VOLUME 47, NUMBER 1, MARCH 2024

HADRONIC JOURNAL Volume 47, Number 1, March 2024

HADRONIC JOURNAL

Founded in 1978 by Prof. R. M. Santilli at Harvard University. Some of the past Editors include Professors S. L. Adler, A. 0. Barut, L. C. Biedenharn, N. N. Bogoliubov, M. Froissart, J.Lohmus, S. Okubo, Nobel Laureate Ilya Prigogine, M. L. Tomber, J. P.Vigier, J. Wess, Nobel Laureate Chen Ning Yang.

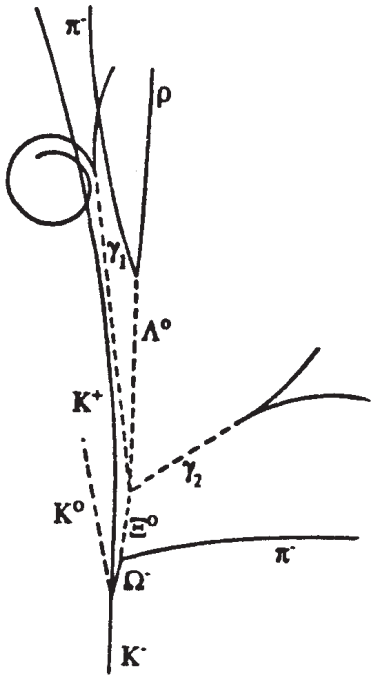

HADRONIC PRESS, INC.

HADRONIC JOURNAL

Established in 1978 by Prof. R. M. Santilli at Harvard University Hadronic Journal and Algebras, Groups and Geometries have been regularly published since 1978 without publication charges and are among the few remaining independent refereed journals.

This Journal publishes advances research papers and Ph. D. theses in any field of mathematics without publication charges.

For subscription, format and any other information please visit the website
http://www.hadronicpress.com

HADRONIC PRESS INC.
35246 U. S. 19 North Suite 215
Palm Harbor, FL 34684, U.S.A.
http://www.hadronicpress.com
Email: info@hadronicpress.com
Phone: +1-727-946-0427

HADRONIC JOURNAL

Founder and Editor in Chief
RUGGERO MARIA SANTILLI
The Institute for Basic Research
35246 U. S. 19 North Suite 215, Palm Harbor, FL 34684, U.S.A.
Email: resarch@i-b-r.org; TEL: +1-727-688-3992

ISSN: 0162-5519

Established in 1978 by Prof. R. M. Santilli at Harvard University Hadronic Journal and Algebras, Groups and Geometries have been regularly published since 1978 without publication charges and are among the few remaining independent refereed journals.

This Journal publishes advances research papers and Ph. D. theses in any field of mathematics without publication charges.

For subscription, format and any other information please visit the website http://www.hadronicpress.com

HADRONIC PRESS INC.
35246 U. S. 19 North Suite 215
Palm Harbor, FL 34684, U.S.A.
http://www.hadronicpress.com
Email: info@hadronicpress.com
Phone: +1-727-946-0427

HADRONIC JOURNAL Volume 47, Number 1, March 2024

HADRONIC PRESS, INC.

HADRONIC JOURNAL

VOLUME 47, NUMBER 1, MARCH 2024

HADRONIC JOURNAL 47, 1 - 14 (2024)
DOI 10.29083/HJ.47.01.2024/SC1

SCATTERING OF FREE ELECTRONS WITH HYDROGEN ATOMS IN PROTON EXCHANGE MEMBRANE FUEL CELL

[1,3,4]Saddam Husain Dhobi, [2,3]Anup Pudasaini, [3,5]Dipak Oli, [6]Subash Khatiwada, [2]Keshab Ghimire, [5]Om Shree Rijal, [2]Sudeep Ghimire, [2]Tashi Lama Yonjan, [4]Roshan Pandey, [5]Ganesh Paudel

[1]Central Department of Physics, Tribhuvan University, Kirtipur, Kathmandu, Nepal
[2]Department of Physics, Patan Multiple Campus, Tribhuvan University, Lalitpur Nepal
[3]Innovative Ghar Nepal, Lalitpur, Nepal
[4]Nepal Academy of Science and Technology, Khumaltar, Lalitpur, Nepal
[5]Department of Physics, Amrit Science Campus, Lainchaur, Kathmandu
[6]Department of Physics, St. Xavier's College, Maitighar, Kathmandu
saddam@ran.edu.np

Received October 18, 2023

Abstract

This study examines the evolution of the Klein-Nishina (KN) cross section for hydrogen and platinum atoms in relativistic and non-relativistic scenarios. Using online MATLAB tools, the constructed model of KN cross section for both situations is calculated. The observation demonstrates that as electron energy increases, electronic and atomic KN cross section lowers, which lessens the relationship between the incoming electron and the target atom. The importance of atomic size is demonstrated by a comparison of the KN cross sections of hydrogen and platinum, with platinum possessing a higher cross section because of its greater size and more scattering centers. Higher atomic numbers result in greater interaction between sites and bigger cross sections, and they also play a role in this relationship. The variations in cross sections are also influenced by electron binding effects, especially in the instance of hydrogen. It is demonstrated that relativistic effects have a major impact on the KN cross section, including an exponential decline seen as the energy of electrons increases. In the relativistic domain, the electron's increased mass and decreased wavelength increase scattering probability and produce a greater cross section than in the non-relativistic case. This research sheds light on the variables affecting KN cross sections and their influence on radiation therapy, medical imaging, and materials science.

Keywords: KN cross section, Hydrogen, Platinum, relativistic and non-relativistic

1. Introduction

In recent years, fuel cells made from hydrogen have drawn interest as a practical alternative energy source. Generally speaking, fuel cells use fuels like the gas hydrogen, methanol, or natural gas to transform the chemical energy contained in the fuel they contain into direct current (DC) without intermediary the combustion process, as is the case of traditional engines [1]. Fuel cells are a potential candidate for an environmentally friendly form of energy technology in the future due to their increased efficiency and low emissions. The fuel cells market and, consequently, the shift to a hydrogen economy are determined by the kind of fuel cell, the cost of the components, and the production processes. The price of fuel cells has dropped by 80% in the last couple of decades (since the 1990s), thanks to technological developments. Additionally, it is anticipated that the price of platinum will decline due to the rising demand for natural resources [2]. An fuel cell is an electrochemical machine that uses two redox processes to transform the chemical energy of a fuel (typically hydrogen) plus an oxidizing agent (commonly oxygen) into electrical energy [3]. Over the past three decades, as clean energy technologies are sought after globally for environmental and sustainable development goals, the proton exchange membrane fuel cell (PEMFC) has attracted a lot of interest. PEMFCs are devices which employ hydrogen fuel and transform chemical energies directly into electricity, bypassing the limitations of the Carnot cycle. As a result, they are more efficient and emit almost no emissions in comparison to conventional electricity-generating technologies and direct consuming of fossil fuels.

A single PEMFC is typically built in a hierarchical form, with a proton exchange membrane serving as the center layer through which primarily protons can pass. The catalyst layer (CL) of the anode and cathode, the gas diffusion layer (GDL) between the two electrodes, and the bipolar plates are arranged in order from the center to the edges. Together, the membrane, CLs, and GDLs are referred to as membrane electrode assemblies (MEA), and their physical makeup could be compared to that of porous media with multi-scale pores. Grooves called gas flow channels (GFCs) are mechanically carved into the innermost layer of the polar plate [4]. During cell operation, hydrogen and air are delivered into the cell via the flow channel and, in turn, pass through the anode's and cathode's respective gas diffusion layers to reach the catalyst layer. The molecules of hydrogen are depleted of their electrons and broken down into protons in the catalyst, which is the layer of the anode. To create an electric current, electrons are required to move through an external circuit. The formed electron, proton and residue goes interaction in effective area called, scattering cross sections. The scattering region can be

calculated by using equation (1) from differential cross section phenomenon [5].

$$\frac{d\sigma}{d\Omega} = \frac{r_e^2}{2}\left(\frac{k'}{k_0}\right)^2 (1 + cos^2\theta) \quad (1)$$

In terms of the wavelengths of the photons, Compton described this relationship as follows:

$$\lambda' - \lambda = 1 - cos\theta \quad (2)$$

where $\boldsymbol{\lambda}$ and $\boldsymbol{\lambda'}$ are the photon's pre- and post-deflection Compton wavelengths [6].

In this work authors are applying Klein-Nishina (KN) cross section in the framework of electrode scattering which helpful insights about the connection among electrons and the electrode materials. In order to maximize the effectiveness and effectiveness of PEMFCs, it is essential to comprehend the KN cross section in this particular system. Electrochemical reactions in PEMFCs are greatly aided by electrode materials like platinum or other catalysts. As they engage with electrode surfaces during fuel cell operation, produced electrons experience scattering events. The likelihood of each of these scattering events occurring is measured using the KN cross section. The information regarding scattering in PEMFCs and its effects on performance can be examined by the KN cross section around an electrode scattering. On taking account the KN cross section in electrodes dispersion within PEMFCs offers useful knowledge for enhancing the design, functionality, and longevity of these energy-converting devices. It may direct the choice of materials and electrode engineering, and it can promote PEMFC technology for a variety of uses, such as transport and stationary power generation.

II. Literature Review

The initial gas-based voltaic cell powered by a mixture of hydrogen and oxygen was created by Sir William Grove in 1839, the same year he also put forth the notion of the fuel cell's effect. Ostwald laid the theoretical groundwork for fuel cell research in 1894. When attempting to understand the rate of electromechanical processes in fuel cells, Van Santen developed the Ostwald-proposed step rule concept [7]. In the 1920s, Lawaczek created numerous schemes for hydrogen-powered automobiles, trucks, buses, trains, and engines. He also made a substantial contribution to the development of pressurized electrolyzes. Although knowing that the idea for fuel cells first

emerged in the beginning of the 1840s, it wasn't until Francis T. Bacon began researching them between 1932 and 1952 that this technology was once again developed, allowing the very first time the development and evaluation of a 5 kW hydrogen fuel cell stack. Later, this technology was created for the life support, guiding, and navigation systems used in NASA's Gemini and Apollo programs [8]. During the course of the last 20 years, the fuel cell sector has made enormous strides, leading to discussions about making investments in hydrogen. The development of fuel cell automobiles was a focus for several decades for automakers from various nations. The first commercially available fuel cell vehicle was released by Toyota in 2014, capping years of research and development work. As a result, the public began to view fuel cell cars as a significant component of the next generation of mobility rather than as an experimental technology. Countries including China, the US, Japan, and a number of European nations concentrated their efforts on advancing this technology throughout the course of the following five years [9].

From 2022 and 2027, the worldwide fuel cell industry is anticipated to increase from an USD 3 billion economy to a USD 9 billion economy at a 26.0% CAGR [10]. Over the course of the last few years, scientific research has also grown more interested in fuel cells. The peak growth in patent applications in the hydrogen-based fuel cell industry [11] (23% increase) from 2016 to 2020 confirms the aforementioned claim. The development of these technologies is driven by personal goals and international obligations in nations including the United States of America, China, India, Japan, South Korea, and several European nations. On the other hand, the efficiency of the fuel cell is affected by the quantum species (electron, proton, hydrogen and oxygen) formed during the interaction of inlet fuel (hydrogen and oxygen) with platinum. KN cross section during the collision of free electrons with atoms (H-atom and Pt-atom) close to the cathode of proton exchange membrane fuel cells (PEMFCs) is the goal of this work. During the collision of free electrons with H and Pt atoms, respectively, the maximum KN cross section measured for single scattering is approximately 70.2 m^2 and 66.0 m^2. The maximum KN cross section recorded for 1ml flow of hydrogen is about −26.6 m^2 and −22.3 m^2 [12]. In 2004, Roy and Pratt used X-ray generator to test KN cross section theory with observations (from 11 to 40 keV) of the entire atom and the observations shows conventional sources ranged from 5% to 50%, but the measurements made with a synchrotron source indicated a small percentage difference. The Compton scattering measures in a range below 10 keV with a broader range of works using angles other than 90 and distinct atomic number Z values in order to confirm the sufficiency of the theoretical treatment.

The KN cross section behavior for H and Pt atoms is the main topic of the current investigation. Future studies may look into a larger range of topics to develop a more thorough grasp of the elements affecting the KN cross section. Understanding how these variables affect the KN cross section would require research into many elements with various atomic sizes, atomic numbers, and material characteristics. Dhobi et al. conducted research on the KN cross section for non-relativistic scenarios and the scattering zone surrounding the electrode in 2023. Furthermore, Dhobi et al. (2022) did not analyze the KN cross section in either the relativistic or non-relativistic case, but rather the interaction of quantum species created around the electrode of PEMFC [13]. There are numerous projects underway to increase the PEMFCs cell's efficiency through experimentation, theory, modeling, etc. Additionally, study is being done on scattering fields theoretically, practically, virtually, etc. However, there aren't many PEMFC and scattering coupled works. Given that PEMFC and scattered are both novel in the fields of research, academia, and industry. Consequently, it is crucial to research dispersion around the PEMFC electrode.

III. Methods and Materials

Hydrogen fuel cell electric vehicles (FCEVs), when compared with traditional internal combustion engine vehicles, they are more efficient from a different perspective. They have a range for driving of more than 300 miles and can be fueled similarly to vehicles with traditional internal combustion engines in around 5 minutes. The technology of FCEVs boost efficiency, like regenerative brakes that collect the electrical power lost during brakes and store it in batteries [14]. Due to their ease of use, quiet operation, high efficiency, and modular design, fuel cells (FCs) have attracted a lot of attention in the automotive sector in recent decades. The usage of FCs in electric automobiles (EVs) is predicted to grow quickly, spark a revolution, and eventually replace conventional vehicles, according to technological breakthroughs. Commercial cars, programs, and research demonstrate that efforts are being made to guarantee that FCEVs have performance improvements sufficient for daily transportation requirements. First, the application areas, distinguishing characteristics, and operational circumstances of FC types and electrical motors are reviewed. According to their structure, complexity, and architectural frequency of use, power converters—voltage regulating and motor drive topologies—that are employed in FCEVs are described in depth [15].

Free electrons, protons, and leftover hydrogen are created when hydrogen comes into touch with the electrodes' catalyst. When the formation electron collides with the atom of hydrogen, a great deal of collisions occurs in the system, which causes heat to be produced. However, in this instance, we take into account the collision that occurs of the hydrogen atom and a free electron. PEMFCs have a serious issue with fuel cell efficiency because of the heat produced during collisions. We are interested in studying the Kelin-Gordan differential cross section that results from the collision of an electron and a hydrogen atom. The classical Thomson scattering can be described using a generalized Klein-Nishina differential equation for Compton scattering with a limited train of pulses. The quantity of scattering photons produced at a particular solid angle $d\Omega$ is

$$\frac{dN_{scat}}{d\Omega} = \int_{-\infty}^{\infty} \frac{\epsilon_0 c|E_x(\omega)|^2}{2\pi\hbar|\omega|} \frac{d\sigma}{d\Omega} d\omega \tag{3}$$

And because the scattered photon has energy $\hbar\omega'$, the total scattered energy is:

$$\frac{dU_r}{d\Omega} = \int_{\infty}^{\infty} \frac{\epsilon_0 c|E_x(\omega)|^2}{2\pi} \frac{\omega'}{\omega} \frac{d\sigma}{d\Omega} d\omega \tag{4}$$

The input gamma ray impacts an atomic electron, causing atomic ionization, and this is the primary scattering mechanism that produces 511 Kev photons. The KN differential cross section formula will determine the angle at which the incident photon will scatter,

$$\left(\frac{d\sigma}{d\Omega}\right)_a = \frac{Zr_e^2}{2}\left(\frac{1}{1+\alpha(1-cos\theta)}\right)^2 \left((1+\cos^2\theta) + \frac{\alpha^2(1-cos\theta)^2}{[1+\alpha(1-cos\theta)]}\right) \tag{5}$$

A variation of the differential atomic cross sectional area equations for K-N can be found here. Additionally, Knoll discovered the complete KN cross section per atom in 1989;

$$\sigma_a = 2\pi \int_0^{\pi} \left(\frac{d\sigma}{d\Omega}\right)_a sin\theta d\theta \tag{6}$$

Where θ is scattering angle overall photons. Now from (5) and (6), we get:

$$\sigma_a = 2\pi \int_0^{\pi} \frac{Zr_e^2}{2}\left(\frac{1}{1+\alpha(1-cos\theta)}\right)^2 \left((1+\cos^2\theta) + \frac{\alpha^2(1-cos\theta)^2}{[1+\alpha(1-cos\theta)]}\right) sin\theta d\theta \quad (7)$$

After solving, the following is the total KN cross section per atom:

$$\sigma_a = Z2\pi r_e^2 \left\{\frac{1+\alpha}{\alpha^2}\left[\frac{2(1+\alpha)}{1+2\alpha} - \frac{\ln(1+2\alpha)}{\alpha}\right] + \frac{\ln(1+2\alpha)}{2\alpha} - \frac{1+3\alpha}{(1+2\alpha)^2}\right\} \quad (8)$$

Since electronic cross-sections are multiplied by each element's charge number Z to get Klein-Nishina atomic cross-sections, equation (7) states that $\sigma_a = Z.\sigma_e$ the electronic cross-sectional area for KN is

$$\sigma_e = 2\pi r_e^2 \left\{\frac{1+\alpha}{\alpha^2}\left[\frac{2(1+\alpha)}{1+2\alpha} - \frac{\ln(1+2\alpha)}{\alpha}\right] + \frac{\ln(1+2\alpha)}{2\alpha} - \frac{1+3\alpha}{(1+2\alpha)^2}\right\} \quad (9)$$

where $r_e = 2.818\, fm$ is the classical electron radius, Z is the nuclear charge of the target molecule and $\alpha = \frac{E}{m_e c^2} = \frac{E}{0.511MeV}$, for non relativistic case. For relativistic case, energy of electron $E_r = \frac{mc^2}{\sqrt{1-v^2/c^2}} = \frac{mc^2}{\sqrt{\beta}}$ [16] and $mc^2 = 0.511MeV$ [17]. Also, $E_r = \frac{1}{\sqrt{1-v^2/c^2}}$ therefore for relativistic case $\alpha_r = \frac{1}{\sqrt{1-v^2/c^2}}$. Now equation (11) can be modified as

$$\sigma_e^r = 2\pi r_e^2 \left\{\frac{1+\alpha_r}{\alpha_r^2}\left[\frac{2(1+\alpha_r)}{1+2\alpha_r} - \frac{\ln(1+2\alpha_r)}{\alpha_r}\right] + \frac{\ln(1+2\alpha_r)}{2\alpha_r} - \frac{1+3\alpha_r}{(1+2\alpha_r)^2}\right\} \quad (10)$$

Also from, $\sigma_a = Z.\sigma_e$ we have

$$\sigma_a^r = 2Z\pi r_e^2 \left\{\frac{1+\alpha_r}{\alpha_r^2}\left[\frac{2(1+\alpha_r)}{1+2\alpha_r} - \frac{\ln(1+2\alpha_r)}{\alpha_r}\right] + \frac{\ln(1+2\alpha_r)}{2\alpha_r} - \frac{1+3\alpha_r}{(1+2\alpha_r)^2}\right\} \quad (11)$$

IV. Results and Discussion

The KN cross sections for electron and atom interactions are shown in Figure 1 as a function of electron energy. With increased electron energy, the cross section is seen to decrease. The cross section is initially large at lower energy, indicating a greater likelihood of interaction. But as electron energy rises, the cross section gradually contracts until it reaches a fixed value. It is clear from comparing the cross sections of platinum and hydrogen that platinum has a higher KN cross section than hydrogen and electronic interaction. The size of the atoms under consideration accounts for the majority of this variation.

Platinum atoms' increased size increases the scattering likelihood and raises the cross section.

By taking into account the energy dependency of scattering processes, it is possible to explain the decreasing pattern of the KN cross section with rising electron energy. Because their energy scales are more closely matched at lower energies, the relationship between an incoming electron and the object being targeted atom has a greater impact. The contact, however, weakens with increasing electron energy, resulting in a decrease in the width of the cross section. The significance of atomic size is demonstrated by comparing the cross sections of hydrogen and platinum. The cross section of platinum is higher because platinum atoms are bigger than hydrogen atoms. This is explained by the fact that there are more scattering centers accessible, which increases the likelihood of scattering occurrences. The KN cross section obtains a constant value in the high-energy area. This tendency implies that the incident electron's interaction with the target atom weakens and becomes less reliant on electron energy. Due to the predominance of relativistic effects, whereby the wavelength of the input electron shrinks dramatically relative to the size of the scattering centers, the interaction is diminished.

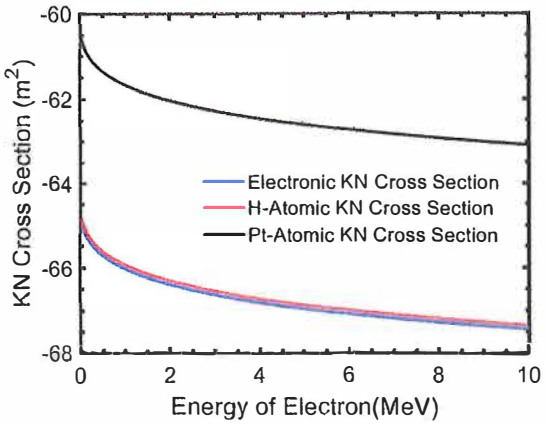

Figure 1: KN cross section with electron energy

Figures 2, 3, and 4 depict the KN electron and atomic cross section together with the electron's velocity. The KN electronic and atomic cross sections fall exponentially with increasing energy of electrons in the relativistic situation. The two main causes of this phenomena are the contraction of the electron wavelength and the relativistic mass increase. For the relativistic situation of mass, an electron's mass grows noticeably when it approaches relativistic energies, which are energy close to the speed of light. The relativistic mass

of an object traveling at a high speed is determined by, in accordance with Einstein's theory of special relativity. The trajectory of the electrons during scattering events is impacted by the increase in mass. At greater energies, the electron behaves resembles a heavy particle because its relativistic mass is much more than its rest mass. The KN cross section decreases as a result of the higher mass since it lowers the likelihood of scattering.

In the relativistic wavelength situation, the electron's wavelength gets shorter as its energy rises. An electron's de Broglie wavelength is calculated using the formula ($\lambda = h/p$), where λ is the wavelength, h is Planck's constant, and p is the electron's momentum. A shortened de Broglie wavelength results from the electron's momentum increasing as its energy does. By decreasing the true dimension of the scattered centers (atoms), the diminishing electron wavelength has an impact on the scattering process. The efficiency of scattering decreases when the wavelength of the electron approaches or falls below the dimensions of the scattering centers. The KN cross section decreases as a result of this decline in scattering effectiveness. As a result, the KN electronic and atomic cross sections exponentially drop with increasing electron energy due to the interaction between the relativistic mass increase and the decreasing electron wavelength in the relativistic regime.

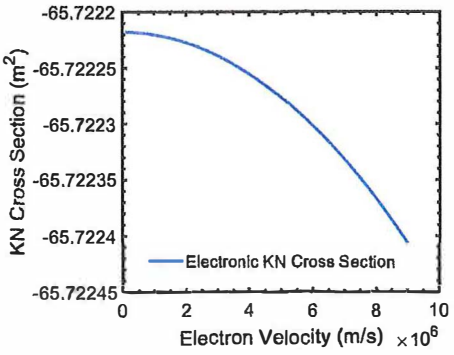

Figure 2: KN Electronic cross section with electron energy

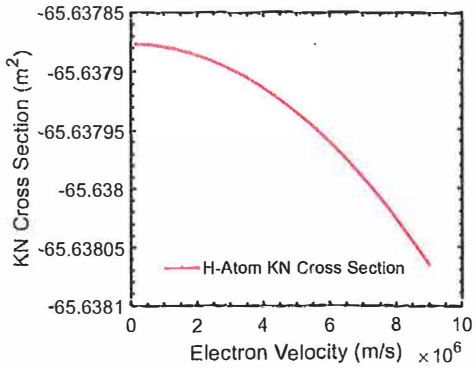

Figure 3: H-Atom KN cross section with electron energy

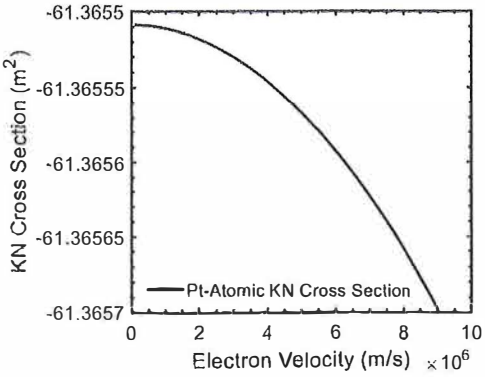

Figure 4: Pt-Atom KN cross section with electron energy

The KN cross section for Pt is greater than the KN cross section for hydrogen (H), as well as the KN electronic cross section, when the KN cross sections from Figures 2, 3, and 4 are compared. Additionally, it is discovered that the KN cross section for hydrogen is greater than that of the KN electronic cross section. There are various underlying causes for this variation in cross section values. The atomic size of the particles that interact is a significant factor for the observed variations in the KN cross sections. Hydrogen atoms are much smaller than platinum atoms. Due to their bigger size, platinum atoms offer a larger target region for the incoming electrons to engage with during the scattering process. Since there are more scattering events as a result, platinum has a greater cross section than hydrogen and electronic interactions.

The target atoms' atomic number is another element that affects the cross section discrepancy. Compared to hydrogen, Pt has a higher atomic number. Higher atomic numbers equate to more electrons in the atom's outer shells, which increases the number of potential places for interaction for the incoming electrons and affects the scattering likelihood. As a result, platinum has a greater cross section than electrical and hydrogen interactions. The difference in cross section between electronic interactions and hydrogen is also influenced by the electron binding effects. The attractive force of the charged proton in its nucleus is felt by an incident electron when it comes into contact with a hydrogen atom. In comparison to the KN electronic cross section, which solely takes into account the scattering of electrons without taking into account the influence of a bonded nucleus, this attractive force increases the scatter probability, resulting in a greater KN cross section for hydrogen.

Overall, the differences in the KN cross sections are caused by the interaction of atomic size, atomic number, and electron binding effects. Platinum has a bigger cross section than hydrogen and electrical interactions due to its bigger dimensions and higher atomic number. In addition, compared to electronic interactions, the effects of hydrogen's electron binding contribute to its greater cross section.

It is found that the KN cross section in the relativistic case is greater than in the non-relativistic case when compared the KN cross sections in the relativistic and non-relativistic instances, as shown in figure 5. The scattering is governed by classical electromagnetic theory in the non-relativistic situation, where the electron energies are substantially lower than the speed of light (c). Assuming the amount of electron mass stays constant during the scattered process and ignoring relativistic effects, Thomson scattering is used to characterize the cross section for this case. On the other hand, relativistic effects become important in the case where the electron energy approach or surpass a large proportion of the speed of light. The KN formula, which integrates relativistic adjustments to the scatter amplitude and accounts for the fluctuation of electrons mass with energy, describes relativistic scattering.

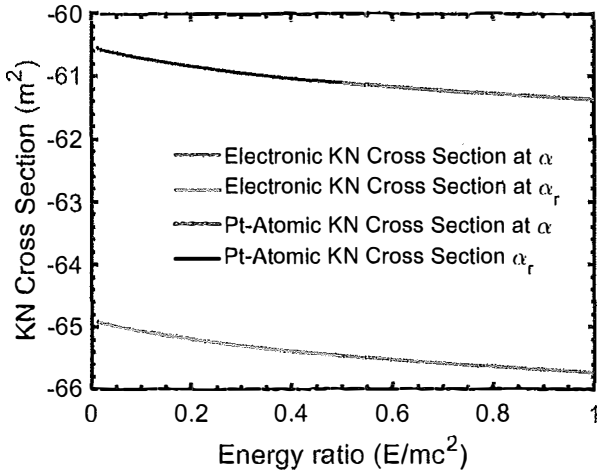

Figure 5: KN cross section with energy ratio for relativistic and non-relativistic case

Additionally, the electron's mass greatly increases in the relativistic zone as its kinetic energy approach the speed of light. The enhanced contact between an incoming electron and the intended atom caused by the higher mass has an impact on the scattering process. A higher scatter probability and, as a result, a greater KN cross section are produced by this increased contact. The KN formula considers the energy dependency of the scattering process while calculating the relativistic scattering amplitude. When an electron is struck at a greater energy, its wavelength approaches or even falls below the dimension of the scattering centers (atoms). Comparing to the non-relativistic scenario, this enables more effective scattering and increases the cross section. As a result, the relativistic situation has a greater KN cross section than the non-relativistic case due to the combination of the relativistic mass increases and the dependent on energy scattering amplitude. The increased cross section is due to relativistic phenomena that increase the scattering probability and enable stronger interactions among the incoming electron and the target atom.

V. Conculsion

In conclusion, the energy dependency of scattering processes can be used to explain the declining tendency of the KN cross section increasing electron energy. In comparing the cross sections of hydrogen and platinum, it is clear how important atomic size and number are; platinum has a higher cross section because of its bigger dimensions and greater atomic number. Additionally, the KN cross section remains constant in the high-energy area, indicating weaker and fewer energy-dependent interactions, possibly as a

result of relativistic processes. The KN cross section is found to be greater in the relativistic domain when compared the relativistic and non-relativistic situations. This is attributable to the relativistic mass rise and energy-dependent scattered amplitude. A larger range of atomic sizes, numbers, and substances should be investigated in order to better comprehend KN cross sections. Radiation therapy, medical imaging, and materials science can all benefit from the findings. Computer simulations are useful for understanding complex systems.

REFRENCES

[1] Y. Manoharan, S. E. Hosseini, B. Butler, H. Alzhahrani, B. T. F. Senior, T. Ashuri, and J. Krohn, Applied Sciences, 9 (2019).

[2] G. Reverdiau, A. Le Duigou, T. Alleau, T. Aribart, C. Dugast, and T. Priem International Journal of Hydrogen Energy, 46 (2021).

[3] K. Jain, and K. Jain, International Journal of All Research Education and Scientific Methods (IJARESM), 9 (2021).

[4] J. P. Kone, X. Zhang, Y. Yan, G. Hu, and G. Ahmadi, Journal of Computational Multiphase Flows, 9 (2017).

[5] Caltech. (2023). Experiment 32. Retrieved from http://www.sophphx.caltech.edu/Physics_7/Experiment_32.pdf

[6] J. H. Hubbell, Center for Radiation Research, National Bureau of Standards, Washington, D.C. (1969). Retrieved from https://nvlpubs.nist.gov/nistpubs/Legacy/NSRDS/nbsnsrds29.pdf

[7] R. A.V. Santen, Journal of Physics and Chemistry, 88 (1984).

[8] K. A. Burke, In Proceedings of the 1st International Energy Conversion Engineering Conference, Portsmouth, VA, USA, (2003).

[9] M. Bodke, R. G. Shriwastava, and R. U. Shelke, International Journal of Research in Electronics and Computer Engineering, 8(4), (2020).

[10] A. M. Elberry, J. Thakur, A. Santasalo-Aarnio, and M. Larmi, International Journal of Hydrogen Energy, 46 (2021).

[11] S. C. Ma, J. H. Xu, and Y. Fan, Journal of Cleaner Production, 338 (2022).

[12] S. H. Dhobi, S. P. Gupta, J. J. Nakarmi, B. Koirala, K. Yadav, S. K. Oli, M. Gurung, International Annals of Science, 13 (2023).

[13] S. H. Dhobi, K. Yadav, A. K. Jha, B. Karki, and J. J. Nakarmi, ECS Transactions, 107 (2022).

[14] AFDC. (2023). How do fuel cell electric cars work? Retrieved from https://afdc.energy.gov/vehicles/how-do-fuel-cell-electric-cars-work

[15] M. Nci, M. Büyük, M. H. Demir and G. İlbey, Renewable and Sustainable Energy Reviews, 137 (2021).

[16] Y. Z. Umul, Optik, 231 (2021).

[17] MIT. (2013). Relativistic Dynamics: The Relations Among Energy, Momentum, and Velocity of Electrons and the Measurement of e/m. Department of physics. Retrieved from http://web.mit.edu/8.13/www/JLExperiments/JLExp09.pdf

HADRONIC JOURNAL 47, 15 - 29 (2024)
DOI 10.29083/HJ.47.01.2024/SC15

POSSIBLE DEVELOPMENT DIRECTIONS OF PARTICLE PHYSICS AFTER STANDARD MODEL

Yi-Fang Chang

Department of Physics
Yunnan University
Kunming, 650091, China
yfc50445@qq.com, yifangch@sina.com

Received July 3, 2023

Abstract

After three generations of quarks-leptons and Higgs boson have been confirmed, we research some possible development directions of particle physics. First, particles of three generations are extended. Second, the hadronic theory must precision quantification such as heavy flavor hadrons and the lifetime formula, etc. Third, various unifications of interactions are discussed. Fourth, some basic principles (Pauli Exclusion Principle, duality, uncertainty principle, etc.) are probably violated under some cases. Fifth, Santillli, Penrose, et al., proposed some new mathematical methods. Sixth, particle astrophysics, the negative matter as unified dark matter and dark energy, and the extensive quantum theory are searched.

Key words: hadron, three generation, unification, basic principle, mathematics, astrophysics.

I. Introduction

It is well-known that the three generations of quark-lepton in the standard model is:

$$\begin{array}{cccc} q=(2/3)e & -(1/3)e & -e & 0 \\ \begin{pmatrix} u \\ c \\ t \end{pmatrix} & \begin{pmatrix} d \\ s \\ b \end{pmatrix} & \begin{pmatrix} e \\ \mu \\ \tau \end{pmatrix} & \begin{pmatrix} \nu_e \\ \nu_\mu \\ \nu_\tau \end{pmatrix} \end{array}. \qquad (1)$$

So far these quarks-leptons and Higgs boson are confirmed. In this model the second and third generations of quark-lepton are the different excited states of the first generation. The standard model implies that third generation quarks are already final from bottom to top.

After the basic elements and structure of the particle are determined, what is the further development direction of particle physics? In this paper, we research some possible directions.

2. Extension of Three Generations

The extension of three generations may be: 1. The most common method is to further confirm those new particles composed of the standard model, but these particles not yet being discovered. Different generations of quarks have a certain periodicity, most notably heavy quark charmonium and bottomonium $\eta_c = c\bar{c}$ and $\Upsilon = b\bar{b}$, which agree with Cornell potential [1]:

$$V = -\frac{\alpha_s}{r} + Kr . \qquad (2)$$

For $c\bar{c}$, $b\bar{b}$ and $t\bar{t}$, α_s=0.35, 0.22 and 0.11. They become smaller with the bigger quark mass. Further, the mesons with c-quark are $D^+ = \bar{d}c$, $D^0 = \bar{u}c$ (I=1/2), and $D_s^+ = c\bar{s}$ (I=0). The mesons with b-quark are $B^+ = u\bar{b}$, $B^0 = d\bar{b}$ (I=1/2), and $B_s^0 = s\bar{b}$ (I=0). Both are complete symmetry. The baryons with c-quark are (Λ_c^+, Σ_c^+)=udc, Σ_c^{++}=uuc, Σ_c^0=ddc, Ξ_c^+=usc, Ξ_c^0=dsc, and Ω_c^0=ssc. Other Ξ_{cc}^{++}=ucc, Ξ_{cc}^+=dcc, $\Omega_{cc}^+ = scc$, Ω_{ccc}^{++}=ccc and so on. In 1990s, the heavy quark symmetry and heavy quark effective theory (HQET) are proposed [2-7], in which interactions between heavy quarks are mainly achieved by exchanging soft gluons and other light-flavor particles inside the heavy hadron. Usually phenomenological models are combined by some nonperturbative QCD.

2. Find the gluon and whether it has three generations, or some excited states of the known first generation. 3. Whether W-Z have three generations,

or which are only excited states of W-Z. 4. Are there three generations of Higgs particles?

It is known that K is weaker than π interactions. If it is generalized, D and B interactions should be weaker. Further, the three-generation interactions are getting weaker and weaker. If the interaction is the same, three quark-lepton exchange particles must be zero mass.

3. Precision Quantification of Three Generations of Hadronic Theory

The first quark-lepton and QED is very precise, which includes the anomalous magnetic moments of electron by the renormalization theory, and Lamb shift. Second and third quark-lepton should first be specifically renormalized. This corresponds probably to the Rosen-Ross mass formula of leptons-meson [8,9]:

$$M = m_e(1+\frac{n}{2\alpha}). \quad (3)$$

We proposed a modified accurate mass formula [8,10-12]:

$$M = M_0 - AS + B[I(I+1) - S^2/2]. \quad (4)$$

For the $J^p = 1^+/2$ baryon octet, let M_0 =910.75MeV, *A*=222.04MeV and *B*=38.43MeV, so

$$m(N) = 939.5725, m(\Lambda) = 1115.6MeV,$$
$$m(\Sigma^0) = 1192.46, m(\Xi^0) = 1314.89MeV. \quad (5)$$

For the $J^{pc} = 0^{-+}$ meson octet, let *A*=0, M_0 =549.4MeV and $B = -207.22$ MeV, so

$$m(\pi^0) = 134.96, m(K^0) = 497.6, m(\eta) = 549.4MeV. \quad (6)$$

The neutral baryons and mesons agree completely within the range of error, and are unified M=m.

According to the symmetry of s-c quarks in the same generation, the heavy flavor hadrons which made of u,d and c quarks should be also classified by SU(3) octet and decuplet. Such we derived the symmetrical mass formula [10-12]:

$$M = M_0 + AC + B[I(I+1) - C^2/2]. \quad (7)$$

Let M_0 =875, A=1453, B=84MeV, so m(N)=938, $m(\Lambda_c^+) = 2286$, $m(\Sigma_c) = 2454$ MeV, and we predicted $m(\Xi_{cc}) = 3676$MeV and so on. In July 2017 LHC observed a new and very charming baryon $\Xi_{cc}^{++} = ucc$, whose mass is 3621*MeV* [13]. Then m(Ξ_{cc}^+)=3621.4MeV, and J=1/2. It agrees with Eq.(7), whose error only is 1.4%.

For QCD, SU(3) has [7],

$$m_{\pi^\pm}^2 = \frac{4v}{f^2}(m_u + m_d), \quad (8)$$

$$m_{K^\pm}^2 = \frac{4v}{f^2}(m_u + m_s), \quad (9)$$

$$m_{K^0}^2 = \frac{4v}{f^2}(m_d + m_s). \quad (10)$$

By the experiments, (9)/(8) obtains m_s / m_u =11.507. (10)/(8) obtains m_s / m_d =11.70. Further, m_d / m_u =11.70/11.507=1.0168. But, (10)/(9) obtains m_d / m_u =0.01586. Both are complete different. Assume usually that m_d / m_u =2:1. It is that 4 parameters m_u, m_d, m_s and $\frac{4v}{f^2}$ determine 3 masses $m_{\pi^\pm}, m_{K^\pm}, m_{K^0}$, and which is not agree with experimental data.

Various masses of different quarks mass are very uncertain. And the quark mass change is irregular. Does it conform to the power $M = m^k$, $\log M = k \log m$?

Free quark not exist that can be considered in particle with the infinite deep potential well, which will only have several separate states $E_n = n^2 E_0$. This should be related to the masses of the different quarks. However, only m(d):m (u)=4, and other does not conform.

In the mass formula (4) the quantum number S corresponds to vibration, and I corresponds to rotation. C is also vibrations, both are basically symmetrical, A=228, and 1453. Quarks u-d only rotation I=1/2, s and c are I=0, do not form rotation.

The Planck blackbody radiation formula and Bohr orbit are based on oscillators. The GMO mass formula corresponds to diatomic molecules with vibration-rotation. It corresponds to ud-s two bodies, and may develop to ud-c, etc. Assumed that rotation I is the same, while vibrations S and C are different. Further, S-C-B-T are all different vibrations, and probably correspond to $n, n^2, ...n^m$ and so on.

The heavy flavor hadrons include c, b, t quarks, but t quark is very unstable, and soon decays by the form t→b+W. But, its theory obtained only few quantitative results, and some introduce too many parameters.

Based on the Y-Q and I-U symmetries between mass and lifetime on the general SU(3) theory, we obtained the lifetime formulas of hyperons and mesons [8,10-12]. Based on the new data, we proposed various lifetime

formulas of heavy flavor hadrons, which very agree with experiments. This is a new method on lifetime of hadrons described by quantum numbers, and can be unified for mass and lifetime [12]. But these still need to be precise and systematized.

Present the mass formula is determined according to octet and decuplet. Whether there is a similar lifetime formulas? For octet p, n, Λ_c^+(I=0), Σ_c(I=1) and Ξ_{cc}(I=1/2) are a side of the SU(4). For decuplet three side masses are isometric or add one interaction term. m(Ω^-)=1672.5, m(Ω_c^0)=2695.2, the mass difference is 1022.7. Isometry m(Ω_{cc}^+)=3717.9, m(Ω_{ccc}^{++})=4740.6 (J=3/2). But, m(Δ^{++})=1232, m(Σ_c^{++})=2520, isometry m(Ξ_{cc}^{++})=3808, m(Ω_{ccc}^{++})=5096 (J=3/2).

Moreover, m(Δ^-)=1232, m(Σ_c^0)=2520, isometry m(Ξ_{cc}^+)=3808, m(Ω_{ccc}^{++})=5096 (J=3/2). Both m(Ω_{ccc}^{++}) are different, so we may determine that isometry is only approximate.

Other aspects, various quantitative descriptions of decays and collides on particles still remains to be identified and developed.

4. Unifications of Various Interactions

In QCD, the function is [7]

$$\beta(g) = -\frac{g^3}{16\pi^2}(11 - \frac{2}{3}N_q) + O(g^5), \qquad (11)$$

where N_q is the number of quark flavors. 1. If g>0, β<0; if g<0, β>0; if g=0, β=0. 2. For g>0, if N_q<33/2, β<0; if N_q>33/2 which may not possible, β>0; if N_q=33/2, β=0. Usual $\beta(g_l)$ depends on the running coupling g_l.

$$\alpha_s(Q^2) = \frac{12\pi}{(33 - 2N_f)\ln(Q^2/\Lambda^2)}. \qquad (12)$$

When $Q^2 \to \infty$ (higher energy and shorter range), α_s =0, i.e., the asymptotically freedom. SU(3) is asymptotically free, which first is discovered by Gross and Wilczek [14] and Politzer [15] in 1973.

$\beta(g_l)$ may be positive or negative or 0 [16-18]. $\beta(g_l)$<0 (for 0< g_l<q), $\beta(g_l)$=0 (when g_l=q), and $\beta(g_l)$>0 (for g_l>q). From infrared attraction to ultra-violet repulsion [18],

$$\alpha_s(Q^2) = \frac{g_S^2}{4\pi} = \frac{4\pi}{\beta_0 \ln(Q^2/\Lambda^2)}. \qquad (13)$$

When energy $Q^2 \rightarrow \infty$, the coupling constant of strong interaction $\alpha_s(Q^2) \rightarrow 0$. Further, reduction of distance should be weak interaction with repulsive force. It can be inaccessibility and exclusion, are repulsion.

We proposed that $\beta(g_I)>0$ is strong interaction with big g_I and attraction, $\beta(g_I)<0$ is weak interaction with small g_I and opposite repulsion, and $\beta(g_I)=0$ with g_I =q is the asymptotic freedom. The theory of strong interactions based on the gauge group [19-21]. This is also the unity of strong and weak interactions with short-range [19-21].

5. Possible Violations of Some Basic Principles

So far the universality of Pauli exclusion principle (PEP) was queried some times. First in 1978-1980 Santilli proposed the rest of PEP, in particular, under strong interactions [22,23]. Based on some experiments and theories of particles at high energy, we investigated violation of PEP at high energy begin from 1984 [24-28], and researched some possible tests of violation of PEP (VIP) [25,27]. Recently, we researched another possibility on VIP at ultra-low energy, which is similar to superconductivity, superfluids and Bose-Einstein condensation (BEC), etc. Further, we proposed a possible mechanism of VIP: Cooper pairs extend to general fermion pairs, so they transform to bosons with VIP. From this we may predict some characters of this like-boson, as in nuclei and atoms, etc. Moreover, we researched some possible VIP in mathematics and physics. Based on the extensive quantum theory, its PEP may be violated [29]. At very low temperature two fermions can constitute a boson like the Cooper pair, and perform Bose-Einstein condensation.

The ghost field has gone beyond the distinction of two kinds of quantum statistics, under what conditions does it hold? Is it at very high or at ultra-low energy?

In 1995, the condensation numbers of ^{87}Rb and ^{7}Li atoms may be high as 10^5 under this extreme condition [30]. In 1999 DeMarco and Jin cooled the potassium atomic gas with fermion characteristics to 10^{-9} K, so that the potassium atom pairs to realize quantum degeneracy to Fermi atomic gas [31]. Its quantum effects are different from Bose atomic gas, such as Fermi pressure, Pauli blocking and superfluid, etc. The interaction leads to the formation of Cooper pairs by Fermi atoms and the change of resonance interaction to realize the phase transition from the supercurrent of BCS to BEC [32-34]. At ultra-low temperature fermion pairs can VIP. Contrarily, in 1960 Girardeau proposed a gas model under the hard core boson limit, that is, Tonks-Girardeau gas, at this case the boson is confined to one-dimensional space and the repulsion is very strong. It is similar to PEP. In 2004 Paredes, et al., confirmed this case by cold atomic experiments [35]. This is a boson

similar to a fermion. So boson and fermion are symmetry and unification. In this case PEP has not played a role in the ultra-cold structure, and VIP may be tested.

VIP Collaboration searched new experimental limit on VIP by electrons [36-38], and experimental tests of quantum mechanics on VIP and future perspectives [39]. Chakraborty, et al., discussed sufficient condition for the openness of a many-electron quantum system from the violation of a generalized PEP [40]. Abgrall, et al., researched new limits on bosonic dark matter, solar axions, PEP violation, and electron decay from the low-energy spectrum [41]. Shi, et al., searched experiments for VIP [42].

Based on the analysis of the logical structure [43], the duality, the wave-property is the basic principle of quantum mechanics. But, the wave property seems to have not been well tested under some conditions. We assume that wave should be corrected and developed, and for example, it is nonlinear wave, and a development of the linear superposition principle [8,44]. The quantitative restrict of wave property is mainly determined by $\lambda = h/p$. For particles with high energy or large mass, the wavelength is particular small. The relativity is a range of high velocity and large momentum, while microphysics wave property exhibits easily only with low velocity and small momentum. We suggested that the basic characteristic of particles is the symmetry-statistics duality [8].

K. Shoulders (1991,1992,1999) found the charge cluster (Exotic Vacuum Objects, EVO): When 10 billions of electrons are compressed into an area of a millionth of a millimeter in diameter or less, they began to stick together. This not only violates the charge exclusion, but also fails PEP at high energy. It violates probably the charge and matter conservation laws. In 2000 Puthoff proposed a model attributed to the Casimir force produced by zero energy.

Santilli proposed a unified form of possible generalizations of Heisenberg uncertainty principle for strong interactions [45]. Hadronic mechanics (HM) [46-48] has generalized the uncertainty relations in the only non-trivial way.

In 2023 Santilli reviewed and updated that the insufficiencies of quantum mechanics in nuclear physics; the completion of quantum mechanics into the axiom-preserving, Lie-isotopic branch of hadronic mechanics for the invariant representation of extended protons and neutrons under potential and contact/non-potential interactions; the exact hadronic representation of all characteristics of the neutron in its synthesis from the proton and the electron at the non-relativistic and relativistic levels; the completions of Bell's inequalities with ensuing iso-deterministic principle for strong interactions. Santilli then presented the apparent resolution of the historical objections against the reduction of all stable matter in the universe to protons and electrons and point out a number of open problems whose treatment is beyond the capabilities of quantum mechanics, such as: the cosmological

implications of the missing energy in the neutron synthesis, the prediction of negatively charged pseudo-protons, and the possible recycling of radioactive nuclear waste by nuclear power plants via their stimulated decay [49].

We researched uncertain relations of entropy, information and thermodynamics, and proposed the speed of light and some fundamental constants should be uncertain. Further, we searched its possible development in the entanglement, superstring, and the extensive quantum theory, various matters and different phases, etc. Moreover, the irreversibility and statistics are discussed, and we derived operators of entropy, etc [50]. New measuring technology and some developed theories already challenge the uncertainty principle, which may not be held under certain conditions, and must be modified and developed.

6. Some New Mathematical Methods

From 1978 Santilli discovered the new Iso-Mathematics, which includes isonumbers, isorepresentation [51-53], etc. In Iso-Mathematics, isonumbers and genonumbers of dimensions 1, 2, 4, 8, and their isoduals and pseudoduals may extend to "hidden numbers" of dimension 3, 5, 6, 7 [52]. They are applied for many regions [53,54]. In 1998 Santilli shown that the objections against the Einstein-Podolsky-Rosen (EPR) argument are valid for point-like particles in vacuum (*exterior dynamical systems*), but the same objections are inapplicable (rather than being violated) for extended particles within hyperdense physical media (*interior dynamical systems*) because the latter systems appear to admit an identical classical counterpart when treated with the isotopic branch of hadronic mathematics and mechanics. Now Santilli reviewed, upgraded and specialized the basic mathematical, physical and chemical methods for the study of the EPR prediction that quantum mechanics is not a complete theory. This includes basic methods [55], apparent proof of the EPR argument [56], and examples and applications, in which the validity of the EPR final statement is the effect that the wavefunction of quantum mechanics does not provide a complete description of the physical reality. The axiom-preserving “completion” of the quantum mechanical wavefunction due to deep wave-overlapping when represented via isomathematics, and shown that it permits an otherwise impossible representation of the attractive force between identical electrons pairs in valence coupling, as well as the representation of *all* characteristics of various physical and chemical systems existing in nature [57]. Moreover, Santill studied the classical determinism of EPR prediction by isomathematics [58].

It is known that field theory has scalar, vector, tensor, spinor, torsion and so on. Penrose proposed twistor [59]. Penrose and MacCallum proposed twistor theory as an approach to the quantisation of fields and space-time [60]. Penrose searched nonlinear gravitons and curved twistor theory. Twistor

space is a parameter space-time with complex structure [61]. Penrose and Rindler discussed spinor and twistor methods in space-time geometry [62].

The space-dimension of mathematics and physics can be extended to higher n-dimensions geometry [63]. It may be Hilbert space and corresponding quantum mechanics, and superstring. In mathematics, physics and many regions the field theory is all a very important problem. When the space-dimension is extended to n, fractal and complex, and various number-systems, the field theory and its formulas may be correspondingly extended. In these cases, Gauss's theorem and Stokes's theorem, and corresponding extensions on gradient, divergence and curl are searched [64]. Further, they are combined each other, and form multiple combinations, such as the scalar-tensor fields, the scalar-spinor fields, the vector-spinor fields, etc. These fields can be applied to physics, biology, earthquakes and social science, etc. Field theory has been widely applied in many regions of natural and social sciences, and its any development will necessarily inspire and apply to more aspects [65].

In quantum mechanics the time-space operators of energy-momentum representation in quantum mechanics are [66]:

$$x_\mu \psi = i\hbar \frac{\partial}{\partial p_\mu} \psi . \qquad (14)$$

Based on Eq.(48) we discussed the space-time operators and their generalization, and some applications of this method. In particular, the lifetime formulas of particles are obtained from the time equation, and they agree better with the experimental data. We proposed some operator equations of general relativity and special relativity. This is the simplest unifying quantum theory and general relativity, and corresponds to the extensive quantum theory, and may overcome the singularity problem in general relativity. It is the combination and unification on quantum mechanics and general relativity [67].

Further, based on the non-commutation

$$[A,B] = AB - BA = \eta \neq 0 , \qquad (15)$$

of matrix, group, tensor and so on, we propose the mathematical quantum theory. If η is imaginary number, it will correspond to the extensive quantum theory. If η is real number, it will be development of quantum theory. Moreover, η may be complex number, etc. We introduce a similar wave function and corresponding operators, various similar quantum results will be derived. Next, we discuss its physical meaning and various applications. Third, based the general matrix we research mathematics of unified gravitational and electromagnetic fields. Fourth, we discuss the space-time equations and the simplest unifying quantum theory and general relativity. Further, we can combine general discrete mathematics [68].

The nonlinear approach of quantum mechanics is continuously an important direction. We propose mathematically the basic nonlinear operators

$$p_\mu = -i\hbar(F\frac{\partial}{\partial x_\mu} + i\Gamma_\mu), \qquad (16)$$

so Klein-Gordon equation and Dirac equations turn out to be

$$(F^2\Box + \Gamma_\mu^2 - m^2)\varphi = -J. \qquad (17)$$

Dirac equations are:

$$\gamma_\mu(F\partial_\mu + i\Gamma_\mu)\psi + \mu\psi = j. \qquad (18)$$

We obtained the corresponding Heisenberg equation. Then the present applied superposition principle is developed to the general nonlinear form. The quantum commutation and anticommutation belong to F and Γ_μ. This theory may include the renormalization, which is the correction of Feynman rules of curved closed loops [44]. We think the interaction equations must be nonlinear. Many theories, models and phenomena are all nonlinear, for instance, soliton, nonabelian gauge field, and the bag model, etc. The superluminal entangled state, which relates the nonlocal quantum teleportation and nonlinearity, should be a new fifth interaction. Moreover, the nonlinear effects exist possibly for various interactions, for single particle, for high energy, and for small space-time, etc. The relations among nonlinear theory and electroweak unified theory, and QCD, and CP nonconservation, etc., are expounded. Finally, some known and possible tests are discussed [44].

We proposed that a trefoil knot of left hand and a trefoil knot of right hand is possibly similar to two spins s=1/2 and -1/2 of three quarks (nucleons p and n, etc) [69]. Two topological structures should differ in their energy levels in the magnetic field. Basic mesons of two quark form a line, and s=0. This model is first applied to proton and neutron, then it may be extended to other particles.

7. Particle Astrophysics and Extensive Quantum Theory

The particle astrophysics is a new modern intersecting science. Perkins published a book *Particle Astrophysics* [70]. In book some of the most perplexing cosmic and astrophysical phenomena are inextricably intertwined with the quantum world of elementary particles. Cosmologists have developed a "concordance model" that accounts for the observed global properties of the universe and the cosmic structures that were probably seeded by primordial quantum fluctuations. The standard model of particle physics accommodates all experimentally observed properties of elementary particles. But it completely fails to account for key elements of the concordance model—the dark matter that dominates the dynamics of galaxies and the dark energy that accelerates the expansion of the universe. Nor can it explain the cosmic preponderance of ordinary matter over antimatter, an asymmetry necessary

for our very existence. Well-motivated extensions of the standard model suggest novel particles as dark-matter candidates.

The Dirac negative energy state corresponds to a negative matter with some new characteristics, which are mainly the gravitation each other, but the repulsion with all positive matter. Such the positive and negative matters are two regions of topological separation in general case, and the negative matter is invisible. It is the simplest candidate of dark matter, and is unified with dark energy, and can explain their some phenomena. We researched possible quantum theory of dark energy. The negative matter is related with inflation cosmos and many worlds, and discussed eight possible tests of this hypothesis, in particular, the season effect [71].

Based on Dirac negative energy, Einstein mass-energy relation and principle of equivalence, we propose the negative matter as the simplest model of unified dark matter and dark energy. All theories are known, only mass includes positive and negative. Because there is repulsion between positive matter and negative matter, so which is invisible dark matter, and repulsion as dark energy. It may explain many phenomena of dark matter and dark energy. We derived that the rotational velocity of galaxy is approximate constant. Assume that dark matter is completely the negative matter, so we may calculate an evolutional ratio between total matter and usual matter from 1 to present 11.82 or 7.88. Further, the mechanism of inflation is origin of positive-negative matters created from nothing, whose expansion is exponential due to strong interactions at small microscopic scales. The negative matter as a candidate of dark matter and dark energy is not only the simplest, and is calculable and testable [72]. Generally, cosmology must be related to particles, in particular, for early Universe [73,74].

According to Feynman's idea [75] and based on a new form of the Titius-Bode law [76,77]:

$$r_n = an^2, \qquad (19)$$

we developed a similar theory with the Bohr atom model, and obtain the quantum constants $H = (aGM_{\odot})^{1/2}$ of the solar system and corresponding Schrödinger equation [76,77]:

$$iH\frac{\partial\psi}{\partial t} = -H^2\nabla^2\psi + (U - Q)\psi\,. \qquad (20)$$

Further, we proposed the extensive quantum theory in which the formulations are the same with the quantum mechanics and only quantum constant h and corresponding basic quantum elements are different [77,78].

8. Discussion

In 2005, CERN experiments concluded that a new high-temperature and high-dense substance state has been produced. The quark-gluon plasma

(QGP) predicted by the original theory should be an approximate ideal gas composed of weakly coupled quark-gluons, but the result is that this matter exhibits extremely strong interaction, nearly perfect liquid (sQGP) [79], and may be described accordingly by the string theory of twin ecology [80]. This seems to violate the asymptotic freedom.

Basis of quantum biology and quantum consciousness and quantum society [81-83] must be the extensive quantum theory [76-78], which includes the extensive quantum biology [84-86], and the extensive quantum sociology [87,88]. General drugs are always quantized. Only intravenous infusion is continuous, which corresponds to fluid mechanics. Its mathematical foundation and extension are mathematical quantum theory [68].

References

[1]E. Eichten, et al. *Phys.Rev.* D21(**1980**):203.
[2]N. Isgur and M.B. Wise, *Phys.Lett.* B. 232(**1989**): 113.
[3]N. Isgur and M.B. Wise, *Phys.Lett.* B. 237(**1990**): 527.
[4]H. Georgi, *Phys.Lett.* B. 264(**1991**): 447.
[5]M. Neubert, *Phys.Rep.* 245(**1994**): 259.
[6]M.B. Wise, hep-ph/9805468.
[7]A.V. Manohar and M.B. Wise, *Heavy Quark Physics*. Cambridge University Press. **2000**.
[8]Yi-Fang Chang, *New Research of Particle Physics and Relativity*. Yunnan Science and Technology Press. **1989**; Phys.Abst. 93(**1990**)No1371.
[9]Yi-Fang Chang, *Hadronic J.* 45(**2022**):253.
[10]Yi-Fang Chang, *International Review of Physics*. 6(**2012**)3:261.
[11]Yi-Fang Chang, *Hadronic J.* 41(**2018**):221.
[12]Yi-Fang Chang, *Hadronic J.* 41(**2018**):335.
[13] R. Aaij, B. Adeva, M. Adinolfi, et al. (LHCb Collaboration). *Phys.Rev.Lett.* 119(**2017**): 112001.
[14] D.J. Gross and F. Wilczek, *Phys.Rev.Lett.* 30(**1973**):1343.
[15] H.D. Politzer, *Phys.Rev.Lett.* 30(**1973**):1346.
[16] T.D. Lee, *Particle Physics and Introduction to Quantum Field Theories.* Amsterdam: OPA. **1981**.
[17] S. Weinberg, *The Quantum Theory of Fields II. Modern Applications*. Cambridge University Press. **1995**.
[18] Bing-Lin Yong, *Introduction to Field Theory*. Science Press. **1987**.
[19]Yi-Fang Chang, *European Journal of Applied Sciences*. 8(**2020**)5:28.
[20]Yi-Fang Chang, *International Journal of Modern Theoretical Physics*. 11(**2022**):1.
[21]Yi-Fang Chang, *Hadronic J.* 46(**2023**):97.
[22] R.M. Santilli, *Hadronic J.* 1(**1978**): 223.
[23] C.N. Ktorides, H.C. Myung and R.M. Santilli, *Phys.Rev.* D22(**1980**): 892.

[24] Yi-Fang Chang, *Hadronic J*. 7(**1984**): 1118.
[25] Yi-Fang Chang, *Hadronic J*. 7(**1984**): 1469.
[26] Yi-Fang Chang, *In Hadronic Mechanics and Nonpotential Interactions*, Par2. H.C. Myung, Ed. Nova Science Publishers, Inc. **1992**. 169.
[27] Yi-Fang Chang, *Hadronic J*. 22(**1999**): 257.
[28] Yi-Fang Chang, *International Review of Physics*. 7(**2013**): 299.
[29]Yi-Fang Chang, *Hadronic J*. 43(**2020**):161.
[30] C.C. Bradley, C.A. Sackett, J.J. Tollett, et al., *Phys.Rev.Lett.* 75(**1995**): 1687.
[31] B. DeMarco and D.S. Jin, *Science*. 285(**1999**):1703.
[32] M. Olshanii, *Phys.Rev.Lett*. 81(**1998**):938
[33] M.D. Girardeau and E.M. Wright, *Phys.Rev.Lett*. 87(**2001**):210401.
[34] C.A. Rrgal, et al., *Phys.Rev.Lett*. 92(**2004**):040403.
[35] B. Paredes, et al., *Nature*. 429(**2004**):277.
[36] VIP Collaboration, S. Bartaluccia, S. Bertoluccia, M. Bragadireanuab, et al., *Phys.Lett.* B. 641(**2006**): 18.
[37] D. Pietreanu, S. Bartalucci, S. Bertolucci, et al., *International Journal of Modern Physics* A. 24(**2009**): 506.
[38] S. Bartalucci, S. Bertolucci, M. Bragadireanu, et al., *Foundations of Physics*. 40(**2000**): 765.
[39] C. Curceanu, S. Bartalucci, S. Bertolucci, et al., *International Journal of Quantum Information*. 9(**2011**)11:145.
[40] R. Chakraborty and D.A. Mazziotti, *Phys.Rev*. A 91(**2015**): 010101.
[41] N. Abgrall, I.J. Arnquist, F.T.A. Iii, et al., *Phys.Rev.Lett*. 118(**2016**): 161801
[42] H. Shi, E. Milotti, S. Bartalucci, et al., *The European Physical Journal* C. 78(**2018**): 319.
[43]Yi-Fang Chang, *International Journal of Modern Theoretical Physics*. 7(**2018**):16.
[44]Yi-Fang Chang, *International Journal of Modern Mathematical Sciences*. 11(**2014**):75.
[45] R.M. Santilli, *Hadronic J*. 4(**1981**):642.
[46] R. M. Santilli, Elements of Hadronic Mechanics, Ukraine Academy of Sciences, Kiev, Volume I (1995), Mathematical Foundations.
[47] R. M. Santilli, Elements of Hadronic Mechanics, Ukraine Academy of Sciences, Kiev, Volume II (1994), Theoretical Foundations.
[48] R. M. Santilli, Elements of Hadronic Mechanics, Ukraine Academy of Sciences, Kiev, Volume III (2016), Experimental verifications.
[49] R. M. Santilli, *Progress in Physics*. 19(**2023**):73.
[50]Yi-Fang Chang, *Hadronic J*. 44(**2021**):357.
[51] R.M. Santilli, *Hadronic J*. 8(**1985**): 36.

[52] R.M. Santilli, *Algebras, Groups and Geometries*. 10(**1993**): 273.
[53] R.M. Santilli, *Acta Applicandae Mathematicae* 50(**1998**): 177.
[54] R.M. Santilli, *Hadronic Mathematics, Mechanics and Chemistry*, Vol.s. I, II, III, IV, and V, International Academic Press. **2008.**
[55] R.M. Santilli, Ratio Mathematica. 38(2020)5.
[56] R.M. Santilli, Ratio Mathematica. 38(2020)71.
[57] R.M. Santilli, Ratio Mathematica. 38(2020)139.
[58] R.M. Santilli, Ratio Mathematica. 37(2019)5.
[59] R. Penrose, *J.Math.Phys*. 8(**1967**):345.
[60] R. Penrose and M.A.H. MacCallum, *Phys.Rep*. 6(**1972**):241.
[61] R. Penrose, *Int.J.Theor.Phys*. 1(**1968**):61.
[62] R. Penrose and W. Rindler, *Spinors and Space-time: Spinor and twistor methods in space-time geometry*. Vol. 2. Cambridge University Press. **1986.**
[63] R.Courant and F.John. *Introduction to Calculus and Analysis*. John Wiley and Sons, Inc. **1982**.
[64] Yi-Fang Chang, *International Journal of Physics and Applications*. 3(**2021**):25.
[65]Yi-Fang Chang, *Algebras, Groups, and Geometries*. 39(**2023**):113.
[66] L.E. Ballentine, *Quantum Mechanics: A Modern Development*. Singapore: World Scientific Publishing. **1998**.
[67]Yi-Fang Chang, *International Journal of Modern Applied Physics*. 10(**2020**):16.
[68]Yi-Fang Chang, *Hadronic J*. 44(**2021**):251.
[69]Yi-Fang Chang, *Hadronic J*. 44(**2021**):311.
[70]D. Perkins, D. *Particle Astrophysics* (Second Edition). Oxford University Press. **2003.**
[71]Yi-Fang Chang, *Hadronic J*. 40(**2017**):291.
[72]Yi-Fang Chang, *SCIREA Journal of Astronomy*. 5(**2023**):1.
[73]S. Weinberg, *The First Three Minutes*. Basic Books. **1988**.
[74]S. Weinberg, *Cosmology*. Oxford University Press. **2008**.
[75]R.P. Feynman, R.B. Leighton and M. Sands, *The Feynman Lectures on Physics*. V.3. Ch.21. Addison-Wesley Publishing Company. **1966**. 21-1.
[76]Yi-Fang Chang, *Publications of the Beijing Astronomical Observatory*. 16(**1990**):16.
[77]Yi-Fang Chang, *Physics Essays*. 15(**2002**):133.
[78]Yi-Fang Chang, *International Journal of Modern Mathematical Sciences*. 16(**2018**):148.
[79]B. Muller, J. Schukraft and B. Wyslouch, *Ann.Rev.Nucl.Part.Sci*. 62(**2012**):361.
[80]J. Casalderrey-Solana, H. Liu, D. Mateos, et al. arXiv:1101.0618.
[81]D. Zohar and I, Marshall, *The Quantum Society: Mind, Physics and a New Social Vision*. New York: Morrow. **1994**.

[82]E. Haven and A. Khrennikov, *Quantum Social Science*. Cambridge University Press. **2013**.
[83]A. Wendt, *Quantum Mind and Social Science: Unifying Physical and Social Ontology*. Cambridge University Press. **2015**.
[84]Yi-Fang Chang, *NeuroQuantology*. 10(**2012**):183.
[85]Yi-Fang Chang, *NeuroQuantology*. 12(**2014**):356.
[86]Yi-Fang Chang, *NeuroQuantology*. 13(**2015**):304.
[87]Yi-Fang Chang, *International Journal of Modern Social Sciences*. 2(**2013**):20.
[88]Yi-Fang Chang, *Sumerianz Journal of Social Science*. 6(**2023**):1.

HADRONIC JOURNAL 47, 31 - 48 (2024)
DOI 10.29083/HJ.47.01.2024/SC31

A DOZEN PARADOXES OF SPECIAL RELATIVITY

Libor Neumann

Prague, Czech Republic
libor.neumann@email.cz

Received February 10, 2024
Revised February 21, 2024

Abstract

In more than a dozen examples, the coordinate transformation known as the Special Relativity Theory is applied. The exact application of this transformation results in disagreement with generally known natural phenomena and with 5 experimentally verified laws of physics. At the same time, there is a disagreement with the first principle of Special Relativity Theory.

1 Introduction

In 1905, Albert Einstein published a paper "On the Electrodynamics of Moving Bodies" ("Zur Elektrodynamik bewegter Körper") [1], which is now known as the Special Relativity Theory (SRT). Today, this theory is accepted by the mainstream of physicists. Challenging this theory threatens the professional careers of physicists.

The mainstream physicists believe that there is ample experimental evidence for the validity of SRT. Nevertheless they continue to invest huge amounts of time and effort to validate relativity (special and general), e.g. LIGO [2].

The "twin paradox" is well known [3] and less well known is the "Bell spaceship paradox" [4].

Special isorelativity (SIR) - [5] which has been developed for the dynamics of extended particles contains paradoxes as well (see in particular Sect. 8 on).

2 SRT

First, let's quote the necessary parts of the text from the translated original SRT [6].

p. 41: **§2. On the Relativity of Lengths and Times**

"The following reflexions are based on the principle of relativity and on the principle of the constancy of velocity of light. These two principles we define as follows:

1. The laws by which the states of physical systems undergo change are not affected, whether these changes of state be referred to one or the other of two systems of co-ordinates in uniform translatory motion.

2. Any ray of light moves in the "stationary" system of co-ordinates with the determined velocity c, whether the ray is emitted by stationary or by a moving body."

p. 48: "so that the transformation equations which have been found become

$$\tau = \beta(t - vx/c^2)$$
$$\xi = \beta(x - vt)$$
$$\eta = y$$
$$\zeta = z$$

where

$$\beta = 1/\sqrt{1 - v^2/c^2}."$$

p. 48: **§4. Physical Meaning of the Equations Obtained in Respect to Moving Rigid Bodies and Moving Clocks**

"We envisage a rigid sphere of radius R, at rest relatively to the moving system k, and with its centre at the origin of co-ordinates of k. The equation of the surface of this sphere moving relatively to system K with velocity v is

$$\xi^2 + \eta^2 + \zeta^2 = R^2$$

The equation of this surface expresed in x,y,z at time $t=0$ is

$$\frac{x^2}{(\sqrt{(1 - v^2/c^2)})^2} + y^2 + z^2 = R^2$$

A rigid body which, measured in the state of rest, has the form of sphere, therefore has in a state of motion - viewed from stationary system - the form of an ellipsoid of revolution with axes

$$R\sqrt{(1 - v^2/c^2)}, R, R.$$

Thus, wheras the Y and Z dimensions of the sphere (and therefore of every rigid body of no matter what form) do not appear modified by the motion, the X dimension appears shortened in the ratio $1 : \sqrt{1 - v^2/c^2}$, i.e. the greater the value v, the greater the shortening."

p.49: "It is clear that the same results hold good of bodies at rest in the "stationary" system, viewed from a system in uniform motion."

From the described transformations of the coordinate system, we prepare relations for the transformation of the distance l between two points and time interval τ:

$l_\xi = \beta l_x$; $l_\eta = l_y$; $l_\zeta = l_z$; $\tau = \beta t$ where $\beta = 1/\sqrt{1 - v^2/c^2}$ - **(1)**

3 Alien Bob

To describe the implications of using SRT transformations, we use the example of a second coordinate system moving at v=*0.87c* in the ecliptic plane of the Earth. Thus β (or γ) = 0.5.

To illustrate, let us use the idea of an alien Bob moving towards (or away from) Earth at velocity v. It is irrelevant whether Bob has technology unknown to us or whether we use the idea of an alien Bob moving away from Earth at velocity v due to the expansion of the Universe.

3.1 Earth rotation effect

According to SRT, Bob sees, in accordance with [6] i.e. **(1)**, a rotational ellipsoid with an axis ratio of 1:2. The orientation of the flattening of the ellipsoid depends on the direction in which Bob is moving.

We know that the Earth rotates once every 24 hours, but the ellipsoid does not rotate, it is fixed in the direction of Bob's movement.

3.2 Elevator on the equator

In areas on the equator, e.g. in Ecuador, everything moves up and down during the day. Like being in a huge elevator. It moves away from the center of the Earth and moves closer again. This is repeated twice a day.

The size of the movement is remarkable. The height difference (the difference in the distance between the surface of the Earth and the center of the Earth) is more than 3,000km.

The maximum speed of upward movement is 825km/h, i.e. the height of 93 Mount Everests per hour, that means the rise to the height of Mount Everest measured from sea level to the top in less than 39 seconds.

And then fall back down at the same speed. And this is repeated every 12 hours. It is noteworthy that the time when the ascent and descent occur does not depend on anything on Earth, but depends on the direction of movement of the coordinate system, that is, the direction of movement of the alien Bob.

It is also remarkable that the air pressure does not change during such movement, so there is no risk of mountain sickness like on Mount Everest. At the same time, the height difference is 360 times greater than the height of Mount Everest.

It is remarkable that all rocks shrink and expand again even at great depths without mechanical damage. Reducing the height of a granite or limestone massif by half and then increasing it to its original height without cracking the granite or limestone is incredible.

3.3 The orbit of the Earth around the Sun

Alien Bob also tracks the Earth's orbit around the Sun. It is not almost circular in his coordinate system as we know it, but elliptical. At first glance, this is nothing extraordinary, the planets move in elliptical orbits.

It is noteworthy that the orientation of the ellipse, i.e. the direction of their axes, is not related to the movement of the Earth or something from the Solar System, but depends on the direction of movement of the coordinate system, i.e. the direction of movement of the alien Bob.

Another oddity is the fact that the Sun is not in one of the foci of the ellipse, as it should be according to Kepler's 1st law, but is in the center of the ellipse.

The eccentricity of the ellipse $e = \sqrt{a^2 - b^2}$ where a=*1au*, b=*0.5au* is e=*0.87au*. This is the distance of the focus of the ellipse from the center of the ellipse. Because $1au \approx 150\, mil.\, km$. So the Sun is about 130 million km away from where it should be according to Kepler's 1st law.

Also, the area described by the Earth's line segment is not constant. It differs by more than 20% 4 times a year, so the movement of the Earth does not coincide with Kepler's 2nd law.

Analysis of the measured speed and acceleration of the Earth's elliptical orbit brings another surprise.

The speed of the Earth's movement changes in a ratio of 1:2 2 times per year, i.e. 2x per one revolution of the Earth around the Sun. This is 2 times more often than is measured for bodies observed from Earth moving in elliptical orbits.

Also noteworthy is the centripetal acceleration calculated from the curvature of the Earth's trajectory. The acceleration drops to $\frac{1}{2}$of the maximum value twice a year, precisely at the point when the Earth is closest to the Sun. The maximum curvature of the Earth's trajectory is when the Earth is farthest from the Sun. This contradicts at least Newton's law of gravity.

According to the law of gravity, the gravitational force should be 4 times greater when the Earth is closest to the Sun than when it is farthest from the Sun. The curvature of the trajectory should be proportional to the gravitational force. Thus, according to Newton's laws, the curvature of the Earth's trajectory should be greatest at the time when the Earth is closest to the Sun.

3.4 The train effect

For trains traveling on the east-west track in the equatorial region, two effects occur (2 times a day).The wagons and the people in the wagons are reduced to half their height. Twice a day, the distances between stations are halved and at the same time the tracks are shortened (including the shortening of the distances between track connectors and between sleepers).

For trains traveling on the north-south line, the effect of changing the track gauge occurs twice a day. So the tracks will approach each other at half the distance. At the same time, the length of the sleepers and the length of the axles of the wagons and locomotives also change. So a normal train becomes a narrow-gauge train twice a day.

3.5 Subway effect

In the case of the subway (metro) line in the east-west direction, the height of the tunnel is reduced twice a day. At the same time, the height of the subway train, the height of the people in the subway, and the height of the seats in the carriages are also reduced. At the equator it is halved, at higher

latitudes less. In London or Paris it is only about a third.

In the case of the metro line in the north-south direction, the gauge of the tracks changes twice a day, the width of the tunnel and also the width of the metro carriages also change at the same time. In them, the width of the seats located perpendicular to the direction of travel changes, and the width of the seats located along the walls of the wagons does not change.

Passenger dimensions also change. Either nose size or shoulder width.

3.6 Bridges effect

Bridges are lowered and raised again twice a day. The height of the bridges is changing, including the height of the support columns. These change the more the higher they are. Although the support columns of different heights change differently, the bridge remains straight.

If the bridge supports are made of concrete, they shorten and then lengthen without damaging the concrete.

In addition, the bridges in the east-west direction change their length twice a day. Unlike bridges in the north-south direction, which change their width. In all cases, this is without damage to the material of the bridges and without external forces.

E.g. Great concrete bridge in China [7], length 721m, length of the main field 445m, height above the valley 295m. Orientation east-west, position 25°N. Twice a day, the concrete arch of the bridge lowers by approx. 135m and then rises again, while the ends of the arch come closer by more than 220m. Although the bridge is made of concrete, it will not be damaged during such huge changes in dimensions. The deep valley over which the bridge leads does the same.

3.7 Buildings effect

Buildings also change their height twice a day, including lowering the ceilings and lowering the height of their residents.

At the same time, buildings change their width or length twice a day. Windows in the south or north facade change their width and height, unlike

windows in the east or west facade/wall, which change their height and glass thickness.

And that twice a day and without damaging the glass or frames. E.g. a window in a house in the equatorial area with dimensions of 2x2m in the south facade will decrease in height by 1m twice a day and narrow by 1m twice a day. And without damaging the glass or frames.

E.g. the tallest building in the world, Burj Khalifa, 828m high, lowers twice a day and rises again by more than 350m without any damage. The relatively smaller reduction is a result of the building's off-equatorial location.

3.8 Ship effect

Ships change draft (and height) twice a day, including large seagoing ships. The height of the locks and the depth of the canals (e.g. Panama, Suez) are changing. During handling in the port, the behavior of ships changes twice a day.

Twice a day, when the ship is turned by 90°, the ship shortens and widens or, on the contrary, lengthens and narrows. The draft does not change.

2 times a day it will decrease (including reducing the draft) and it will not change either length or width when rotated.

For example, the passenger ship Oasis of the Seas [8], which has a length of 360m, a width of 60m and a draft of 9m.

This ship will shorten by 180m or narrow by 30m at the equator depending on the turn of the ship. The draft changes twice a day by 4.5m.

3.9 Carousel effect

People sit on the carousel and it spins. Twice a day, the situation occurs that the skull of each person on the carousel is deformed at each revolution, so that during one revolution of the carousel, it narrows twice and widens twice, and also shortens twice and lengthens twice.

So, for example, on the carousel near the equator, during one rotation of the carousel, the skull, including the eyes, is halved twice, and the length of the skull, including the nose, is preserved. This alternates with a situation

where the width of the eyes and skull is normal, but the length of the skull is halved, the nose is halved, and the eye sockets are shallower and the eyeballs are flattened.

This is replaced in 6 hours by a situation where the width and length of the passengers' skull does not change when the carousel rotates, but is deformed from above, i.e. it is half the height of the forehead, half the height of the eyes, half the teeth.

3.10 The effect of high-voltage distribution systems

Let's observe the transmission routes of high-voltage power lines in the east-west direction.

Twice a day the columns will decrease and increase again. Twice a day the distance between the pillars is shortened and increased again.

When the columns get closer to each other, the wires will not sag more, but the opposite. The lowest point is higher than when the columns are further apart. The length and also the shape of the wires changes. When the columns are closest to each other, the cross-section of the conductors is circular, when they are farthest from each other, the conductors are flattened with an elliptical cross-section.

Let us recall that the resistance of a conductor is directly proportional to the length of the conductor and inversely proportional to the cross-section of the conductor, i.e. if the conductor is lengthened, its resistance will increase, if the cross-section is reduced, the resistance will also increase.

In the case of high-voltage lines near the equator, the situation is as follows. When the distance between the columns is halved, the length of each conductor is halved and thus the resistance drops by 50%.

In case of flattening of the conductor, i.e. in 6 hours after the shortening of the conductor, the cross-section will be reduced by half and thus the resistance will double.

This means that the resistance of the conductor changes twice a day in a ratio of 1:4.

The power loss in a conductor at constant current is directly proportional to the resistance of the conductor. So the power loss on the line conductors should change twice a day in a ratio of 1:4.

This ratio of resistances and therefore power loss depends on the speed of movement of the coordinate system, i.e. on the speed of movement of the alien Bob. The measuring instruments of the distribution network operator on Earth do not show this.

3.11 Glasses effect

Two people in the equatorial region have glasses, beautiful glasses with round frames. Bob observes what is happening with their glasses. One of them faces west and the other faces north.

For those who look to the west, the thickness of the glasses changes twice a day and thus the shape of the lens, which determines the optical parameters of the glasses (focal length / optical power - diopters). This alternates with a period when the shape of the frames, including the glass of the glasses, is deformed from circular to elliptical (recumbent ellipse). This is also reflected in the optical properties where the optical parameters of the glasses are different in different directions (cylindrical lens effects). Thus, the number of diopters of the glasses is reduced twice a day, and this alternates with the flattening of the frames and an increase in the optical power (increasing the number of diopters) depending on the direction (glasses with toric lenses compensating for astigmatism).

The glasses behave differently for those who look to the north. The shape of the frames changes from a lying ellipse to a standing ellipse. Four times a day, the frames of the glasses have a circular shape.

The thickness of the lens glass does not change. The optical properties of the glasses also change. The axis of the cylindrical component rotates by 90°(in steps four times a day). Cylindrical component in one direction increases, then decreases, axis changes, followed by growth and then decrease in the other axis and again direction change, increase and decrease...

Like the lens of glasses, the lens of the eye and the eye deform. When the optical power (number of diopters) of the glasses decreases, the optical power of the lens of the eye and the eye itself also decreases. Optical effects add up.

None of the users of the glasses subjectively noticed a change in the optical properties of the glasses.

3.12 Formula 1 races

Cars driving on a race track have interesting behavior. This depends on direction as well as time (due to the rotation of the Earth).

For example, let's look at what Bob observes while watching the famous 24 Hours of Le Mans race.

During the race, the shape of the cars on the east-west sections of the track changes from short with tall elliptical wheels to long and low with flat elliptical wheels.

On the north-south sections, low cars with flat wide wheels will change to narrow cars with narrow round wheels. The shape of the car and the wheels change when cornering because the direction of movement changes.

Let's take a closer look at the behavior of racing car wheels. That is, for spinning elliptical wheels. The car does not rattle as it should if the wheels were not circular. The ellipse does not rotate with the wheel. Only the wheel rotates and it deforms during rotation so that the flattening of the ellipse does not change direction.

It's easy to see if we look at the wheel valve. At maximum speeds, the wheels of the car rotate approximately 50 times per second. So the valve "circulates" the center (bearing) of the wheel 50 times per second. The wheel disc and tire are deformed 100 times in 1 second so that the valve moves closer to the center of the wheel and moves away again at exactly twice the wheel rotation speed. When the car drives slower, the valve approaches less often, when faster, more often. At the same time, the disc of a racing wheel is made of very high-quality and strong materials, which require enormous forces for such large deformations.

When Bob chooses a suitable spot on the Le Mans track, he can observe the effect of flattened (elliptical) wheels with a large flattening that occurs many times per second. And in the same place, the behavior changes during the race.

When Bob chooses one car and follows it around the circuit, he notices that both the car and its wheels are changing. In addition, the transformation also changes during the race.

A short car with tall elliptical wheels turns into a long car with flat elliptical wheels and also a narrow car with narrow round wheels.

And since the Le Mans circuit lies at 48° latitude, these effects do not have the same magnitude (length ratios).

3.13 Free fall effect

Bob observes a repeated free fall on the equator (e.g. in Ecuador) performed using a measuring device allowing the measurement of the free fall time from a height of 5m. From the measured values (fall length and fall time), Bob calculates the gravitational acceleration on Earth. They find that repeated free falls performed in the same location with the same equipment give different results.

At the moment when the measuring device is farthest from the center of the Earth, it observes a free fall from a height of 5m, which lasts according to Bob's clock $\Delta\tau = 0.505s$ and has a gravitational acceleration of $g = 39.2m/s^2$.

At the second moment, 6 hours after the first experiment, when the measuring device is closest to the center of the Earth, it finds that the fall from a height of 2.5m also takes $\Delta\tau = 0.505s$. The resulting acceleration is $g = 19.6m/s^2$.

Thus, the gravitational acceleration changes in a ratio of 1:2 2 times a day and is the largest at the place that is farthest from the center of the Earth, and the smallest gravitational acceleration is at the place when the measuring device is closest to the center of the Earth.

3.14 Pulley effect

The use of the pulley has an interesting effect on the rope that passes over the pulley. On the equator, a situation occurs twice a day when the rope leading over the pulley lengthens or shortens during movement.

When a rope is used that has marks on it that are equidistant from each other, and such a rope is guided over a pulley where it is almost horizontal on one side and vertical on the other (for example, when lowering and pulling a water bucket from a well), then the marks in the vertical part of the rope are closer together than in the horizontal part. When lowering, the marks on the rope that passed over the pulley get closer (the rope gets shorter).

On the contrary, when pulling out, the mark on the rope that passed over the pulley moves away. Both are without damage to the rope which is still taut. So the jack moves slower than the horizontal part of the rope moves.

3.15 Tides

Bob also observes the Moon and its orbit around the Earth. It is also elliptical with a semi-axis ratio of 1:2. The orientation of the flattening is the same as the flattening of the Earth and also the flattening of the Earth's orbit around the Sun.

According to Newton's law of gravity, the tides should respect this geometry of the motion of the Earth and the Moon. The maximum size of the tide occurs at the moment when the Moon is between the Sun and the Earth, that is, at the time of the new moon. Because the orbits of the Earth and the Moon are flattened, the distance of the Earth from the Sun and from the Moon at the time of new moon depends on the season.

The amplitude of tides is inversely proportional to the cube of the distance, according to Newton's law of gravity. Therefore, the height of the highest tide should change in a ratio of 1:8 twice a year. A period of low tide should alternate with a period of up to 8 times larger tide after about 3 months.

Because the position of the Earth in its orbit around the Sun changes at the same time, the influence of the Earth's flattening effect changes. At the time of the greatest approach, i.e. the greatest flattening, the height of the tide is also reduced on the equator to 1:2 due to the flattening. In Canada, the effect is smaller, so the height of the tide should be only 5.6 times greater.

Additionally, there is a length contraction effect that applies to a partial extent. So overall only 4x bigger.

The highest measured tide is in Neah Bay, Nova Scotia, Canada [9], it has a size of about 11.5m.

Due to the flattening of the Earth's orbit and the Moon's orbit, according to Newton's law of gravity, a situation should occur twice a year that Bob will measure the height of the tide at about 11.5m and twice a year he

should measure the tide with a level difference of over 45m.

It is noteworthy that the effect of buildings also occurs at the same time, i.e. the maximum tide according to Newton's law of gravity is greater than a building 60m high. Because even the height of the building observed by Bob will decrease.

This is not the case when Bob measures the sea level difference of Neah Bay so he measures the tide height in the range of 8.1 to 11.5m. At the same time, paradoxically, it will measure the maximum height of the tide at the time when the Moon and the Sun are farthest from the Earth and the minimum at the time when they are closest to the Earth. This is another contradiction to Newton's law of gravity.

3.16 The effect of the definition of the physical unit of distance

In the history of physics, the distance unit meter has been defined in different physical ways:

- 1791 - ten-millionth of the earth's quadrant
- 1799 - 1960 - the distance between the lines of the reference bar
- 1960 -1983 - a multiple of the wavelength of krypton radiation
- 1983 - fraction of the speed of light (distance in 1s).

Let us analyze the properties of these definitions.

3.16.1 Earth Quadrant

The circumference of an ellipse with an eccentricity corresponding to Bob's speed is 0.77 times smaller than the circumference of a circle. Thus, the length of a meter according to the definition from 1791 will be 0.77 less and therefore all distances measured by this shorter meter will be 1.3 times larger.

As the Earth rotates, the length of the meridian changes. The meridian in the direction of Bob will be shortened, the perpendicular meridian will

remain unchanged. The length of the meridian will change twice a day, so the length of the distance unit will also change twice a day. And therefore the distances measured by this variable reference meter will also change twice a day.

3.16.2 The distance of the lines of the standard

The length of the standard will change depending on the direction and the time. Since the standard of the meter shortens as well as the dimensions of the objects measured by it, the numerical values of the distances come out unchanged. And therefore the length contraction by SRT will not be measurable.

3.16.3 Wavelength of light

There are two possible interpretations of the application of SRT transformations to the wavelength of light.

It is a distance and thus distance transformations are applied. This means that the wavelength depends on the direction of the beam. This will change with time due to the rotation of the Earth. So the light will change its color (wavelength) and the effects will be the same as in the case of lines on the standard.

The second interpretation is that the wavelength of light is given by the relation $\lambda = c/f$ where f is the frequency of the light, i.e. $f = 1/T_0$ where T_0 is the period of oscillation.

Time is transformed by SRT and c is constant. Time transformation is independent of direction.

In this case, Bob measures half the period of the oscillation and therefore twice the frequency. Therefore, the wavelength of light is halved regardless of direction.

This means that the effect of length contraction in the direction of movement will numerically be zero, the numerical value of the distance will be the same, thus contradicting SRT. On the contrary, the distances measured in the perpendicular direction will be numerically doubled, i.e. also contrary to SRT.

3.16.4 The speed of light

According to the SRT axiom, the speed of light is constant in all coordinate systems.

Time transforms. Time transformation does not depend on the direction of movement of the coordinate system. The distance transformation is dependent on the direction of movement.

Light travels 300 thousand km in 1s in the direction perpendicular to Bob's motion. Bob will measure a time of 0.5s, i.e. the length of the meter in Bob's coordinate system will be 2m. This means that the distances measured with such a meter will be halved, i.e. contrary to SRT.

Light travels 300 thousand km in 1s also in the direction of Bob's movement. Bob measures a time of 0.5s, and at the same time measures a distance of 150 thousand km. So the length of the meter in Bob's coordinate system will be 1m. So the distances measured with this meter will be in agreement with the SRT.

The length of a unit of distance depends on the direction and therefore also on time due to the rotation of the Earth.

3.16.5 Summary

Thus, all definitions of meter used in history, except for one variant of the interpretation, have the physical effect of the time dependence of the reference. That is, the time dependence of all measured distances using a physical unit defined in this way.

The only exception is the interpretation based on the frequency of the reference light source. In this case, the length of the reference is independent of the direction and therefore of the rotation of the Earth. In this case, the length of the reference meter depends on the speed of movement of the coordinate system. In this case, the numerical values of the measured distances will contradict the SRT regardless of the direction.

4 Alien Alice

The alien Alice, unlike Bob, moves at a speed of $v = 0.44\ c$, i.e. roughly half the speed of Bob. It also moves in the plane of the Earth's ecliptic. For Alice, β or $\gamma = 0.9$.

In Alice's coordinate system, all the described effects are visible as in Bob's coordinate system, except that the numerical values are significantly different.

For example, the maximum speed of upward movement due to the Earth's rotation is 165km/h at the equator. That's 5x slower than Bob observes.

The eccentricity of the Earth's orbit is 0.14 and thus 6 times smaller. The ratio of resistances of distribution network conductors is only 4:5, i.e. roughly 13 times smaller. A concrete bridge in China lowers "only" by about 30m, the passenger ship Oasis of the Seas changes its draft by less than a meter. In both cases, 5 times less.

Gravitational acceleration calculated from free fall experiments from data measured by Alice is 3.2x smaller than from data measured by Bob.

When Alice communicates with Bob and they share the results of their observations, they discover that they are observing the same effects but the measured values are many times different, i.e. as if different physical laws work for different observers on Earth.

Therefore, together they compile a table of contradictions of observed effects with experimentally verified physical laws. They find that the following laws of physics are violated:

1. 1st and 2nd Kerpler's law
2. Newton's law of gravity
3. Laws of strength and elasticity, including Hooke's law
4. Ohm's law
5. Laws of classical (geometric) optics

This means that the 1st SRT principle is not fulfilled

5 Conclusion

SRT coordinate transformations violate the first principle of SRT. SRT contradicts at least five experimentally verified laws of physics and practical experience of earthlings.

6 Acknowledgement

Many thanks go to my family, especially my wife Světla. The contribution could not be made without tolerance and support. I also thank Prof. Jan Rak for his support

References

[1] A. Einstein, *Zur Elektrodynamik bewegter Körper*, Annalen der Physik, 17, 1905

[2] Laser Interferometer Gravitational-Wave Observatory (LIGO), https://cs.wikipedia.org/wiki/LIGO.

[3] Twin paradox, https://en.wikipedia.org/wiki/Twin_paradox

[4] Bell spaceship paradox, https://en.wikipedia.org/wiki/Bell%27s_spaceship_paradox

[5] R. M. Santilli, *Overview of historical and recent verifications of the Einstein-Podolsky-Rosen argument and their applications to physics, chemistry and biology,* APAV - Accademia Piceno Aprutina dei Velati, Pescara, Italy (2021), http://www.santilli-foundation.org/epr-overview-2021.pdf

[6] A. Einstein, *On the Electrodynamics of Moving Bodies, The Principle of Relativity,* A collection of original memoirs on the special and general theory of relativity, Dover Publications, Inc., 2017, ISBN: 978-0-486-60081-9, pp. 37-65

[7] Qinglong Railway Bridge, China, https://en.wikipedia.org/wiki/Qinglong_Railway_Bridge

[8] Oasis of the Seas, https://en.wikipedia.org/wiki/Oasis_of_the_Seas

[9] NOAA, Where is the highest tide?, https://oceanservice.noaa.gov/facts/highesttide.html

HADRONIC JOURNAL 47, 49 - 88 (2024)
DOI 10.29083/HJ.47.01.2024/SC49

WORK PRODUCTION BY THERMODYNAMICALLY-REVERSIBLE, IDEAL-GAS REACTIONS IN A VAN'T HOFF CHEMICAL-POTENTIAL ENGINE

José C. Ìñiguez

Independent Researcher
1227 21st Street, Douglas, AZ 85607
iniguezjosec@outlook.com

Received February 9, 2024
Revised February 24, 2024

Abstract

Once a number of fundamental thermodynamic notions associated to a reversible, ideal-gas phase chemical reaction were determined, among them the equation for its path, the equation for its driving force, and via this last one, the equation quantifying its work output at any given point along its unfolding, we proceeded to study in detail the occurrence of this reaction in a van't Hoff equilibrium box. The results obtained not only evinced the similarity existing between the way work is produced in both, the van't Hoff equilibrium box and Carnot's heat engine, but also the fact that like the latter, the former is also a cyclical process. The fundamental difference between the two being that while in Carnot's engine work is produced out of the heat transferred from a hotter to a colder heat reservoir, in van't Hoff's work comes out of the transfer of chemical matter between two different chemical states described by chemical potentials.

1. Introduction: The system of interest and its associated thermodynamic data.

The arguments to be here presented will be centered on the following thermodynamically-reversible, stoichiometric, isothermal, and isobaric chemical reaction taking place in the ideal-gas phase:

$$1\ \text{Butane (ideal gas, 1 bar, 298.15 K)} = 1\ \text{Isobutane (ideal gas, 1 bar, 298.15 K)} \quad (1)$$

For the purposes of this discussion reversible is any process which in concatenation with its inverse restores the condition existing before any change had taken place, the so-called initial condition.

In the thermodynamic analysis of reaction (1) performed in the first six sections of this paper, the reaction system, namely pure butane at the initial state, pure isobutane at complete conversion, and any intermediate reaction mixture constitutes the system. The surroundings are constituted by a heat bath, in charge of maintaining the system's isothermal condition, and a mechanical or work reservoir acting as depository or supplier of the work either produced or demanded by the reaction system. These three bodies constitute the universe of the process. Serves to note that on reason of it taking place without change in total mole number, isothermal and isobaric reaction (1) is also isochoric, that is, it also evolves at constant volume. The relevant thermodynamic properties for this reaction are given in Tables 1, and 2.

Substance	ΔH_f^o	ΔS_f^o	ΔG_f^o
butane	-126.1476	-0.3657	-17.1141
isobutane	-134.516	-0.3812	-20.8612

Table 1 Relevant standard thermodynamic data for butane and isobutane at 298.15 K (Stull et al., 1969, pp. 209, 245). ΔS_f^o stands for the standard molar entropy of formation in kJ K^{-1} mol^{-1}, with ΔH_f^o and ΔG_f^o respectively representing the standard molar enthalpies, and standard molar Gibbs energies of formation, both in kJ mol^{-1}.

Reaction	ΔH^o kJ mol^{-1}	ΔS^o kJ K^{-1} mol^{-1}	ΔG^o kJ mol^{-1}
butane → isobutane	-8.3684	-0.0155	-3.7471

Table 2. Standard enthalpy, entropy, and Gibbs energy changes for reaction (1) per mole of reaction. These values were obtained as the difference of the corresponding enthalpies, entropies, and Gibbs energies of formation of isobutane minus those of butane given in Table 1.

2. The chemical potentials and the chemical force

The Gibbs energy change for a homogeneous, closed system capable of undergoing changes in composition, can be written as follows:

$$dG = VdP - SdT - dW \qquad (2)$$

The previous equation can be obtained from the combination of the defining equations for the internal energy $dU = TdS - PdV - dW$; enthalpy $dH = dU + PdV + VdP$; and Gibbs energy $dG = dH - TdS - SdT$.

In eq. (2) dW represents work different from the work of displacement PdV, that is, different from:

> … the work done by the system in displacing its environment at the steady pressure P… (dW) is the chemical work … a form of work which can be done by a system in the absence of any change of volume and due to its change of composition …and which can be attained by use of the van't Hoff equilibrium box or the galvanic cell." (Denbigh, pp. 68, 81)

If the evolution of the system is isobaric and isothermal, then eq. (2) takes the following form:

$$-dG = dW \qquad (3)$$

It is on reason of the state function nature of the Gibbs energy that the previous equation applies to both, the reversible as well as the irreversible transit of the system between identical initial and final states:

$$-dG = dW_{rev} = dW_{lost} \qquad (4)$$

Or, equivalently

$$-\Delta G = W_{rev} = W_{lost} \qquad (5)$$

Equations (4) and (5) make clear the fact that for isothermal and isobaric processes the Gibbs energy change represents the work transferred to the mechanical reservoir along the reversible path (W_{rev}), as well as the dissipated work-producing potential (W_{lost}) transferred in the form of heat to the heat reservoir along the irreversible path:

> The change in G is, of course, the same for the same initial and final states of the reaction system, whether the process is conducted reversibly or not. It is the output of work which varies … (Denbigh, p. 76)
>
> A system undergoing change can perform maximum work only when the change is carried out reversibly. If the process is not completely reversible, the amount of work obtainable is always below the maximum, the difference appearing as heat. (Maron & Prutton, p. 189)

If the system under consideration turns out to be a homogeneous mixture of two components, α and β, then the following equation, making explicit the dependence of its Gibbs energy from temperature, pressure, and composition, also applies:

$$G = G(T, P, n_\alpha, n_\beta) \qquad (6)$$

In what follows α is to be an alternative descriptor of butane, and β of isobutane, as they appear in reaction (1).

The total differential of eq. (6) has been written below:

$$dG = (\partial G/\partial T)_{P,n_i} dT + (\partial G/\partial P)_{T,n_i} dP + \sum_i (\partial G/\partial n_i)_{T,P,n_j} dn_i \qquad (7)$$

The usual provisos apply regarding the n_i and n_j constraints appearing in the partial derivatives of the previous equation.

For a constant temperature and pressure evolution of the reaction system, the previous equation reduces to:

$$dG = \sum_i (\partial G/\partial n_i)_{T,P,n_j} dn_i \qquad (8)$$

The comparison of equations (8) and (3) allows us to write:

$$dG = -dW = \sum_i (\partial G/\partial n_i)_{T,P,n_j} dn_i \qquad (9)$$

The partial derivatives appearing on the right-hand side of equations (8) and (9), of capital importance in the thermodynamic theory of spontaneity, chemical, and phase equilibrium, are also represented in the following simpler manner:

$$\mu_i = (\partial G/\partial n_i)_{P,T,n_j} \qquad (10)$$

This intensive quantity μ_i, with units of energy/mole, is the chemical potential of species i in the reaction mixture. As such, its value is dependent on the pressure, temperature, and composition of the said mixture.

The chemical potential of component i can be interpreted as the amount by which the capacity of the reaction mixture for doing work (other than work of expansion) increases per mole of i added at constant temperature, pressure, and composition. The following example provided by Denbigh might serve to make its meaning clearer:

> ...the chemical potential of copper sulphate in its acqueous solution in a Daniel cell is equal to the increased capacity of the cell to provide electrical energy, per mole of copper sulphate added (the addition actually being an infinitesimal). (Denbigh, p. 79)

Even if the 'infinitesimal addition' referred above by Denbigh is a way of satisfying the constant composition constraint implicit in eq. (10), a more sensible way to this end would have consisted in adding a small fraction of a mole of copper sulphate to a finite quantity of solution followed by the calculation of the proportionate increase per mol. "If (this) is done, for strict accuracy one must pass to the limit of $(\Delta G_i/\Delta n_i)$, as Δn_i approaches zero for the substance in question. The limit of this ratio, however, is exactly μ_i: $\mu_i = \lim_{\Delta n_i \to 0} (\Delta G_i/\Delta n_i)$" (Aston &Fritz, p. 89; The quote includes minor changes in notation.)

In terms of the chemical potential, the following equivalent expressions for equations (8) and (9) will be written:

$$dG = \sum_i \mu_i \, dn_i \qquad (11)$$

$$dW = -\sum_i \mu_i \, dn_i \qquad (12)$$

Let us now bring here the thermodynamic variable known as the degree of advancement, or reaction coordinate ξ, defined as follows (Moore, pp. 283-284):

$$\xi = \frac{\Delta n_i}{\nu_i} \text{ mol} \qquad (13)$$

In the previous equation Δn_i represents the change in number of moles experienced by chemical species i at the point at which ξ is being evaluated, with ν_i representing its unitless stoichiometric coefficient, negative for reactants, and positive for products. For reaction (1) it adopts the following forms:

$$\xi = \frac{\Delta n_i}{\nu_i} = \frac{n_\alpha - 1}{-1} = \frac{n_\beta - 0}{1} \qquad (14)$$

From the previous expressions we get:

$$n_\alpha = 1 - \xi\,, \quad n_\beta = \xi \qquad (15)$$

The fact that the total number of moles is equal to one:

$$n_\alpha + n_\beta = 1 - \xi + \xi = 1 \qquad (16)$$

allows us to realize that the mole fractions (y_i) of these chemical species in the reaction mixture, as well as their respective partial pressures (p_i) in it, this on reason of the total pressure being equal to 1 bar, are numerically identical to their respective number of moles, as given by eq. (15), i.e.,

$$n_\alpha = y_\alpha = p_\alpha = 1 - \xi\,, \quad n_\beta = y_\beta = p_\beta = \xi \qquad (17)$$

The corresponding differential expression for eq. (13) is given below:

$$dn_i = \nu_i d\xi \qquad (18)$$

The substitution of eq. (18) in eq. (12) leads to:

$$dW = \left(-\sum_i \nu_i \mu_i \right) d\xi \qquad (19)$$

In terms of the definition of work, thermodynamic or otherwise, as the product of force times displacement (Klotz & Rosenberg, p. 45), we can express dW as follows:

$$dW = \text{chemical force x reaction's displacement} = f\, d\xi \qquad (20)$$

A simple comparison between equations (19) and (20) allows us to identify the chemical force as the expression between parenthesis in eq. (19), i.e.,

$$f = -\sum_i \nu_i \mu_i \qquad (21)$$

When the properly signed stoichiometric coefficients $\nu_\alpha = -1$ and $\nu_\beta = 1$ for reaction (1) are substituted in eq. (21), we get:

$$dW = \left(1\mu_\alpha - 1\mu_\beta\right) d\xi \qquad (22)$$

The previous equation permits writing the following expression for the chemical force driving reaction 1 Butane → 1 Isobutane:

$$f = 1\mu_\alpha - 1\mu_\beta \qquad (23)$$

The following equation, coming out of the combination of equations (20) and (22), can now be written for reaction (1):

$$dW = \left(1\mu_\alpha - 1\mu_\beta\right) d\xi = f d\xi \quad (24)$$

The fact that $d\xi$ is, by definition, a measure of the change in the number of moles of reactants and products allows us to bring here the interpretation provided by Brønstead of the dW term appearing in the previous equations, as "... the work associated to the transport of chemical matter between two different chemical states described by chemical potentials." (Gill, p, 507)

The following statement of Maron & Prutton (p. 189, italics are ours), asserting that:

> Work results only when the tendency of systems to attain equilibrium is harnessed in some way. *From a system in equilibrium no work can be obtained*, but a system in its way to equilibrium may be made to yield useful work.

will be given here the following representation:

$$\left(\frac{dW}{d\xi}\right)_{eq} = 0 \qquad (25)$$

Combination of equation (25) with eq. (24) leads us to:

$$\left(\frac{dW}{d\xi}\right)_{eq} = 1\mu_{\alpha,eq} - 1\mu_{\beta,eq} = f_{eq} = 0 \qquad (26)$$

The previous result allows us to trace this $(dW/d\xi)_{eq} = 0$ characteristic of a reaction in equilibrium to an even more fundamental condition: the fact that at this point the chemical force f —and with it the difference in chemical potentials it represents— is equal to zero, i.e.,

$$f_{eq} = 1\mu_{\alpha,eq} - 1\mu_{\beta,eq} = 0 \qquad (27)$$

Once the chemical force has been re-expressed as a function of ξ, then the work associated, say, to the transit $(0 \rightarrow \xi)$ of the reaction system, can be evaluated via the following integral:

$$Work = \int_0^{\xi} f(\xi) d\xi \qquad (28)$$

3. Thermodynamic work

Work, says J. C. Maxwell (p. 54), *"...is the act of producing a change of configuration in a system in opposition to a force which resists that change."*

Regarding the work of expansion of a gas, the fact that "... for a given expansion the work performed depends upon the external pressure resisting the expansion...," makes it necessary to distinguish the (internal) pressure of the gas, P, from the external one, P_{ex}. "In order that an expansion may occur, the internal pressure, must, of course, be greater than the external, but this difference may be made as small as is desired, and as a limit we may consider the case in which the internal pressure is equal to the external pressure or differs from it by a negligible amount." The work produced under this condition is the reversible work. (Quotes from Pitzer and Brewer, p.35)

In general, while the work of expansion can be represented as $W = \int P_{ex} dV$; the reversible work, on its part, takes the following form $W_{rev} = \int P(V) dV$.

The previous statements require the following clarification:

While thermodynamics cannot do away with the infinitesimal difference between driving and resisting forces in reversible processes —making them equal makes the process impossible; mathematics certainly can, this on reason of the fact that the numerical results obtained with one or the other are for all practical purposes, identical.

This seems the proper place state that reversible processes are ideal, that is, practically impossible processes, and this is on reason of the impossibility of achieving an infinitesimal difference between driving and resisting forces. It is not uncommon to find the impossibility of reversible processes also defined in the following manner: "Strictly speaking, all reversible processes are impossible in nature, as they would require an infinite time for their accomplishment." (Maron & Prutton, p. 110) Even if practically unrealizable, the fact that they represent the efficient limit to natural processes, makes of them an indispensable tool for the theoretical analysis of thermodynamic processes.

Now, the following words from Denbigh (p.78):

> The chemical potential has an important function analogous to temperature and pressure. A temperature difference determines the tendency of heat to pass from one body to another and a pressure difference determines the tendency towards bodily movement... a difference of chemical potential may be regarded as the cause of a chemical reaction or of the tendency of a substance to diffuse from one phase to another. The chemical potential is thus a kind of 'chemical pressure' and is an intensive property of a system, like the temperature and pressure themselves.

allows us to make a simile (with all the appropriate reservations) between the chemical force given above by eq. (21), and the internal pressure of the gas. The internal qualifier comes on reason of the fact that the chemical force finds definition in terms of the chemical potential of the substances constituting the reaction system; it is thus, as Denbigh notes, a property of the system, just like P is a property of the gas.

Just like the equation $W_{rev} = \int P(V)dV$ is used under the assumption that a pressure infinitesimally smaller than that of the gas is resisting the expansion, the same can be done with equation $W_{rev} = \int f(\xi)d\xi$ to evaluate the chemical work. This procedure de facto exempts us to provide any details as to the nature of this resisting force, or about the mode in which it performs its opposing or resisting role. Further comments on this issue in the discussion section. All we need to know to perform these integrations is knowledge of the functional relation connecting P and V in the former, and f with ξ in the latter. The interesting thing to be noted here is that even if f is the explanation for the occurrence of the reaction, and $f d\xi$ is the quantifier of its reversible work output, this pair plays, however, no role in the *actual* production of this work. As will be seen below, for chemical reactions taking place in the van' Hoff equilibrium box, this task, the actual production of work is carried on by the pair PdV. A similar thing happens in heat engines. While it is a temperature difference the one driving the flow of heat from the hot to the cold reservoir, work appears in the surroundings via the net result of two isothermal and reversible volume changes: one expansion, and one compression.

Even, if the work defined by the integral $W_{rev} = \int f(\xi)d\xi$ is, as made explicit by the '*rev*' subscript, reversible work, it also quantifies, for an irreversible transit between the same initial and final states, the work lost in it. Being this so, we will abstain from attaching any superscript to W.

4. The functional connection between chemical force and reaction extent or degree of advancement in reaction (1)

According to Denbigh (p. 115):

> … a gaseous mixture (is) said to be perfect if the chemical potential of each of its components is given by the following relation, in which μ_i^o *is a function of temperature only,*
>
> $$\mu_i = \mu_i^o + RT \ln P + RT \ln y_i$$
>
> Where P is the total gas pressure and y_i is the mole fraction of component i. Now, since μ_i^o is independent of composition it retains the same value when y_i is brought up to unity. It is thus precisely the … value of the Gibbs free energy per mole of the gas i in its pure state at unit pressure.
>
> This equation … can be put in a more compact form by means of the *partial pressure* p_i. Thus
>
> $$\mu_i = \mu_i^o + RT \ln p_i \qquad (29)$$

The combination of the previous equation with the relations established by eq. (17), allows us to write the chemical potentials of butane and isobutane, and the chemical force by them defined, as they all pertain to reaction (1), in the following manner:

$$\mu_\alpha = \mu_\alpha^o + RT \ln(1-\xi) \qquad (30)$$

$$\mu_\beta = \mu_\beta^o + RT \ln(\xi) \qquad (31)$$

$$f = 1[\mu_\alpha^o + RT \ln(1-\xi)] - 1[\mu_\beta^o + RT \ln(\xi)] \qquad (32)$$

After rearrangement and simplification, the previous equation becomes:

$$f = -\Delta\mu^o - RT \ln\left(\frac{\xi}{1-\xi}\right) \qquad (33)$$

Further replacement of $\Delta\mu^o$ for the standard Gibbs energy change of reaction (1), produces:

$$-f = \Delta G^o + RT \ln\left(\frac{\xi}{1-\xi}\right) \qquad (34)$$

In which case, and in accord with equations (4), (24), and (34), we can write the following equation:

$$dG = -dW = -f d\xi = \left[\Delta G^o + RT \ln\left(\frac{\xi}{1-\xi}\right)\right] d\xi \qquad (35)$$

Which can also be written as follows:

$$\frac{dG}{d\xi} = -\frac{dW}{d\xi} = \Delta G^o + RT \ln\left(\frac{\xi}{1-\xi}\right) \qquad (36)$$

Applying the equilibrium condition stated above in eq. (25), which given eq. (4) can also be expressed as $(\frac{dG}{d\xi})_{eq} = 0$, we obtain the well-known equation:

$$\Delta G^o = -RT \ln(\frac{\xi}{1-\xi})_{eq} = -RT \ln K \qquad (37)$$

While $(\frac{dW}{d\xi})_{eq} = 0$ expresses, on one side, that at the state of equilibrium, as the previous quote of Maron and Prutton states, no more work can be obtained from a reversible chemical reaction, nor dissipated by an irreversible one; the $(\frac{dG}{d\xi})_{eq} = 0$ condition identifies, on the other side, the state of equilibrium as the minimum of the graph $G - vs. -\xi$:

> The criterion of equilibrium for a system of prescribed temperature and pressure is that G has reached its minimum possible value. (Denbigh, p. 83)

5. Numerical values for the chemical potentials and the chemical force for reaction (1)

With $R = 8.314\ \text{JK}^{-1}\text{mol}^{-1}$ and the respective standard Gibbs energies of formation of butane, and isobutane at 298.15 K, namely $-17{,}114.1\ \text{Jmol}^{-1}$ and $-20{,}861.2\ \text{J mol}^{-1}$, we will have equations (30), (31), and (32) taking the following forms:

$$\mu_\alpha = -17{,}114.1 + 2478.8 \ln(1-\xi)\ \text{J mol}^{-1} \qquad (38)$$

$$\mu_\beta = -20{,}861.2 + 2478.8 \ln(\xi)\ \text{J mol}^{-1} \qquad (39)$$

$$f = 1\mu_\alpha - 1\mu_\beta = 3747.1 + 2478.8 \ln\left(\frac{\xi}{1-\xi}\right)\ \text{J mol}^{-1} \qquad (40)$$

The evolution of these magnitudes along the course of reaction (1) can be read from Table 3, constructed by the simple expedient of substituting a few selected values of ξ into each of the three equations given immediately above, and performing the indicated operations.

In column 1 of Table 3, $\xi_{eq} = 0.82$ was calculated by solving eq. (37) once $\Delta G^o = -3747.1\ \text{J mol}^{-1}$, and $RT = 2478.8\ \text{J mol}^{-1}$ were substituted in it.

The combination of equations (28) and (34) produces the following equation for the work associated to reaction (1):

$$W = \int -[\Delta G^o + RT \ln(\frac{\xi}{1-\xi})]\, d\xi \qquad (41)$$

Performance of the previous indefinite integral produces:

$$W = -\xi\, \Delta G^o - RT[\xi \ln(\xi) + (1-\xi)\ln(1-\xi)] - RT + C$$

The constant of integration C in the previous equation, evaluated with the known fact that at complete conversion, $\xi = 1$, it is true that $W = -\Delta G^o$, turns out to be equal to $C = RT$, in which case, we can write it in the following manner:

$$W = -\xi\, \Delta G^o - RT[\xi \ln(\xi) + (1-\xi)\ln(1-\xi)] \qquad (42)$$

The substitution in eq. (42) of the thermodynamic magnitudes there involved produce, in turn, the following equation:

$$W = 3747.1\, \xi - 2478.8\, [\xi \ln(\xi) + (1-\xi)\ln(1-\xi)] \qquad (43)$$

It was via the simple expedient of substituting in eq. (43) selected values for ξ, that the numbers for W appearing in columns 5 and 6 of Table 3 were obtained.

6. About the results consigned in Table 3

The results produced by equations (38), (39), and (40), for the chemical potentials of butane, isobutane, and for their difference, that is for the chemical force, at various degrees of advancement of reaction (1), are those respectively contained by columns 2, 3, and 4. In accord with their respective dependence of the concentration of butane and isobutane, we see μ_α decreasing, and μ_β increasing as the reaction progresses, up to that point, the state of chemical equilibrium, at which no more difference exists between them. In accord with these considerations, we see the chemical force transiting from an arbitrarily large magnitude at $\xi = 0$, to a value of zero at equilibrium. The work calculated with the previous equation, identical at every ξ with the negative of the corresponding Gibbs energy change, quantifies, as explained above, the work gained, that is the work available in the work reservoir at any given ξ along the reversible path, as well as the work lost at same degree of advancement, along the irreversible path. The numbers in column 5 corresponding to post-equilibrium $\xi's$, applying only to the reversible path, are smaller than those corresponding to $\xi_{eq} = 0.82$. The decrease obeys to the fact that work must be

removed from the work reservoir in order to be spent in forcing the system to go beyond its equilibrium condition, that is, into the region of conversions of isobutane larger than $\xi_{eq} = 0.82$. Concomitant to the decrease in the work available in the work reservoir, we find, on reason of this work being done in the system, an increase in its Gibbs energy. For example, the 63 J decrease in the content of the work reservoir, from 4241 J to 4178 J, spent in pushing the system along the transition $(\xi_{eq} = 0.82) \rightarrow (\xi = 0.9)$, appear as an increase in the system's Gibbs energy, from $-4241\,\mathrm{J}$ to $-4178\,\mathrm{J}$ J along the same transition.

ξ	$-1\,\mu_\alpha$	$-1\,\mu_\beta$	$f = \frac{-\partial \Delta G}{\partial \xi} = \frac{\partial W}{\partial \xi}$	$W = -\Delta G$	$W_j - W_i$
0.00	17114.1	∞	∞	0	0
0.10	17375.3	26568.8	9193.5	1180	1180
0.20	17667.2	24850.7	7183.5	1990	810
0.30	17998.2	23845.6	5847.4	2638	648
0.40	18380.3	23132.5	4752.2	3167	529
0.50	18832.3	22579.4	3747.1	3592	425
0.60	19385.4	22127.4	2742.0	3916	324
0.70	20098.5	21745.3	1646.8	4137	221
0.80	21103.6	21414.3	310.7	4238	101
$\xi_{eq} = 0.82$	21364.7	21353.1	≈ 0	4241	3
0.90	22821.7	21122.4	-1699.3	4178	-63
1.00	∞	20861.2	$-\infty$	3747	-431

Table 3. Column 1 in mol, Columns 2 through 4 in Joules/mol, and columns 5 and 6, in joules. The graphs of these numbers are shown in Figures 2 and 3.

That the numbers in column 5 for $\xi > \xi_{eq}$ do not apply to the irreversible path obeys to the fact that at no point along this path, including the state of chemical equilibrium, we find any work available in the work reservoir.

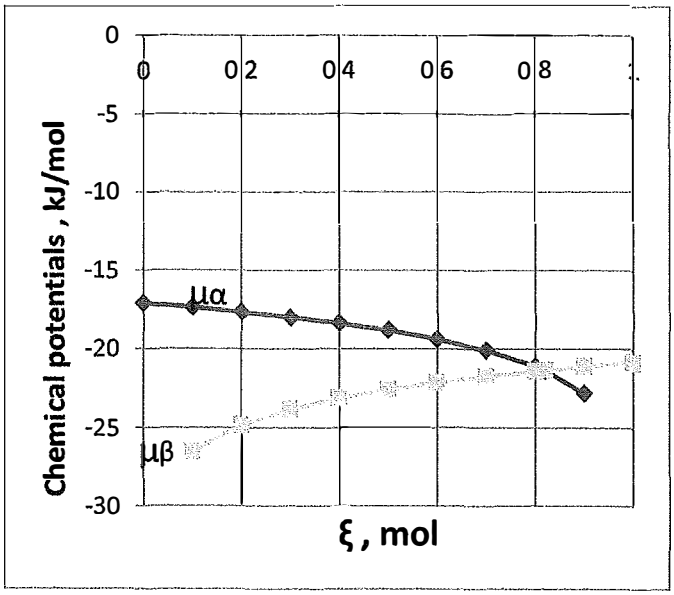

Figure 2 The chemical potentials of butane (α) and isobutane (β) vs. ξ.

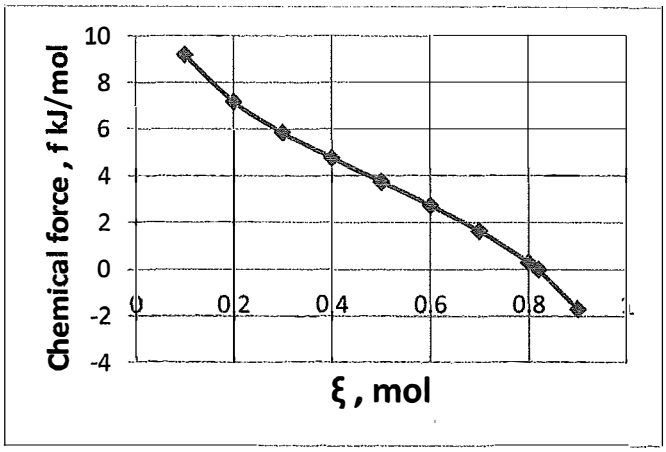

Figure 3 The chemical force f is positive for $\xi_{eq} < 0$, zero at $\xi_{eq} = 0.82$, and negative for $\xi_{eq} > 0$

It is this fact, the absence of available work in this irreversible universe, what makes any transit beyond the equilibrium condition, impossible. To make it happen we must re-define our universe to accommodate in it a new work-supplying body to carry on this task.

That the chemical force f is, as shown by equation (36), the instantaneous rate at which the work-producing potential of the reaction, as measured by ΔG, is being transformed into actual work along the reversible path, or dissipated into heat along the irreversible one, explains the heading of column 4.

The diminishing amounts of work produced (dissipated) as the reaction proceeds are the matter of the numbers in column 6. Thus, while the contribution of the transit from $(\xi = 0) \rightarrow (\xi = 0.1)$ amounts to 1180 J, the one from $(\xi = 0.1) \rightarrow (\xi = 0.2)$ reduces to 810 J; the one from $(\xi = 0.8) \rightarrow (\xi_{eq})$ only amounts to 3 J. This trend is a consequence of the fact that the value of the chemical force decreases as the reaction proceeds.

Let us now address the issue of how is it that the work producing potential of reaction (1) becomes gained work, that is, work available to us in a work reservoir.

7. A thermodynamically-reversible chemical reaction in the ideal gas-phase

7.1 The isomerization of butane into isobutane in the van't Hoff Equilibrium Box

The present section is a modified version of the one appearing in a previous paper by this author on a related subject (Íñiguez, 2014)

The detailed description of the mechanism through which the efficient conversion of the work producing potential of a chemical reaction into actual work takes place, will be done in what follows by studying the occurrence *at equilibrium* of reaction (1). The device in which this reaction is to take place, known as the van' Hoff equilibrium box (*EB*), has been represented in Figure 1.

The operation of the *EB* for different types of chemical reactions, namely homogeneous reactions in the gas phase, and heterogeneous solid-gas reactions, has been described with various degrees of detail by Kauzmann, pp. 291-297; Denbigh, pp. 72-74; Smith and Van Ness, pp. 409-410; Fermi, pp. 101-106, and Pauli, pp. 54-56. among others.

The salient features of a reaction occurring at equilibrium in a van't Hoff equilibrium box, are the following:

1) It will take place without the production of work; conclusion which in terms of our previous discussions, finds explanation in the fact that at equilibrium it is true that $f_{eq} = 0$, and if so, also true that $dW_{eq} = f_{eq} d\xi = 0$. For such a reaction, the expression of the first law, $\Delta U = Q - W$, reduces to $\Delta U = Q$, which means that all the energy released by the reaction ends up as heat in its heat bath. The bath will later exchange some of this energy with a number of isothermal and reversible volume changes involving reactants and products, for it to be transformed, via the action of the pair PV, into the thermodynamically predicted maximum possible amount of work.

2) The final result of the operation to be described of the equilibrium box, takes the form of a standard reaction as in it the reactants remaining and the products produced appear in their pure states, that is separate from one another, each at the standard pressure of 1 bar at the temperature of the reaction.

The thermodynamic analysis starts with the reaction box, designated as C_R in Figure 1, containing a *vast* amount of reaction (1) in chemical equilibrium at 298.15 K and 1 bar total pressure. It is to this equilibrium mixture that n moles, $0 < n \leq 1$, out of the initial mole of butane available for reaction (1), will be added, and n moles of isobutane removed. It is in this vast amount of reaction mixture in equilibrium where we will see the said n moles of butane (α) introduced in it, isomerized into n moles of isobutane (β). The $(1 - n)$ moles of α remaining and the n moles of β produced will be found at the end, separate of one another, and each of them at 1bar and temperature T.

The result of the four processes which described below, constitute van't Hoff's box mode of operation, can be represented as follows:

$$1\alpha\ (g, 1\ \text{bar}, T) \rightarrow [(1 - n)\alpha\ (g, 1\ \text{bar}, T)] + [n\beta\ (g, 1\text{bar}, T)] \qquad (44)$$

The brackets appearing in the right-hand side of the previous equation emphasize that these chemical species are found at the end of said four processes, separate from one another and at the indicated conditions.

Let us now center our attention on the situation depicted in Figure 1. In it C_α and C_β are cylinders fitted with weightless and frictionless pistons. The connection of the cylinders to the reaction box C_R includes valves V_α and V_β −initially closed− as well as semi-permeable membranes M_α and M_β; the former permeable only to ideal gas α; the latter only to ideal gas β. The reaction box C_R

contains a *vast amount of a mixture of gases α and β* at their respective equilibrium pressures $P_{\alpha,eq}$, $P_{\beta,eq}$, at temperature T, i.e., in C_R:

$$\alpha(P_{\alpha,eq}, T) = \beta(P_{\beta,eq}, T) \qquad (45)$$

The pressure inside the box is constant and equal to $P_{C_R} = P_{\alpha,eq} + P_{\beta,eq}$. The pistons have been properly coupled to a work or mechanical reservoir (*mr*) -not shown- whose function is to serve as deposit or provider of the work either produced or demanded by the operation. Initially, while cylinder α contains 1 mole of α at 1 bar and temperature T, cylinder β is empty, with its piston in its extreme leftmost position. At this point the pressures keeping these pistons in place are 1 bar, and $P_{\beta,eq}$, respectively. The equilibrium box is in thermal contact with a heat bath or heat reservoir (*bath*) –not shown- of temperature T.

Gases α and β in the cylinders, as well as their equilibrium mixture in the reaction box, constitute the thermodynamic system (*sys*); with the heat and mechanical reservoirs constituting the surroundings. Combined, system and surroundings constitute the universe of the process. The mechanical device constituted by reaction box, cylinders, pistons, valves, and semi-permeable membranes is called the *van't Hoff Equilibrium Box* (*EB*).

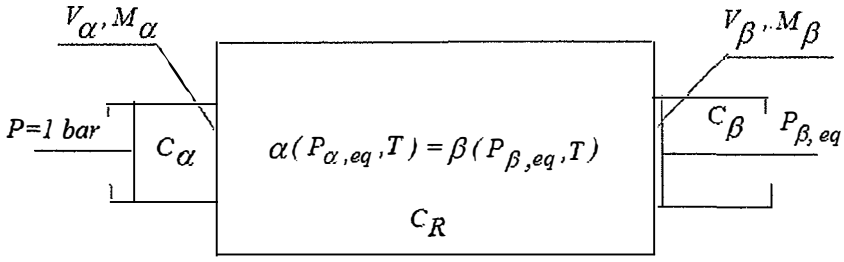

Figure 1. The van't Hoff Equilibrium Box.

The form of the first law to be here used to describe and quantify the energy exchanges of the system with its surroundings, is the following: $\Delta U = Q - W$. In it, heat absorbed, and work done by the system are positive magnitudes; their inverses, negative. It is understood that in the universe just described, the only bodies capable of exchanging heat are the heat bath and the system, in which case heat lost by one, is heat gained by the other. Likewise, the only bodies capable of exchanging energy in the form of work are the system and the work or mechanical reservoir, in which case, work done by one is work done on the

other. It will be further assumed that the reader is knowledgeable about the thermodynamics of ideal gases.

7.2. The four processes taking place in the van't Hoff equilibrium box

Process 1: The mole of gas α in cylinder C_α is expanded isothermally (T) and reversibly from 1 bar to $P_{\alpha,eq}$. At the end of this process the pressure keeping this piston in place is $P_{A,eq}$. In accordance with the isothermal nature of this process, and the sole dependence of the internal energy of ideal gases with the temperature, we will have:

$$\Delta U_{sys,1} = 0 \qquad (46)$$

As indicated by the form adopted by the first law for this process, namely $Q_{sys} = W_{sys}$, the reversible work transferred by the system to the work reservoir, comes from an equivalent amount of heat absorbed by it from the heat bath. It is with base on these considerations that the following equation will be written:

$$-Q_{bath,1} = Q_{sys,1} = W_{sys,1} = -W_{mr,1} = -nRT\ln(P_{\alpha,eq}) \qquad (47)$$

In it, the last term on the right-hand side quantifies, as should be known, the reversible work of expansion produced by the ideal gas in its transit from $P = 1$ to $P_{\alpha,eq}$. It should be noted that the argument of the logarithmic term in the previous expression is a quotient whose denominator, omitted here for reasons of economy of expression, is the unit valued initial pressure of the said expansion.

At the conclusion of this process both valves are opened for Process 2 to occur.

Process 2. Here n moles of gas $\alpha(P_{\alpha,eq}, T)$ are introduced into the reaction box, and n moles of gas $\beta(P_{\beta,eq}, T)$ simultaneously removed from it, $0 < n \leq 1$. The respective representations of these two processes, given below:

$$[n\mu_\alpha(p_{\alpha,eq}, T)]_{before\ adddition} = [n\mu_\alpha(p_{\alpha,eq}, T)]_{after\ addition}$$

$$[n\mu_\beta(p_{\beta,eq}, T)]_{before\ extraction} = [n\mu_\beta(p_{\beta,eq}, T)]_{after\ extraction}$$

allows us to realize that:

> Since the fugacities are the same in the cylinder as in the mixture, there is no change in free energy; the process occurs at equilibrium (Smith and Van Ness, pp. 409-410)

The fact that no change in free energy means no exchange of energy in the form of work, leads us to:

$$W_{\alpha,2} = 0 \qquad (48)$$

$$W_{\beta,2} = 0 \qquad (49)$$

The combination of the work associated to these two processes determines the work of the system for Process 2:

$$W_{sys,2} = W_{\alpha,2} + W_{\beta,2} = 0 \qquad (50)$$

The sub-indexes here used refer to the changes experienced by the system, in the form of gases α or β, in process 2

That the temperature of each of these two gases remained constant along the processes just described, means that they experienced no change in their internal energies, i.e.,

$$\Delta U_{sys,2} = \Delta U_{\alpha,2} + \Delta U_{\beta,2} = 0 \qquad (51)$$

The substitution of the two previous results in the equation for the firs law, $\Delta U_{sys} = Q_{sys} - W_{sys}$, leads to the conclusion that:

$$Q_{sys,2} = 0$$

The previous results evince the fact that no heat exchange takes here place between the system and the heat bath, that is:

$$Q_{bath,2} = Q_{sys,2} = 0 \qquad (52)$$

Additional comments on this process can be found in Section 15.

At the conclusion of this process the valves are closed.

Process 3. Following the introduction/removal process just described, the following reaction takes place:

$$n\alpha\left(P_{\alpha,eq}, T\right) \rightarrow n\beta\left(P_{\beta,eq}, T\right) \qquad (53)$$

The fundamental assumption behind the modus operandi of the van' Hoff equilibrium box in general, and of reaction (53) in particular, or of the inverse of this reaction, is that even if the disequilibrium created on the vast amount of reaction in the reaction box by the addition of n moles of α, and the removal of n moles of β produces no measurable effect on the respective partial pressures or concentrations of these two chemical species, it will be however (this disequilibrium) the reason for the occurrence of reaction (53) through which equilibrium in the box will be restored.

In Fermi's words:

> We assume that the content of the large box is so great that the relative changes in concentration resulting from this inflow of gases is negligible. The concentrations of the gases during this process, therefore, remain practically constant ...Moreover, since the temperature and volume of the large box do not change, the chemical equilibrium of the gases in the box readjusts itself... (pp. 103, 105).

The fact that in this reaction butane at its equilibrium conditions is transformed into isobutane at the same conditions is the reason why this reaction is said to be taking place 'at equilibrium.' The fact shown above in eq. (27), that at equilibrium the chemical force is zero, means that the occurrence of reaction (53) will take place without any exchange of work with its work reservoir:

$$\text{If } f_{eq} = 0, \text{then } W_{sys,3} = 0 \qquad (54)$$

At the light of the previous result, the expression of the first law for reaction (53), that is for the system in process 3, namely $\Delta U_{sys,3} = Q_{sys,3} - W_{sys,3}$, reduces to:

$$\Delta U_{sys,3} = Q_{sys,3} \qquad (55)$$

The previous equation shows that the whole of the internal energy or enthalpy change of reaction (53), which is the energy coming from the breaking and forming of chemical bonds defining this chemical process, appears as an equivalent amount of heat.

The situation to be noted at this point in process 3 is that there exists no avenue open, no mechanism at play which could take this energy (the thermodynamically mandated fraction of it, that is), as it is being made available by reaction (53), and transform it into work. The only path open to it is the one leading to the heat bath, and it is this fact what defines the way through which the said fraction of this energy is to be converted into work.

Let us acknowledge now the following two facts: 1) The internal energy, and the enthalpy, of an ideal gas are sole functions of its temperature (Denbigh, p. 113). The previous statement implies that said functions are independent from the pressure; 2) Any ideal-gas phase, isothermal, and isobaric reaction taking place with constant total mole number, $\Delta n = 0$, like the one being here considered, is also isochoric; and on reason of this, for any such reaction the internal energy and enthalpy changes become identical: $\Delta U = \Delta H - P\Delta V = \Delta H - RT\Delta n = \Delta H$.

It is with the previous notions in mind that the following equation will be written:

$$\Delta U_{sys,3} = \Delta H_{sys,3} = \Delta H\left[n\alpha\left(p_{\alpha,eq}, T\right) \rightarrow n\beta\left(p_{\beta,eq}, T\right)\right] = n\Delta H[\alpha(1\text{bar}, T) \rightarrow \beta(1\text{ bar}, T)] = n\Delta H^o = n\Delta U^o \qquad (56)$$

From which the following equation will be excerpted:

$$\Delta U_{sys,3} = n\Delta U^o = n\Delta H^o \qquad (57)$$

The combination of equations (55) and (57) leads us to the following equation in which we have included the change experienced by the heat bath:

$$n\Delta H^o = Q_{sys,3} = -Q_{bath,3} \qquad (58)$$

Process 4. Here, the amounts of α and β in C_α and C_β at the end of process 3, namely $(1-n)\alpha\ (P_{\alpha,eq}, T)$ and $n\beta\ (P_{\beta,eq}, T)$, will be now compressed isothermally (T) and reversibly to a final pressure of 1 bar. The amounts of work involved are the following:

$$W_{\alpha,4} = Q_{\alpha,4} = -Q_{bath,\alpha,4} = (1-n)RT \ln P_{A,eq} \qquad (59)$$

$$W_{\beta,4} = Q_{\beta,4} = -Q_{bath,\beta,4} = nRT \ln P_{B,eq} \qquad (60)$$

Combined, the two previous equations quantify the changes experienced by the system and the bath in this process in the following manner:

$$W_{sys,4} = W_{\alpha,4} + W_{\beta.4} = Q_{sys,4} = -Q_{bath,4} = (1-n)RT \ln P_{\alpha,eq} + nRT \ln P_{\beta,eq} \qquad (61)$$

The isothermal nature of these two processes means that they occur without changes in their respective internal energies. This fact is implicit in the equality between work and heat evinced by the previous three equations. Therefore:

$$\Delta U_{sys,4} = 0 \qquad (62)$$

7.3 A summary of changes

7.3.1 The reaction Box

No change remains in the reaction box once the previous processes have concluded. The original changes consisting in the addition of n moles of α and the simultaneous removal of n moles of β were offset by the occurrence of reaction $n\alpha\left(P_{A,eq}, T\right) \rightarrow n\beta(P_{B,eq}, T)$ through which the n moles of α inserted were consumed in order to replenish the n moles of β extracted; with the constancy of its temperature assured by the action of the heat reservoir.

7.3.2 The Cylinders

Cylinders α and β do experience changes in their respective conditions because of these four processes. Thus, while the former originally contained 1 mole of

$\alpha(1\text{bar}, T)$; at the end it contains only $(1-n)$ moles of this gas at these same conditions. The latter, originally empty, is found at the end containing n moles of $\beta(1\text{ bar}, T)$. Note then that the previous concatenation of processes has managed to reversibly transform the original mole of $\alpha(1\text{bar}, T)$ into pure α and pure β in the amounts and conditions given by $(1-n)\alpha\ (1\text{bar}, T)$, and $n\beta\ (1\text{ bar}, T)$. The former occupying cylinder α and the latter cylinder β. In other words, these four processes combined to bring forward the reversible standard reaction given by equation (44).

7.3.3 The System

The work performed by the system along these four processes, quantified in equations (47), (50), (54), and (61), amounts to:

$$W_{sys} = -RT \ln P_{\alpha,eq} + 0 + 0 + (1-n)RT \ln P_{\alpha,eq} + nRT \ln P_{\beta,eq} \quad (63)$$

Upon simplification, this equation reduces to:

$$W_{sys} = nRT \ln \left(\frac{P_{\beta,eq}}{P_{\alpha,eq}} \right) \quad (64)$$

Recognition of the fact that the pressure quotient in the previous equation is the equilibrium constant K for reaction (1) at temperature T, combined with the fact that:

$$\Delta G^o = -RT \ln K \quad (65)$$

Allows writing equation (64) as follows:

$$W_{sys} = -n\Delta G^o \quad (66)$$

The heat exchanged by the system in each of these processes has been evaluated in equations (47), (52), (58), and (61). It amounts to:

$$Q_{sys} = -RT\ ln\ P_{\alpha,eq} + 0 + n\Delta H^o + (1-n)RT \ln P_{\alpha,eq} + nRT\ ln\ P_{\beta,eq} \quad (67)$$

Simplification of this equation, followed by its combination with equation (65) produces:

$$Q_{sys} = n(\Delta H^o - \Delta G^o) \quad (68)$$

The defining equation of the Gibbs energy, $G = H - TS$, allows writing the previous expression as

$$Q_{sys} = n\,T\Delta S^o \quad (69)$$

The internal energy changes experienced by the system are given in equations (46), (51), (57), and (62). Combined, they amount to:

$$\Delta U_{sys} = 0 + 0 + n\Delta H^o + 0 = n\Delta H^o \qquad (70)$$

The final form of the previous equation comes through the substitution in the equation for the first of the results shown in equations (66) and (67), i.e.,

$$\Delta U_{sys} = n\Delta H^o = Q_{sys} - W_{sys} = n(T\Delta S^o + n\Delta G^o) \qquad (71)$$

7.3.4 The mechanical reservoir

That in the universe of the equilibrium box the only bodies capable of exchanging energy in the form of work are the system and the work reservoir (*mr*) means that work done by one is work done on the other, and vice-versa. In other words, $W_{sys} = -W_{wr}$. According to this, at the end of the four processes above described, the work in the work reservoir finds, in attention to eq. (66), the following quantification:

$$W_{sys} = -W_{mr} = -n\Delta G^o \qquad (72)$$

It should be kept in mind that while ΔG^o in the previous equation is a constant which stands for the difference between the standard Gibbs energies of formation of 1 mole of isobutane and 1 mole butane, as they appear in reaction (1), both work terms there appearing W_{sys}, and W_{mr}, refer to the conversion of n moles of butane into isobutane, $0 < n \leq 1$. As expressed in the previous equation, both these terms are functions of n.

7.3.5 The heat reservoir

That in the universe of the equilibrium box the only bodies capable of heat exchange are the system and the heat bath means that heat gained by one is heat lost by the other. According to this, and in attention to eq. (69), we can quantify the heat exchanged by the heat bath with the following expression:

$$Q_{bath} = -nT\Delta S^o \qquad (73)$$

All the results obtained in the previous discussion agree with thermodynamic theory.

Regarding the standard isomerization reaction of butane into isobutane, we have this exothermic reaction making available in process 3, an amount of heat equal to $n\Delta H^o = n \cdot 8368.4$ J which is originally transferred to the heat bath. A portion of this energy in the amount of $n\Delta G^o = n \cdot 3747.1$ J leaves the heat bath to be transformed into an equivalent amount of work that ends up in the work reservoir. The difference, in the amount of $n \cdot T\Delta S^o = n(298.15 \cdot 15.5) = n \cdot 4621.3$ J remains, as unavailable energy, in the heat bath.

8. Back to the beginning

It was through the concatenation of the four processes just described that the following reaction, as represented in eq. (44), took place:

$$1\alpha\ (g, 1\ \text{bar}, T) \rightarrow [(1-n)\alpha\ (g, 1\ \text{bar}, T)] + [n\beta\ (g, 1\text{bar}, T)]$$

This new concatenation of the four processes to be described below, will be responsible on the other hand, for the inverse change, namely:

$$1\alpha\ (g, 1\ \text{bar}, T) \leftarrow [(1-n)\alpha\ (g, 1\ \text{bar}, T)] + [n\beta\ (g, 1\text{bar}, T)] \qquad (74)$$

The processes and associated changes subsumed by it, will be identified with Roman numerals. When necessary, these processes/changes will also bear the subscript $\beta \rightarrow \alpha$ to distinguish them from those associated to the previous concatenation, which, when needed, will be identified by the subscript $\alpha \rightarrow \beta$.

The new concatenation starts at the conditions we find the universe (system and surroundings) at the conclusion of the previous one. Here, the achievement of the intended change represented in eq. (74) will include, among other processes, the occurrence of the inverse of reaction (53), that is, of reaction:

$$n\beta\left(P_{\beta,eq}, T\right) \rightarrow n\alpha\left(P_{\alpha,eq}, T\right) \qquad (75)$$

The description of these four new processes is given below.

Process I: Gases α and β, in the amounts and conditions they are respectively found in cylinders C_α and C_β at the conclusion of the previous concatenation, namely $(1-n)\alpha(1\ \text{bar}, T)$, and $n\beta(1\text{bar}, T)$, will be isothermally and reversibly expanded to respective pressures $P_{\alpha,eq}$ and $P_{\beta,eq}$. The following changes accompany these expansions:

$$\Delta U_{sys,I} = 0 \qquad (76)$$

$$W_{sys,\alpha,I} = Q_{sys,\alpha,I} = -Q_{bath,\alpha,I} = -W_{mr,\alpha,I} = -(1-n)RT\ln(P_{\alpha,eq}) \qquad (77)$$

$$W_{sys,\beta,I} = Q_{sys,\beta,I} = -Q_{bath,\beta,I} = -W_{mr,\beta,I} -= -nRT\ln(P_{\beta,eq}) \qquad (78)$$

The fact that $W_{sys,I} = W_{sys,\alpha,I} + W_{sys,\beta,I}$, leads us to the following expression:

$$W_{sys,I} = Q_{sys,I} = -Q_{bath,I} = -W_{mr,I} = -(1-n)RT\ln(P_{\alpha,eq}) - nRT\ln(P_{\beta,eq}) \qquad (79)$$

After rearrangement and simplification, the previous equation takes the following form:

$$W_{sys,I} = Q_{sys,I} = -Q_{bath,I} = -W_{mr,I}$$
$$= -RT\ln(P_{\alpha,eq}) + nRT\ln\ (P_{\alpha,eq}) - nRT\ln\ (P_{\beta,eq})$$
$$= -RT\ln\ (P_{\alpha,eq}) + nRT\ln\left(\frac{P_{\alpha,eq}}{P_{\beta,eq}}\right)$$
$$= -RT\ln\ (P_{\alpha,eq}) - n\Delta G^{o}_{\beta\to\alpha} \qquad (80)$$

Process II. The fact that the addition/removal process taking place here is essentially the same as that discussed in process 2, allows us to identify the introduction of n moles of gas $\beta(P_{\beta,eq}, T)$ into the reaction box, and the removal from it of n moles of gas $\alpha(P_{\alpha,eq}, T)$ from it, as processes taking place with no change in Gibbs energy, and if so, without any exchange of energy in the form of work. Therefore:

$$W_{\alpha,II} = 0 \qquad (81)$$
$$W_{\beta,II} = 0 \qquad (82)$$

Note here that at the conclusion of this process we will find that while C_α contains 1 mole of α, C_β is, on its part, empty.

The combination of the two previous equations produces:

$$W_{sys,II} = 0 \qquad (83)$$

From the isothermal nature of these two processes, we get:

$$\Delta U_{sys,II} = 0 \qquad (84)$$

And from the first law, in the form $Q_{sys,II} = \Delta U_{sys,II} + W_{sys,II}$, the following result is produced:

$$Q_{sys,II} = 0 + 0 = 0 \qquad (85)$$

Process III. It is in this process where, via eq. (75), the n extra moles of β in the reaction mixture are consumed to offset its n moles of α deficit. The fact that it is a reaction taking place 'at equilibrium,' means, as already noted regarding these reactions, that no work is exchanged by it, if so, then:

$$W_{sys,III} = 0 \qquad (86)$$

In terms of the previous result, the first law reduces to:

$$\Delta U_{sys,III} = Q_{sys,III} \qquad (87)$$

The fact made evident by a simple inspection of eq. (56) that $\Delta U_{sys,III} = -\Delta U_{sys,3}$ allows us, on reason of eq. (57), to re-express eq. (87) in the following manner:

$$\Delta U_{sys,III} = Q_{sys,III} = \Delta H^o_{\beta\to\alpha} \qquad (88)$$

The previous equation shows that along its occurrence, reaction (75) takes away from the heat bath an amount of heat equal to $\Delta H^o_{\beta\to\alpha}$, identical in magnitude to that transferred to the heat bath by reaction (53) in process 3.

The following quote from Clausius serves to set processes 3, and III, in the proper thermodynamic frame:

> … let us consider a cyclical process, which is such that a body passes through a series of changes of condition and at last returns to its original state. This variable body, if placed in connection with the heat reservoir to receive or give heat, must have the same temperature as the reservoir; for it is only in this case that the heat can pass as readily from the reservoir to the body as in the reverse direction, and if the process is reversible it is requisite that this should be the case. (p. 106)

Process IV. At this point the 1 mole of α in cylinder C_α is compressed isothermally and reversibly from $P_{\alpha,eq}$ to 1 bar. The changes associated to this process are the following:

$$\Delta U_{sys,IV} = 0 \qquad (89)$$

$$W_{sys,IV} = Q_{sys,IV} = -Q_{bath,IV} = -W_{mr,IV} = RT \ln P_{\alpha,eq} \qquad (90)$$

8.1 Summary of Changes for the inverse path.

8.1.1 Internal energy: From equations (76), (84), (88), and (89) we can write, for the internal energy change of the system along the inverse process (*inv*), the following equation:

$$\Delta U_{sys,inv} = 0 + 0 + n\Delta H^o_{\beta\to\alpha} + 0 = n\Delta H^o_{\beta\to\alpha} \qquad (91)$$

8.1.2 Work: The work exchanged by the system is determined by the combination of equations (80), (83), (86), and (90):

$$W_{sys,inv} = -RT \ln(p_{\alpha,eq}) - n\Delta G^o_{\beta\to\alpha} + RT \ln(p_{\alpha,eq}) = -n\Delta G^o_{\beta\to\alpha} \qquad (92)$$

8.1.3 Heat: The heat exchanged by the system with the heat bath can be obtained from equations (80), (85), (88), and (90):

$$Q_{sys,inv} == -RT\ln(p_{\alpha,eq}) - n\Delta G^o_{\beta\to\alpha} + 0 + n\Delta H^o_{\beta\to\alpha} + RT\ln(p_{\alpha,eq})$$
$$= n(\Delta H^o_{\beta\to\alpha} - \Delta G^o_{\beta\to\alpha}) = nT\Delta S^o_{\beta\to\alpha} \qquad (93)$$

9. Summary of results for the cycle defined by the combination of the two previous concatenations

9.1 Internal energy: From the combination of equations (70) and (91) we get:

$$\Delta U_{sys,cycle} = \Delta H^o_{\alpha\to\beta} + \Delta H^o_{\beta\to\alpha} = 0 \qquad (94)$$

The equality to zero of the previous equation stems from the state function nature of the enthalpy, which asserts that $\Delta H^o_{\alpha\to\beta} = -\Delta H^o_{\beta\to\alpha}$.

9.2 Work: The work exchange by the system and the work reservoir, calculated with equations (72) and (92), leads us to the following result:

$$W_{sys,cycle} = -W_{mr,cycle} = -n\Delta G^o_{\beta\to\alpha} - n\Delta G^o_{\alpha\to\beta} = 0 \qquad (95)$$

The zero in the previous equation finds the same explanation as that given for eq. (94).

9.3 Heat: The heat exchanged by the system with the heat bath, calculated with equations (69) and (93):

$$Q_{sys,cycle} = -Q_{bath,cycle} = nT\Delta S^o_{\alpha\to\beta} + nT\Delta S^o_{\beta\to\alpha} = 0 \qquad (96)$$

Note that here, again, $nT\Delta S^o_{\alpha\to\beta} = -nT\Delta S^o_{\beta\to\alpha}$.

Equations (94), (95), and (96), make evident the fact that at the completion of the cycle, no change remains in the system, the bath, or the work reservoir. At the end of this cycle, the universe has returned to its original condition, and no evidence remains of any change having ever taken place; which is the essential meaning of the reversibility concept, at least in the way it was originally understood by Carnot (pp. 11, 19). Said restoration implies the reversibility of both, the forward, and reverse processes.

The introduction into the reaction box, in the first concatenation, of only a fraction *n* of the one mole of available butane obeyed to the fact that the results thus obtained could be concatenated with the mixing process to be described below, in such a way that the result of this combination could be compared with that of the chemical-potential centered analysis represented by eq. (43)

10. The mixing process

It was Lord Rayleigh the first to recognize that work might be obtained by the isothermal mixing of gases. In a paper titled "On the work that may be gained during the mixing of gases," published in 1875, he demonstrated, in the words

of Darrigol (2018), that "... the maximal work that can be obtained by mixing (isothermally) two gases initially occupying the separate volumes V_1 and V_2 and finally sharing the volume $V_1 + V_2$ is equal to the work produced by the expansion of the first gas alone from V_1 to $V_1 + V_2$ pus the work produced by the expansion of the second gas alone from V_2 to $V_1 + V_2$. The maximal work is reached when the mixing is reversible."

The following discussion pertains the isothermal and reversible mixing of the product of the first concatenation, that is, of the $(1-n)\alpha(1\text{bar}, T)$ moles of α in cylinder C_α, and the $n\beta(1\text{bar}, T)$ moles of β in cylinder C_β. Apart from saying that this isothermal, reversible, and work producing mixing process takes place in a device in thermal contact with the same bath, and properly coupled to the same work reservoir used in the van' Hoff operation; we will add that excellent discussions about this issue are available in the thermodynamic literature (Klotz and Rosenberg, pp. 271-273; Schmidt, pp. 135-138). In them we find the mixing work given by the following equation:

$$W_{sys,mix} = -(n_\alpha RT \ln x_\alpha + n_\beta RT \ln x_\beta) \qquad (97)$$

In terms of the notation which based on the degree of advancement ξ, was introduced in eq. (17) of Section 2, making $n_\beta = x_\beta = p_\beta = \xi$, and $n_\alpha = x_\alpha = p_\alpha = 1 - \xi$, the previous equation becomes:

$$W_{sys,mix} = -RT[(1-\xi)\ln(1-\xi) + \xi \ln \xi] \qquad (98)$$

Applying the same change of variable to eq. (66), which gives the work produced by non-mixing standard reaction (44) in the first concatenation, we get:

$$W_{sys} = -\xi \Delta G^o_{\alpha\to\beta} \qquad (99)$$

At the end of this mixing process, we find that the total work produced by the system amounts to:

$$W_{sys,tot} = -\xi \Delta G^o_{\alpha\to\beta} - RT[(1-\xi)\ln(1-\xi) + \xi \ln \xi] \qquad (100)$$

In terms of free energy, the two previous equations find, on reason of eq. (5), the following equivalent expressions:

$$\Delta G_{sys} = \xi \Delta G^o_{\alpha\to\beta} \qquad (101)$$

$$\Delta G_{sys,tot} = \xi \Delta G^o_{\alpha\to\beta} + RT[(1-\xi)\ln(1-\xi) + \xi \ln \xi] \qquad (102)$$

A simple inspection will reveal the identity existing between equations (43) and (102), confirming this way the equivalence of the usual thermodynamic procedure with that of the van't Hoff equilibrium box.

11. Discussion

11.1 The previously noted fact that reaction (44) as it takes place in the van't Hoff equilibrium box transits from an initial state represented by 1 mole of pure butane in cylinder C_α to a final state represented by $(1-n)$ moles of pure butane in the same cylinder, and n moles of pure isobutane in cylinder C_β, both at 1 bar of pressure at the selected temperature, is what makes of this reaction a standard reaction:

> The word 'standard refers not to any particular temperature, but to unit pressure of 1 bar for each of the pure reactants and products." (Denbigh, p. 148)

The 'pure' condition means, of course, unmixed.

The standard path for reaction (44), a non-mixing path, is thus the one defined by eq. (101). The fact indicated by Table 2 that $\Delta G^o_{\alpha\to\beta} = -3747.1\ \mathrm{J\ mol^{-1}}$, allows to write this equation in the following manner

$$\Delta G_{sys} = -3747.1n = -3747.1\xi \qquad (103)$$

Any point on the negatively sloped line defined by this equation on coordinates $\Delta G_{sys} - vs. -\xi$ corresponds this way to a different run of reaction (44); Each of these runs, characterized by a given n or ξ, producing a different change in the Gibbs energy of the system, and a different work output. The fact that for all n different from zero, $0 < n \leq 1$, it is true that $\Delta G_{sys} < 0$, means that reaction (44) is spontaneous for all these n.

The fact that the linear path of reaction (44) is negatively sloped or, equivalently, a Gibbs energy decreasing path, means that any number of moles of α introduced into the van't Hoff box will be totally converted into the stoichiometrically corresponding moles of β.

It is interesting to note here that this devoid of mixing, and full-conversion standard reaction comes out of the equilibrium mixture of the same reaction, a reaction which precisely on reason of having taken place along a mixing path, was incapable of complete conversion.

11.2 As proved above, the mixing of the products of reaction (44) transforms the path of reaction (44) from one described by eq. (101) to one described by eq. (102). The graph of this equation takes the familiar form of the concave up curve with its minimum corresponding to the equilibrium mixture.

Of the two sources capable of providing energy for reversible reaction (1) to transform into mechanical work, it is the one coming from the chemical process itself, that is, the one associated to the breaking and forming of bonds ($n\Delta G^{o}_{\alpha\rightarrow\beta}$) the one with which the standard reaction deals with. The 'actual' path of a chemical reaction, deals with both, the previous one, and the one originating in the mixing process ($n_{\alpha}RT\ln n_{\alpha} + n_{\beta}RT\ln n_{\beta}$).

11.3 In thermodynamics, reversible is any process driven by an internal force infinitesimally larger than an external resisting force of the same nature. Thus, the reversible expansion of a gas requires the pressure of the gas being infinitesimally larger than an external, resisting pressure; For example, maximum work is obtained from a chemical reaction taking place in an electrochemical cell working "against an external voltage lower than its own by no more than a differential amount" (Pimentel & Spratley, p. 112).

The fact that in chemical reactions with non-ionic mechanisms, say the gas-phase reaction above considered, it is apparently impossible to oppose a force of the same nature to the one driving the reaction, that is, to the one which called the 'chemical force' and represented by f, finds definition in terms of the difference of the stoichiometrically weighted chemical potentials of reactants minus products, seems to be the reason why the only practical path open to the reversibility of these reactions is the one represented by the van't Hoff equilibrium box in which the reaction of interest is seen taking place 'at equilibrium.' The reason why this is so simple: A reaction taking place at equilibrium does so with a chemical force equal to zero. In this case the opposing force is redundant, there is just no need for it given that there is nothing for it to oppose.

11.4 We have already proved the usefulness of equation $dW = fd\xi$ for the quantification of the work produced by a reversible reaction along any given transit $\xi_1 \rightarrow \xi_2$. The interesting thing to note in this regard is that the work coming out of the van't Hoff equilibrium box does so without the intervention of this force. It could not have been otherwise given that the reaction in it is taking place 'at equilibrium,' condition where this force becomes equal to zero. What we find instead is that the work coming out is actually PdV work. The 'interesting' qualifier used above pertains the fact that the work coming out of a reaction taking place without any change in volume, such as reaction (1), finds evaluation via $dW = PdV$

11.5 The van' Hoff equilibrium box is a tool devised for the theoretical analysis of chemical reactions, with no possibility of practical realization. Even if you succeed in creating infinitesimal gradients, you will have to wait an infinite amount of time for the process to conclude. If these two restrictions were not enough, the case of the equilibrium box faces the additional problem of availability of the required semi-permeable membranes. These are the reasons why instead of using the equilibrium box to produce, for example, mechanical work out of the Gibbs energy change associated to the reversible oxidation of methane in a van't Hoff engine, we are forced to use its enthalpy change for this purpose, and this is done by burning it and feeding the heat thus produced to a less efficient, finite-time, thermodynamic cycle (Denbigh, pp. 72-76), a path associated to an undesirable subproduct: pollution. Let me note in this regard that the theoretical foundation provided by a corrected and extended version of quantum chemistry called Hadronic Chemistry has made possible the development of new clean energies and fuels (Santilli, 2001). This discipline, composed of three branches: Isochemistry, directed to the representation of closed isolated systems such as molecular structures; Genochemistry, directed to the description of "... irreversible chemical processes with unrestricted interactions, as expected in chemical reactions." (ibid, xl); and Hyperchemistry, directed to the representation of "... irreversible biological structures with multi-valued unrestricted internal processes." (ibid, xli), has developed new models for the hydrogen and water molecules in agreement with "... conceptual, theoretical, and experimental evidence." (Santilli & Shillady,1999; Santilli & Shillady, 2000, p. 81)

12. The van't Hoff equilibrium box as the chemical counterpart to Carnot's heat engine

Carnot's reversible heat engine produces work out of heat flowing from a hot reservoir of temperature T_h to a cold reservoir of temperature T_c, and does it by introducing between these reservoirs what is called a Carnot engine, basically a working substance, say one mole of an ideal gas, which contained in a cylinder fitted with a frictionless and weightless piston properly connected to a mechanical reservoir, is subject to the cyclical concatenation of four reversible processes: 1) an isothermal and reversible expansion at the temperature of the hot reservoir. The conditions of the gas in this process change from (T_h, V_A) to

(T_h, V_B); 2) an adiabatic and reversible expansion lowering the temperature of the gas to that of the cold reservoir; the conditions of the gas transit here from (T_h, V_B) to (T_c, V_C); 3) an isothermal and reversible compression at the temperature of cold reservoir, changing the conditions of the gas from (T_c, V_c) to (T_c, V_D); and finally, an adiabatic and reversible compression which starting at (T_c, V_D) ends up with the gas at the same conditions it originally had at the start of the cycle, that is (T_h, V_A). The previous four processes, in the order mentioned, will also, for reasons of economy of expression, be designated as *AB*, *BC*, *CD*, and *DA*. Each of the engine's work producing cycles starts with the hot reservoir transferring to the gas along process *AB*, an amount of heat Q_h. The cyclical work output will, on its part, be designated as *W*.

With the previous antecedents at hand, let us recognize the following salient operational characteristics of this engine:

1. Combined, adiabatic and reversible processes *BC* and *DA* make no contribution to the work output of the cycle. The reason being that the work produced by the former is exactly the amount consumed in the occurrence of the latter. For adiabatic processes, characterized by $Q = 0$, the first law reduces to $\Delta U = w$. For ideal gases, this equation can be written as $\Delta U = C_v \Delta T$. Applied to processes *BC* and *DA*, the previous equation takes the following forms: $\Delta U_{BC} = C_v(T_c - T_h)$ and $\Delta U_{DA} = C_v(T_h - T_c)$. These equations, combined, lead to $\Delta U_{BC} + \Delta U_{DA} = 0$, and on reason of the just noted identity between internal energy change and work, also to $w_{BC} + w_{DA} = 0$. Even if not contributing to the work output of the cycle, isentropic processes *BC* and *DA* are the ones making possible the cycle.

2) The previous result leads to the realization that the work output *W* of the cycle is the sole matter of processes *AB*, and *CD*. In the former, an isothermal and reversible expansion of the ideal gas at the temperature T_h of the hot reservoir, the whole of the heat Q_h received by the gas from the hot reservoir is transformed into an equivalent amount of work w_h which ends up in the work reservoir. Once the temperature of the gas has been taken from T_h to T_c by process *BC*, the gas is subject to an isothermal and reversible compression at the temperature of the cold reservoir, T_c. The work consumed to produced this change, w_c, represents a portion of the one previously deposited in the work reservoir by process *AB*. In line with the mandate of the first law, as it applies to this process, the work spent on it ends up as an equivalent amount of heat Q_c in the cold reservoir.

3. The difference of the temperatures at which expansion *AB* and compression *CD* take place, explains, among other things, the partial conversion into work of the heat released by the hot reservoir.

For isothermal and reversible processes *AB* and *CD*, the following equations can be respectively written: $w_h = Q_h = RT_h \ln(V_B/V_A)$ and $w_c = Q_c = RT_c \ln(V_C/V_D)$, in which case the work output of the cycle will be given by $W = w_h - w_c$. If we now bring here the equation relating the initial and final states of isentropic processes *BC* and *DA*, namely $V_B/V_A = V_C/V_D$, and with it write $w_c = Q_c = RT_c \ln\frac{V_B}{V_A}$, and once this is done, we take the quotient w_h/w_c, we will get $w_h/w_c = T_h/T_c$. This last expression, on substitution of $w_c = w_h - W$, becomes $(w_h - W)/w_h = T_c/T_h$, which on further algebraic rearrangement produces:

$$\frac{W}{w_h} = \frac{W}{Q_h} = \eta_{Carnot} = \frac{T_h - T_c}{T_h}$$

The said difference in temperatures, even if restricting the full conversion of heat input into work output, is the sine qua non condition that opens the door to the continuous transformation of heat into work in a heat engine. When the heat engine returns to its initial condition to start a new cycle, the work reservoir is found holding an additional amount of work $W = \eta_{Carnot} Q_h$ to the one it holds at the conclusion of the previous cycle. Let us now note that an isothermal and reversible ideal gas expansion has the capability to transform its heat input into an equivalent amount of work. This, however is a one-time event. Any attempt to construct a work producing cycle by concatenating this expansion with its inverse will fail on reason of the fact that at the start of the new cycle no work will be found in the mechanical reservoir, the reason being that in the isothermal and reversible compression needed to produce said cycle, the whole of the work initially outputted will be consumed making it a zero efficient cycle. No work can come out of an isothermal Carnot's cycle.

13. The van't Hoff chemical-potential engine in comparison to that of Carnot

The following arguments will refer to the operation of the van't Hoff equilibrium box, when instead of the introduction of $n\alpha(p_{\alpha,eq}, T)$ moles of butane to the vast amount of equilibrium mixture in the reaction box, and the simultaneous removal from it of $n\beta(p_{\beta,eq}, T)$, where $0 < n \leq 1$, we introduce to the said equilibrium mixture 1 mol of butane, and remove from it 1 mol of isobutane,

both at the previously indicated conditions. The benefit of this procedure is the simplicity of description afforded with it.

The form adopted by the four processes constituting the operation of the van't Hoff engine in this new case are the following:

Process *i*: The isothermal and reversible expansion of the 1 mole of butane in cylinder C_α from 1 bar to $p_{\alpha,eq}$. From equations (46), and (47), this last one via the substitution $n = 1$, we get:

$$\Delta U_{sys,i} = 0 \qquad (104)$$

$$-Q_{bath,i} = Q_{sys,i} = W_{sys,i} = -W_{sys,i} = -RT\ln(P_{\alpha,eq}) \qquad (105)$$

Process *ii*: The introduction of 1 mole of $\alpha(p_{\alpha,eq}, T)$ to the vast amount of equilibrium mixture in the reaction box, and the simultaneous removal from it of 1 mole of $\beta(p_{\beta,eq}, T)$. For the reasons already given in regard to processes 2, and II, we will have that:

$$W_{\alpha,2i} = 0 \qquad (106)$$

$$W_{\beta,2i} = 0 \qquad (107)$$

$$W_{sys,2i} = W_{\alpha,2i} + W_{\beta,2i} = 0 \qquad (108)$$

$$\Delta U_{sys,2i} = \Delta U_{\alpha,2i} + \Delta U_{\beta,2i} = 0 \qquad (109)$$

$$Q_{bath,2i} = Q_{sys,2i} = 0 \qquad (110)$$

Note that at the end of this process while cylinder C_α is empty, C_β contains 1 mole of $\beta(p_{\beta,eq}, T)$

Process 3*i*: Equilibrium is restored in the vast amount of reaction inside the reaction box via the occurrence at equilibrium of the following reaction:

$$1\alpha(p_{\alpha,eq}, T) \rightarrow 1\beta(p_{\beta,eq}, T)$$

The 'at equilibrium' nature of the previous reaction means, as already discussed, that:

$$W_{sys,3i} = 0 \qquad (111)$$

From equations (57) and (58), via the same substitution, we get:

$$\Delta U_{sys,3i} = \Delta U^o = \Delta H^o \qquad (112)$$

$$\Delta H^o = Q_{sys,3i} = -Q_{bath,3i} \qquad (113)$$

Process 4*i*: The mole of β in cylinder C_β is compressed isothermally and reversible from $p_{\beta,eq}$ to 1 bar. With base on (60) and (62) and the previously noted substitution, we get:

$$W_{sys,4i} = Q_{sys,4i} = -Q_{bath,4i} = RT \ln P_{B,eq} \qquad (114)$$

$$\Delta U_{sys,4i} = 0 \qquad (115)$$

14. Van't Hoff's chemical-potential engine compared to Carnot's heat engine

With the two previous sections in place, the following statements will be advanced:

1. The obvious difference between Carnot's and van't Hoff's engines is that while the former exploits the work producing potential subsumed by the transfer of heat from a higher to a lower temperature, the latter produces work out of the "… transfer of chemical matter between two different chemical states described by chemical potentials." (Gill, p. 507). The fact that the purpose of one and the other is the same, namely the production of work, is the reason why the van't Hoff equilibrium box is being here referred to as an 'engine.'

Just like no work is outputted in the absence of a temperature gradient in Carnot's engine, neither is, in reference to a chemical reaction, when the value coming out of the combination of the chemical potentials of the reactants, properly weighted by their respective stoichiometric coefficients turns out to be identical to that of a similar combination of the chemical potentials of the products. In both cases the reason is the same: from a system in equilibrium (thermal in the former, and chemical in the latter) no work production is possible.

2. A closer look at equations (105), (108), (111), and (114) allows us to realize that the work output of van't Hoff's engine finds quantification in precisely the same way it happens in Carnot's engine, that is, in terms of the combination of the work produced by an isothermal and reversible expansion, and the work consumed by an isothermal and reversible compression. The difference being that while in Carnot's engine they take place at different temperatures, in van't Hoff's engine they take place at the same temperature.

3. In a heat engine it is the no-work-contributors adiabatic and reversible processes the ones making the reversible cycle possible. They break the finite temperature gradient into an infinity of steps differing infinitesimally in temperature, and in doing so providing, via the working substance, a reversible

connection between them. Once a cycle concludes via process DA, the engine is ready to start a new one in which, again, one portion of its heat input Q_h will be transformed into mechanical work, with the rest discarded into the cold reservoir as the amount of heat $Q_c = Q_h - W$, and so on for each other cycle.

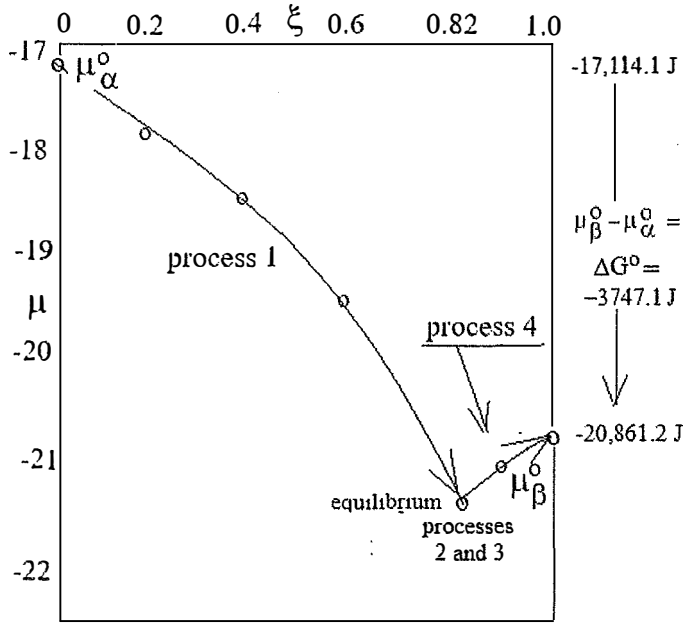

Figure 4. The reversible transit of $1\alpha(1\text{ bar}, T) \rightarrow 1\beta(1\text{ bar}, T)$ in a van't Hoff engine is here shown taking place via the concatenation of work-producing isothermal and reversible expansion 1, work-less processes 2 and 3 jointly representing the 'at equilibrium reaction', and work-consuming isothermal and reversible compression 4.

In van't Hoff's engine, on the other hand, it is the 'at equilibrium reaction' —which for the sake of this argument will be taken as the combination of processes $2i$ and $3i$ (after all, reaction $3i$ won't take place without the previous occurrence of process $2i$) the one which: 1) in combination with work-producing process $1i$, and work consuming process $4i$, provide the reversible path to the transit of chemical matter from μ_α^o to μ_β^o; and 2) by itself makes possible the cyclical operation of van't Hoff's engine. The reason behind this last assertion comes from the fact that the infinitesimal displacement which in the equilibrium condition of the vast amount of reaction in the reaction box is produced by the

addition to it of 1 mole of α, and the simultaneous removal from it of 1 mole of β, finds itself cancelled by the opposite-direction displacement through which said reaction recuperates its initial equilibrium condition via the consumption of the mole in excess of α in order to replenish the lacking mole of β. At this point, it should be noted, with equilibrium restored, the reaction mixture is in the condition to perform a new cycle which starts, as before done, with the addition of a new mole of α and the removal of 1 mole of β. Each cycle responsible for the output of an amount of work $W = -\Delta G^{o}_{\alpha\rightarrow\beta}$.

Figure 4 provides a graphical representation of this operation.

From equations (105) and (114), in combination with the following data, $R = 8.314\ \text{J K}^{-1}\text{mol}^{-1}$, $T = 298.15\ \text{K}$, $p_{\alpha,eq} = 0.18\ \text{bar}$, and $p_{\beta,eq} = 0.18\ \text{bar}$, these last two items from Table 3, we get:

$$w_{sys,i} = 1 \cdot 8.314 \cdot 298.15 \cdot \ln(1/0.18) = 4250.67\ \text{J}$$

$$w_{sys,4i} = 1 \cdot 8.314 \cdot 298.15 \cdot \ln(0.82) = -491.92\ \text{J}$$

The algebraic summation of these two results produces the work output W of van't Hoff's engine:

$$W = w_{sys,i} + w_{sys,4i} = 4250.67 - 491.92 = 3758.5\ \text{J} \qquad (116)$$

The number obtained above for W differs from the expected result, namely $-\Delta G^{0} = 3747.1\ \text{J}$, in 11.4 J, or 0.3%, a reasonable difference explainable in terms of rounding off error.

In a first approximation we could use, save further pondering on this issue, the procedure used in Carnot's engine to determine the efficiency of the present operation of van't Hoff's engine; Thus:

$$\eta_{van't\ Hoff} = \frac{W}{w_{sys,i}} = \frac{3758.5}{4250.67} = 0.88 \qquad (117)$$

As evinced by the figure, process $4i$, the one following the equilibrium restoration of the reaction in the reaction box, is non-spontaneous, and as such work-consuming. The removal of 491.92 J out of the 4250.67 J available in the mechanical reservoir are required to be spent to carry on this compression. The operation of the van't Hoff box will be now complete, with an amount of available work in the mechanical reservoir of 3758.5 J.

15. There is one aspect of the previous graph that needs clarification, and it is the one related to the fact that while the numbers used to draw the paths of processes $1i$, and $4i$ in Figure 4 are those which quoted in Table 3 refer to the

reversible, mixing-included-evolution of reaction (1); the ones that should be defining said paths are those coming out of the isothermal and reversible expansion (process $1i$) and compression (process $4i$) of pure ideal-gases α and β, respectively. To understand that the values of Table 3 are common to both these instances starts by recognizing that the act of *fixing* the value of ξ to be substituted in the equations for the chemical potentials of these substances (equations (30) and (31)) defines a particular mixture of given partial pressures of butane and isobutane. In this mixture no more change takes place. Asserting the contrary implies, contrary to assumption, that ξ can change. It is its unchanging nature what makes of it indistinguishable from a simple, non-reacting mixture of the said gases at the said concentrations or partial pressures: $p_\alpha = (1 - \xi)$ bar for butane, $p_\beta = \xi$ bar for isobutane. But in this simple mixture of ideal-gases we have, in accord with J. W. Gibbs (p. 157), as well as Dalton's law, that each ideal-gas is as a vacuum to the other, or, equivalently, each gas behaves as if it were alone (pure) in the total volume of the mixture at the temperature of the reaction. Thus, the chemical potential of butane in that *reaction mixture* characterized by $\xi = 0.3$ in which, in accord with eq. (17), 0.7 moles of butane exert a partial pressure of 0.7 bar at the temperature of the reaction, is identical to the chemical potential of 0.7 moles of pure butane in the volume of the mixture at the same temperature. The total pressure exerted by 0.7 moles of pure butane at temperature T when confined in a volume V, of magnitude $P_\alpha = 0.7\ (RT/V)$, turns out to be identical to the partial pressure exerted by the same amount of gas in the reaction mixture at the same volume and the same temperature: $p_\alpha = 0.7\ (RT/V)$:

$$\mu_\alpha(\text{pure}, P_\alpha = 0.7\ \text{bar}, T) = \mu_\alpha(\text{mixed}, p_\alpha = 0.7\ \text{bar}, T) = \mu_\alpha^o + RT\ln(0.7) \qquad (118)$$

In the words of Gibbs (p. 158) "... the potential μ_1 has the same value in the gas mixture and in the gas G_1 existing separately as supposed." An exemplification of this notion can be found Castellan (p. 224-224).

The argument leading to eq. (118) is the theoretical foundation of Smith and Van Ness explanation made in regard to the zero Gibbs energy change of process 2:

$$\text{If } \mu_\alpha(\text{pure}, P_{\alpha,eq}, T) = \mu_\alpha(\text{mixed}, p_{\alpha,eq}, T),$$
$$\text{then } \Delta\mu_{sys,2} = \mu_\alpha(\text{mixed}, P_{\alpha,eq}, T) - \mu_\alpha(\text{pure}, p_{\alpha,eq}, T) = 0 \qquad (119)$$

References

Aston, J. G., and Fritz, J. J., 1959, *Thermodynamics and Statistical Thermodynamics*, John Wiley & Sons, Inc., London, UK

Carnot, S., 1824/1960, *Reflections on the Motive Power of Fire*, Dover, New York, NY

Castellan, G. W., 1983, *Physical Chemistry*, Third Edition, Addison-Wesley, Reading, MA

Clausius, R., 1879, *The Mechanical Theory of Heat*, MacMillan and Co., London, UK

Darrigol, O., 2018, The Gibbs Paradox: Early History and Solutions, *Entropy* (Basel), 20 (8), 443

Denbigh, K., 1968, *The Principles of Chemical Equilibrium*, Second Edition, Cambridge University Press, London, UK

Fermi, E., 1956, *Thermodynamics*, Dover, New York, NY

Gibbs, J. W., *Collected Works, Vol 1, Thermodynamics*, Longmans, Green and Co., N.Y., 1928

Gill, S. J., 1962, The Chemical Potential, *J. Chem. Educ.*, 39(10), 506-510

Íñiguez, J. C., 2014, Work Degrading and the Reversible to Irreversible Transition in Chemical Reactions, *International Journal of Chemistry*, Vol. 6, No. 3, pp. 1-13, doi: 10.5539/ijc.v6n3p1

Kauzmann, W., 1967, *Thermodynamics and Statistics*, W. A. Benjamin, Inc., New York, NY

Klotz, I. M., and Rosenberg, R. M., 1986, *Chemical Thermodynamics*, Benjamin/Cummings, Menlo Park, CA

Lord Rayleigh, 1875, On the work that may be gained during the mixing of gases, *Philos. Mag.* 49, 311-319

Maron, S. H., Prutton, C. F., 1965a, *Principles of Physical Chemistry,* 4th. Ed., Macmillan International Student Edition, New York, NY

Maxwell, J. C., 1991/1920, *Matter and Motion*, Dover, New York, NY

Moore, W. J., 1972, *Physical Chemistry*, Fourth Edition, Prentice-Hall, Englewood Cliffs, NJ

Pauli, W., 1973, *Thermodynamics and the Kinetic Theory of Gases*, Dover, New York, NY

Pimentel, G. C., and Spratley, R. D., 1969, *Understanding Chemical Thermodynamics*, Holden-Day, Inc., San Francisco, CA

Pitzer, K. S., and Brewer, L., 1961, *Thermodynamics*, McGraw-Hill, New York, NY

Santilli, R. M. 2001, *Foundations of Hadronic Chemistry: With Applications to New Clean Energies and Fuels*, Kluwer Academic Publishers, Dordrecht.

Santilli, R. M., Shillady, D. D., 1999, A new iso-chemical model of the hydrogen molecule, *International Journal of Hydrogen Energy* 24, 943-956

Santilli R. M., Shillady, D. D., 2000, A new isochemical model of the water molecule, *International Journal of Hydrogen Energy* 25, 173-183

Schmidt, E., 1966, *Thermodynamics*, Dover, New York, NY

Smith, J. M., & Van Ness, H. C., 1965, *Introduction to Chemical Engineering Thermodynamics*, International Student Edition, McGraw-Hill Book Co., México, DF

HADRONIC JOURNAL 47, 89 - 94 (2024)
DOI 10.29083/HJ.47.01.2024/SC89

INTERPRETATION OF THE MECHANISM OF THE INFLUENCE OF π^0 – MESONS ON THE PROCESS OF ATTRACTION OF NUCLEI

Mikhail Kashchenko
Ural Federal University, Ekaterinburg, Russia
Ural State Forestry University, Ekaterinburg, Russia
mpk46@mail.ru
and
Nadezhda Kashchenko
Ural Federal University,
Ekaterinburg, Russia

Received December 28, 2023

Abstract

There are two stages in the process of low-temperature nuclear fusion. The first stage corresponds to the bringing together of nuclei due to attraction to the negative charge in the internuclear space. This charge is formed by massive electron pairs located in a circular orbit. According to hadronic mechanics, the attraction of electrons (with opposite spins) is ensured by contact interaction. The second stage corresponds to the exchange of nuclei by pions, which begins when the nuclei approach each other to a distance equal to the strong interaction radius R_s. To estimate the maximum value of R_S^*, the concepts of hadron mechanics about the π^0 - meson as a bound electron - positron ($e^- e^+$) - pair are used. The main attention is paid to the visual interpretation of the electromagnetic interaction ($e^- e^+$) - pairs with nuclei, promoting the attraction of nuclei.

Key words: low-temperature fusion of nuclei, contact interaction of electrons, strong interaction, pions, electron-positron pairs.

Introduction

Currently, there is a lot of experimental evidence of low-temperature nuclear fusion, ranging from the simplest reactions of muon catalysis to the fusion of complex nuclei. As noted in [1], the synthesis of nuclei when a proton is captured by nuclei with charge numbers an orders of magnitude greater than unity, and, moreover, fusion reactions of complex nuclei at low temperatures should not occur due to tunneling. Such a synthesis requires bringing nuclei closer to distances at which the strong interaction of attraction between nuclei begins to exceed the Coulomb repulsion. Let us introduce the notation R_s for the strong interaction radius. Obviously, the larger the value of R_s, the faster the convergence of nuclei required for the fusion reaction can be achieved.

It is known that the strong interaction is short-range, i.e. R_s is orders of magnitude smaller than the atomic scale $R_a \sim 10^{-10}$ m. Therefore, the "switching on" of the strong interaction must be preceded by the process of bringing nuclei together from R_a to $2d \leq R_s$, where d is half the internuclear distance. According to the authors, this preliminary process is described relatively simply in the intermediate quasi- molecular state (IQS) model. The IQS diagram is shown in Fig. 1.

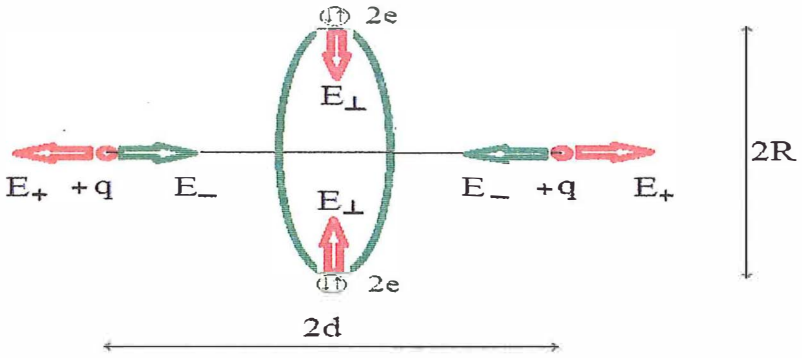

Fig.1. Scheme of the simplest model of a IQS in a state of electrostatic equilibrium (the R/d ratio is reduced compared to the calculated value $\sqrt{3}$, the CC activator contains two electron pairs)

In this model, according to [1-4], the approach of nuclei is achieved due to the attraction of nuclei with a charge +q to a massive negative charge in the internuclear space. The negative charge is associated with a configuration in the form of compact massive electron pairs located in a circular orbit. This object, which catalyzes nuclear fusion, is called, for brevity, a CC activator. Pairs of electrons have opposite spins and are connected by an attractive contact interaction that dominates Coulomb repulsion. Nonpotential contact interaction is described by hadronic mechanics [5].

Estimation of the maximum value of the strong interaction radius

We believe that the conditions for the first stage of nuclear convergence in the IQS model are met. Let us then show, following [1], that for the value of R_s we can use the estimate $R_s \approx 100$ fm.

Let us recall that the mechanism of any type of interaction of objects that are not in contact with each other in quantum field theory is reduced to the exchange of virtual particles - the carriers of this interaction. In the case of strong internuclear interaction of interest to us, the mechanism first proposed by Yukawa [6] remains relevant. In this case, nucleons exchange virtual π - mesons, just as electric charges exchange virtual photons.

Let us also recall that of the three π^0, π^+, π^- - mesons, the π^0 - meson has the smallest rest mass ($\approx$ 135 MeV on the energy scale). Consequently, the estimate of the maximum value of the radius $(R_s)_{max}$ that interests us is associated with the exchange of nucleons by π^0 - mesons. The standard estimate of the interaction radius in quantum mechanics is given by

$$R \approx c\,\Delta t \approx \hbar c / 2\Delta E, \qquad (1)$$

where $c \approx 3\ 10^8$ m/s and $\hbar = h/2\pi \approx 1.05 \cdot 10^{-34}$ J s and it is taken into account that the uncertainties in energy ΔE and time Δt are related by the Heisenberg relation

$$\Delta E\ \Delta t \geq \hbar/2. \qquad (2)$$

It is clear that at finite interaction radii, the maximum value of R corresponds to the minimum value ΔE of the order of the rest energy of the virtual particle, if it is neutral (π^0 - the meson is neutral). If virtual particles have an electric charge, then, in accordance with the law of conservation of electric charge, they should be born in pairs, so that the exchange of nucleons by π^+, π^- - mesons is associated with a smaller radius R_s compared to R_s when exchanging π^0 - mesons.

Moreover, if we assume that, according to hadronic mechanics [5], the π^0 - meson is a bound state of an electron and a positron, then as the maximum value of R_s we can formally take the value $R_s^* \approx 10^{-13}$ m. Indeed, the energy spectrum of the electron is positron pairs (associated with the π^0 - meson) lies in the range $\approx$ (1 - 135) MeV, that is, it is limited from below by the value of the positronium rest energy. Therefore, we take $\Delta E \approx 1.022$ MeV as the minimum value. Then from (1) we obtain $R_s^* \approx 100$ fm $= 10^{-13}$ m. Note that the values of R_s^* and the Compton electron wavelength are of the same order of magnitude. This indicates a characteristic intermediate scale (between the atomic and hadron scales).

"Flickering mode" of the action of (e^-e^+)-pairs on nuclei

Let us recall that the classical model of positronium represents a pair of oppositely charged point particles (with masses equal to the rest mass of an electron) rotating in a circular orbit around a common center of inertia. In this case, the radius of the positronium orbit is approximately twice the Bohr radius, that is,

it has an atomic scale. Then a reasonable question arises: is it possible to compare the formal estimate of R_S^* with an acceptable visual picture of the interaction of nuclei with the participation of positronium? Indeed, for nucleons located at distances d~R_S^* the "exchange" by positronium, the size of which is of the order of $R_a >> R_S^*$, looks, to put it mildly, unconvincing.

Nevertheless, since electromagnetic interaction dominates on the atomic scale, a completely natural and intuitive scenario can be proposed. Namely, we assume that under the conditions of the existence of IQS, the birth of electron-positron (e^-e^+) - pairs from the physical vacuum occurs predominantly with the localization of electrons in the central region of the CC activator. It is clear that such electron localization promotes the approach of nuclei not only due to their attraction to the electron, but also due to repulsion from the positron, whose orbit covers the region containing the nuclei. Of course, under the conditions of the existence of the IQS, the shape of the positron's orbit will differ from a circle. However, when viewed qualitatively, the shape of the orbit does not play a role.

Note that for massive nuclei, the action of the electric field from a fast-moving positron can effectively manifest itself as a "flickering mode" that promotes the approach of one or the other nucleus, as illustrated by the diagram in Fig. 2.

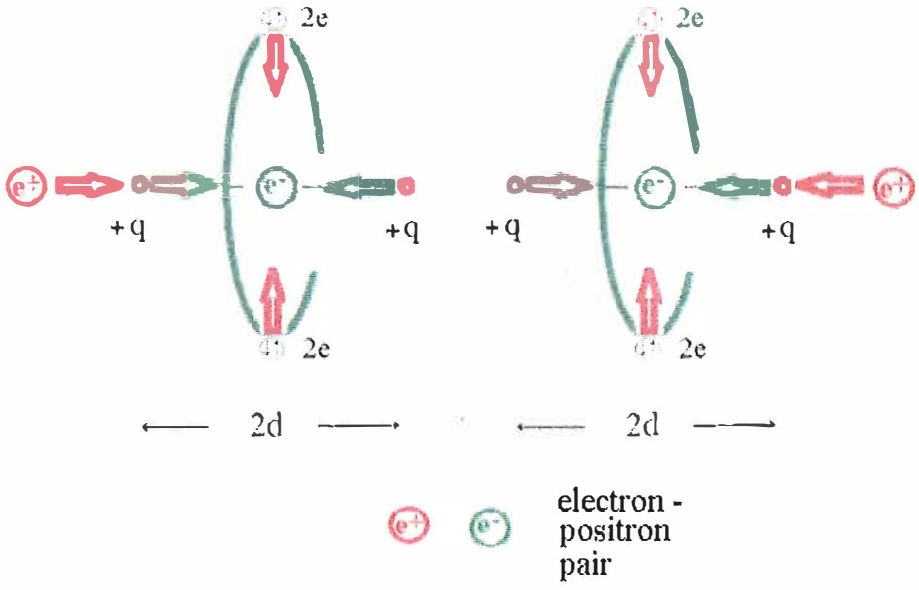

Fig. 2. "Flickering mode" of the action of (e^-e^+)-pairs on nuclei.

Let's give an explanation. Rotation along a circular (or elliptical) orbit is uniquely associated with a pair of oscillations along orthogonal axes. The "flickering mode" can be interpreted as a consequence of the obvious axial symmetry under IQS conditions, which allows one to give preference to one of the vibrations, namely, vibration along the axis of symmetry passing through the nuclei. Indeed, in the presence of an axis of symmetry, the orbits of positrons that enclose nuclei and differ in the orientations of the orbital planes are equally probable. As a result, massive nuclei respond only to the axial component of the electric field of rapidly moving positrons, while the transverse component of the field (due to the rapid change in directions when the orbital plane rotates) is averaged.

It is clear that at a high frequency of appearance and disappearance ($e^- e^+$) - pairs, the "flickering mode" becomes equivalent to the action of an electrostatic field, promoting the convergence of nuclei. In addition, as the process of "exchange" of nuclei ($e^- e^+$) - pairs comes closer, more and more compact and more massive ($e^- e^+$) - pairs are included up to the state of π^0 – meson.

Conclusion

The above considerations demonstrate how, already at distances of the order of 100 fm, interaction with the physical vacuum (PV) can occur, promoting the approach of nuclei. As noted in [4], during nuclear fusion one should expect that the PV is in an excited state and has an energy density comparable to nuclear energy. This means that the frequency and energy of PV oscillations, which include the appearance of (e-e+) pairs, are high.

It is possible that when nuclei approach each other at distances $d \leq 10^{-14}$ m, according to a similar scenario, an electromagnetic contribution to the attraction of nuclei occurs due to ($\pi^+ \pi^-$) - pairs when the π^- - meson is localized in the central region of the CC activator.

It is interesting to note that an interpretation of the complete reduction of short-range strong interaction to electromagnetic interaction is also proposed [7].

It is obvious that if there is a sufficient number of (ee) - pairs in the composition of the CC activator, the process of bringing nuclei closer to distances 2d, significantly smaller than R_s^*, becomes real. Therefore, there is no need to focus on achieving R_s^*. as a prerequisite for starting the second stage of nuclear fusion. This, in turn, ensures the start of strong nuclear interaction, removing the question of overcoming the Coulomb barrier.

References

1. M. Kashchenko and N. Kashchenko, Low-temperature Nuclear Fusion: an Introduction to the Problem and its Conceptual Solution, 180 p. (2022).

2. M. Kashchenko and N. Kashchenko, The Role of the Electronic Current Component in the Formation of a Quasi-Molecular State Leading to the Synthesis of Elements, Letters on Materials **10,** No 3, 266 (2020). DOI: 10.22226/2410-3535-2020-3-266-271

3. Kashchenko M. P., Kashchenko, N. M. (2022). «Development of a model of a quasi- molecular state for low-temperature synthesis of nuclei and interpretation of the formation of chemical elements in the process of vacuum melting of a metal by an electron beam». // In V. L. Derbov (Ed.), *Saratov Fall Meeting 2021: Laser Physics, Photonic Technologies, and Molecular Modeling* [121930V] (Progress in Biomedical Optics and Imaging - Proceedings of SPIE; Vol. 12193). SPIE. https://doi.org/10.1117/12.2626913

4. Kashchenko M. P., Kashchenko, N. M. (2023). Energy density of the physical vacuum and estimation of the mass of a compact electron (ee) – pair. Preprint. https://www.researchgate.net/publication/373650897. DOI: 10.13140/RG.2.2.30521.54880

5. Santilli R.M. Foundations of Hadronic Chemistry. With Applications to New Clean Energies and Fuels. Boston-Dordrecht-London: Kluwer Academic Publishers; 2001. 554 p.

6. H. Yukawa. On the Interaction of Elementary Particles I// Proc. Phys. Math. Soc. Japan. 17(2), 48-57 (1935). DOI: 10.1143/PTPS.1.1

7. Jean Louis Van Belle (2021). Do we need the nuclear force hypothesis? Preprint. https://www.researchgate.net/publication/350872167. DOI: 10.13140/RG.2.2.13315.43042/6

HADRONIC JOURNAL 47, 97 - 126 (2024)
DOI 10.29083/HJ.47.01.2024/SC97

NEW THERMODYNAMICS: WHAT IS THERMAL ENERGY AND ITS DENSITY VERSUS HEAT CAPACITY

Kent Mayhew
68 Pineglen
Ottawa, Ontario
Canada, K2G 0G8
kent.mayhew@gmail.com

Received March 6, 2024

Abstract

Traditional thermodynamics explains what is witnessed when heating matter, at both low and high temperatures, in terms of changes in heat capacities. To enhance our understanding, what constitutes thermal energy will be analyzed. It will then be demonstrated that it is actually the relationship between thermal energy density and temperature that changes, thus allowing heat capacities to theoretically remain constants.

Keywords

Heat Capacity, Thermal Energy Density, Blackbody Radiation, Cut-Off Wavelength

1. Introduction

For: 400 K > T > 250 K, condensed matter has a heat capacity (C_v) that can be approximated by:

$$C_{v-solid} \approx C_{v-liquid} \approx 3R = 24.93 \text{ J/(K mole)} \quad (1)$$

Where the subscript "*v*" signifies the process being isometric (A.K.A. isochoric: dV=0) and "*R*" is the ideal gas constant: R = 8.31 J/mole.

Although not as clear in Fig. 1, for: 400 K > T > 250 K, a monatomic gas has an isometric heat capacity that can be approximated by:

$$C_{v-gas} \approx 3R/2 = 12.46 \text{ J/(K mole)} \quad (2)$$

Similarly, for: 400 K > T > 250 K, a polyatomic gas has its isometric heat capacity approximated by:

$$C_{v-gas} = R(n" + 1/2) \quad (3)$$

where "*n*"" represents the number of atoms in a gaseous molecule. Note that eq. 2 and 3 have been explained in terms of this author's improved kinetic theory [2]-[4].

When an isobaric system expands, it performs lost work onto/into the surrounding atmosphere, as defined by:

$$W_{lost} = (PdV)_{atm} = nRdT \quad (4)$$

Lost work [$(PdV)_{atm}$] has been described by this author as the energy that is expended by an expanding system when lifting the overlying atmosphere's mass. Ultimately, it signifies an atmospheric potential energy increase [4]-[9].

Therefore, for: 400 K > T > 250 K , an expanding monatomic gas has an isobaric (dP=0) heat capacity that can be approximated by [4],[5]:

$$C_{p-gas} = C_{v-gas} + R = 5R/2 = 20.78 \text{ J/(K mole)} \quad (5)$$

where the subscript "*p*" signifies the process as being isobaric (dP=0).

Similarly, for: 400 K > T > 250 K, a polyatomic gas has an isobaric heat capacity that can be approximated by [2]-[4]:

$$C_{p-gas} = R(n" + 1/2) + R = R(n" + 3/2) \quad (6)$$

Equations 1, 2, 3, 5 and 6 are all valid approximations. They are focused upon the molecule's motions. They do not fully consider all the EM components in either gases or condensed matter. Furthermore, equations 2,3, 5 and 6 do not take into account any energy associated with any photons residing in the freespace surrounding the gas molecules.

Furthermore, eq. 1 is isometric. If the condensed matter expands in some isobaric process then one should consider any work done in lifting the atmosphere, as defined by:

$$W_{lost} = (PdV)_{atm} \quad (7)$$

As illustrated in Fig. 1, a solid's heat capacity asymptotically approaches zero, as the solid's temperature approaches absolute zero ($T \rightarrow 0$).

The accepted theory for heat capacities when approaching absolute zero has a certain basis in statistical thermodynamics. A theory that originates in the late 19th/early 20th century from the likes of Maxwell and Boltzmann. This theory is also partially founded in Einstein's (1907) photoelectron model which is based upon a 3-d crystalline solid possessing a large number of quantum harmonic oscillators. Einstein's theory qualitatively explained the heat capacities as $T \rightarrow 0$, but quantitatively there are problems with the analysis. This seemingly was resolved with Debye's analysis.[1]

Debye (1912) extended Einstein's theory with the solid-state equivalent of Planck's law for blackbody radiation, which treated EM radiation as a

---

[1] As a side note, Einstein's theory can be taken as one of the early quantum-founded analysis. Interesting, Einstein, Podosky and Rosen (EPR argument) eventually argued that quantum theory is an incomplete theory [10]. Although quantum theory is currently embraced by the majority, some still argue that there are unresolved issues. One issue being that energy releasing processes tend to be irreversible, while quantum is limited to reversible phenomena [11]. Einstein further noted that quantum mechanics can only represent point-like particles in a vacuum. Of interest, this author's understandings of lost work, limits reversibility of expanding systems to vacuums [4], something that entropy-based traditional thermodynamics fails to elucidate, i.e., work must be done onto something e.g., lifting of the overlying atmosphere's mass against Earth's gravity by an expanding system [4]-[9].

photon gas confined in a vacuum space. Debye T^3 law arrived is accepted as being a superior fit to experimental findings.

Debye's T^3 law considers that the isometric heat capacity at low temperatures, varies as the cube of temperature, e.g.,:

$$C_{v-solid} = A"(T/\theta)^3) = AT^3 \quad (8)$$

where "A" " and "A" are constants and θ is the Debye temperature.

Furthermore, for an ideal gas, the accepted theory for molar heat capacities of gases is based upon the degrees of freedom (f) analysis, i.e.:

$$C_v = \left(\frac{f}{2}\right) R \quad (9)$$

and

$$C_p = C_v + R = \left(\frac{f}{2}\right) R + R \quad (10)$$

Degrees of freedom arguments are founded upon equipartition where a gas molecule has a mean energy of: $kT/2$ per degree of freedom, with "k" being Boltzmann's constant. Such degree of freedom arguments should be questioned because they assert that a gas molecule automatically obtains a mean energy ($kT/2$) per degree, without any clarity explaining the energy's origins.

Furthermore, traditionally one relies upon quantum arguments, e.g., cooling molecules move from a higher to a lower quantized energy state. Moreover, the fraction of molecules in the lowest energy state approaches unity, as the temperature approaches absolute zero. Such arguments have their place when contemplating the excitations of electrons but thermal energy may be better contemplated in terms of broad continuous spectrums of energy rather than discrete/quantized energy states.

A goal of this paper is to explain what has been witnessed without relying upon Einstein's analysis, or Debye's T^3 Law. A result will be an improved understanding concerning what constitutes thermal energy. A result that does not rely upon discrete quantized states.

2. The Essentials For: 400 K > T > 250 K

Eq. 1 can be employed to approximate the thermal energy (Q_{in}) required to raise the temperature of n moles of condensed matter by dT:

$$Q_{in-v} = 3nRdT = nC_{v-solid}dT = nC_{v-liquid}dT \quad (11)$$

For the isometric heating of n moles of a monatomic gas, eq. 2 can be used to approximate the thermal energy (Q_{in}) required to raise the gas' temperature by dT:

$$Q_{in-v} = \left(\frac{3}{2}\right) nRdT \; = \; nC_{v-gas}dT \qquad (12)$$

Similarly, for the isometric heating of n moles of a polyatomic gas, eq. 3 can be used to approximate the thermal energy (Q_{in}) required to raise the gas' temperature by dT:

$$Q_{in-v} = (n" + 1/2)nRdT \; = \; nC_{v-gas}dT \qquad (13)$$

And, for the isobaric heating of n moles of an expanding monatomic gas, eq. 5 can be used to approximate the thermal energy (Q_{in}) required to raise the gas' temperature by dT:

$$Q_{in-v} = (n" + 3/2)nRdT \; = \; nC_{v-gas}dT \qquad (14)$$

Similarly, for the isobaric heating of n moles of a polyatomic gas eq. 6 can be used to approximate the thermal energy (Q_{in}) required to raise the gas' temperature by dT:

$$Q_{in-p} = \left(\frac{3}{2}\right) (n" + \; 3/2)nRdT \; = \; nC_{p-gas}dT \qquad (15)$$

For: $T < 250$ K. Conversely, for the heating of n moles of condensed matter, eq. 8 can be used to approximate the thermal energy (Q_{in}) required to raise the temperature by dT:

$$Q_{in-v} \; = AT^3dT = \; C_{v-solid}dT \qquad (16)$$

Equations 1 through 6, eq. 8, and equations 11 through 16, all assume that the heat capacities are constants and that the thermal energy is some linear increasing function of temperature, i.e., for $T > 250$ K:

$$dT = T_f - \; T_i \qquad (17)$$

where the subscripts "*f*" and "*i*" respectively signify the final and initial states.

3. The Essentials For: $T < 250$ K

For: $T < 250$ K, one can integrate eq. 16 (based upon Debye's T^3 law), thus obtaining for condensed matter:

$$Q_{in-v} \; = \; \int dq_{in-v} = A\int_{T_i}^{T_f} T^3dT = \; (A/4)(T_f^4 - T_i^4) \qquad (18)$$

Generally condensed matter can be contemplated as being isometric. Therefore, one can contemplate eq. 18 in terms of energy density, thus:

$$Q_{in-v}/V = (A/4V)(T_f^4 - T_i^4) \quad (19)$$

Are there any relations in thermodynamics that are a function of T^4? What comes to mind is the Stefan-Boltzmann's equation for a blackbody radiation spectrum:

$$\rho_B = \sigma T^4 \quad (20)$$

where "ρ_B" is the blackbody radiance (energy density), and "σ" is the blackbody radiation constant: $\sigma = 8\pi^5 k^4/15c^3h^3$ = 5.670374419...$\times 10^{-8}$ ($W \cdot m^{-2} \cdot K^{-4}$).

The constants in eq. 19 and eq. 20 are not one and the same, i.e., $a \neq (\frac{A}{4V})$. However, the blackbody energy flux as described by eq. 20 is founded upon the thermal energy emitted by certain closed system's walls, into that closed system's freespace.

4. The Essentials, For All *T*

Certainly, all condensed matter above absolute zero emits energy whose broad continuous spectrum often approximates a blackbody spectrum. This radiated thermal energy is a part of what can be referred to as radiant energy. Radiant energy can take many forms ranging from gamma rays to microwaves. The question then becomes, what part of the spectrum is related to thermal energy in condensed matter?

In order to answer that question, one starts by considering the energy density [$u(v,T)$] associated with blackbody radiation in a closed system. As defined by Planck's formula:

$$u(v,T) = \left(\frac{8\pi h}{c^3}\right) v^n / e^{(\frac{hv}{kT}-1)} \quad (21)$$

The wavelength version of eq. 21, for the energy density of a blackbody spectrum between λ and $d\lambda$ is the energy per mode: ($E = \frac{hc}{\lambda} = hv$), times the density of states per photon, times the probability that the mode is occupied. That being:

$$u(\lambda)d\lambda = \left(\frac{8\pi hc}{\lambda^5}\right)\left[\frac{1}{e^{(\frac{hv}{kT}-1)}}\right]d\lambda \quad (22)$$

Plank's eq. 22 is useful for calculating the total energy density (J/m^3)

associated with a full blackbody spectrum in an enclosed freespace. Based upon eq. 22, plotting the total energy density, one obtains Fig. 2.

Let's reconsider condensed matter. From an energy density perspective condensed matter concentrates thermal energy, when compared to the surrounding radiation density in freespace. It is inarguable that when considering a vacuum in thermal equilibrium that the vacuum's walls must absorb as much thermal energy as they emit.

The exact mechanism for the emittance and absorption of thermal spectrum lacks any clarity. Interestingly, this author has previously proposed that such thermal spectrum is due to inelastic collisions (both intermolecular and intramolecular). Furthermore, a plausible explanation concerning the mechanism that creates the thermal photons associated with radiated thermal energy may be the physical distortions of the electron clouds within molecules and/or atoms, during inelastic collisions [4], [12].

Thermal photons are considered to belong to a broad continuous EM spectrum. The part of the EM spectrum of energy that tends to be both absorbed and emitted by matter.

Whatever the mechanism turns out to be, it must explain why thermal spectrums are:

1) Universal to all condensed matter above absolute zero.
2) Have a temperature functionality.
3) Disappears as: $T \rightarrow 0\ K$

Interestingly, the above 1), 2) and 3) also applies to the thermal energy density within matter. However, the temperature functionality for matter energy density is approximately linear, at least for: 450 K > T > 250 K. Conversely, a blackbody's energy density clearly is not linear, as is illustrated in Fig. 2

Strangely, for T < 250 K, based upon Deby's energy density (eq. 19), one would get a graph similar to that depicted in Fig. 2

As previously stated the above has traditionally been reconciled by contemplating that heat capacities are temperature dependent, rather than constant through all temperature regimes.

5. New Graphical Analysis

The problem with eq. 22 (hence, Fig. 2) is that it considers all wavelengths of a blackbody spectrum. Thermal energy only concerns the

wavelengths (frequencies) that tend to be absorbed by matter, thus becoming thermal energy within that matter. It is accepted (without absolute clarity) that wavelengths associated with thermal energy predominately resides in the infrared part of the spectrum. Therefore, contemplating the total energy density (full spectrum), as sketched in Fig. 2, can be disingenuous.

Accepting that thermal energy consists of only part of the total energy density. Then in order to calculate the thermal energy density, one only needs to consider the part of the spectrum that is predominately thermal energy. What parts of the EM spectrum does one quantify as being thermal energy?

The thermal spectrum resides in the infrared: $0.75\ \mu m = 750nm < \lambda < 100\ \mu m = 100{,}000\ nm$ However, the division between visible light and infrared is founded upon our human vision rather than any concise notions of thermal energy. Accordingly, this analysis depends upon where one chooses to start their consideration of what constitutes thermal energy.

In remote sensing (often used by geologists) the thermal spectrum is considered to be in the range of: $3\ \mu m < \lambda < 15\ \mu m$. In thermodynamics the thermal infrared is considered to be in the range of: $8\ \mu m < \lambda < 15\ \mu m$. The difference can be attributed to the fact that remote sensing sometimes involves spotting forest fires whose emitted wavelengths are close to 3 μm. Again, there is no universal understanding concerning thermal energy.

Based upon Fig. 1, one can speculate that the transition between linear and T^3 functionality for the energy density within condensed matter, occurs near 250 K. Thus, one begins the analysis by examining the energy density for: T = 250 K, as illustrated in Fig. 3. One immediately notices that the peak is near $11.4\ \mu m$. Consider that the thermal energy starts somewhere in the range: $8\ \mu m < \lambda < 12\ \mu m$.

Unfortunately, the integration (of eq. 21 and/or eq. 22) can only be performed over all wavelengths ($0 < \lambda < \infty$) (this is accomplished using mathematical tricks). Therefore, one cannot simply calculate the thermal energy density associated with only some part of a blackbody spectrum. However, one can graphically approximate the thermal energy density associated with various parts of the blackbody spectrum.

One starts by sketching and graphically calculating the total energy density for all temperatures between 50 K and 600 K degrees. This was done at 25 K intervals using graphs obtained from a website that provides the "Planck Curve for Blackbody Radiation", as was published by TU Graz University of Technology [13].

The total energy density of blackbody radiation was obtained using geometric approximations. For example, adding the areas of triangles A, B and C plus the rectangle D, as illustrated in Fig 4 for four different temperatures. The result for the total thermal energy was plotted in Fig. 2.

A similar graphical technique was then used to calculate what is then to be considered as the "thermal energy density". A cut-off wavelength (λ_{cut}) between what is considered thermal energy and non-thermal energy was determined.

Three cut-off wavelengths were chosen: $\lambda_{cut} = 8\,\mu m$, $\lambda_{cut} = 10\,\mu m$ and $\lambda_{cut} = 12\,\mu m$. Fig. 5, illustrates the thermal energy density at four different temperatures (100, 200, 300 & 400 K), for $\lambda_{cut} = 10\,\mu m$, hence over the range: $10\mu m < \lambda < \infty$.

The data table for total energy density and thermal energy density, as well as the energy flux (based upon the Stefan-Boltzmann equation: eq. 20) is given in Table 1, at the end of the paper.

Plotting the total energy density, and the total thermal energy density versus temperature for the three cut-off wavelengths (λ_{cut}), one obtains Fig. 6. It is of interest that the total thermal energy density can be approximated as a linear relation for: 250 K < T < 400 K. The approximate slopes for the thermal energy density using the three cut-off wavelengths are:

$\lambda_{cut} = 8\,\mu m$: (12.58-2.59/ (400-250) = 6.6 x 10^{-2} J/m^3/K
$\lambda_{cut} = 10$ µm: (9.45 -2.27)/(400-250) = 4.8 x 10^{-2} J/m^3/K
$\lambda_{cut} = 12$ µm : (6.99 – 1.95)/(400-250) = 3.4 x 10^{-2} J/m^3/K

It must be emphasized that this analysis was formulated to show that, if the thermal energy density had a thermal energy cut-off wavelength, then one may be able to explain why thermal relationships are approximated as being linear functions of temperature for: 250 K < T < 400 K.

Furthermore, for: T < 250 K the thermal energy density would be a rapidly decreasing function of temperature. Thus, it becomes likely that the heat capacity approximates being a constant through all temperatures.

Moreover, it is the thermal density that is not a linear function of temperature over all temperature regimes.

It becomes a case of our residing on Earth's surface, that we have intuitively come to falsely believe that thermal energy is a linear function of temperature.

In accepting this analysis, one assumes that the thermal energy density associated with matter's thermal spectrum, can be related to the thermal energy density within condensed matter. Based upon the fact that they are both linear relations of temperature, one must conclude that such a relationship may exist. Unfortunately, at this point this relationship is not fully realized. Of interest, one should include the fact that the thermal spectrums emitted by condensed matter, tend to resemble cut-off blackbody spectrums.

Furthermore, the thermal energy cut-off at: 8 μm, 10 μm, and 12 μm, were somewhat arbitrarily made. Certainly, a superior cutoff may be obtained by performing a more exacting analysis over a broader range of wavelengths and by considering various types of condensed matter. Note that this author also tried a cutoff of 3 μm with a preliminary determination that it was too low (see the next section: Weakness of Graphical Analysis).

Moreover, the cut-offs were chosen to be vertical and linear, when in fact it may vary and actually be dependent upon the nature of the condensed matter itself. Even so, there should be a certain degree of universality.

A point becomes that one does not necessarily have to rely upon Einstein's quantum arguments and/or Debye's T^3 law to explain why the total energy required to heat matter has temperature dependence. Again, the simpler explanation may ultimately reside with the realization that it is the thermal energy density that changes with temperature rather than the heat capacity varying in different temperature regimes.

6. A Weakness in this Graphical Analysis

Looking at Fig. 5 one will notice that as the temperature increases, the cut-off wavelength of interest shifts right with increasing temperature. The reason that this analysis was stopped at T = 500 K is that the cut-off wavelength approached C in Fig. 5. At which point, this graphical analysis becomes increasingly inaccurate (see the data points with ** in Table 1).

The expectation should be that as the temperature increases, the thermal energy density continually increases, which is not necessarily what one gets

when doing simple time- consuming geometric analysis, as was done herein. It would be of interest for someone to extrapolate this analysis, perhaps using computing, e.g., artificial intelligence (AI).

7. What does the Cut-Off Represent?

Whether it is ultimately placed at 8 μm, 10 μm, 12 μm, or some other value, the cut-off wavelength (λ_{cut}) represents a theoretical limit for the thermal energy, that being the energy associated with the kinematics within matter. A result of such kinematics is energy radiating from all condensed matter that is above absolute zero. With kinematic energy being the kinetic (translational plus rotational) plus vibrational energy in matter. This statement is partially based upon this author's kinetic theory [2]-[4] wherein the separation of these energies differs from the traditionally accepted degrees of freedom, based theorization.

As stated, there are various types of radiant energy. These include microwave, visible light, ultraviolet, x-rays and gamma rays. What needs to be added to this list is thermal energy, which should be placed between the microwave and visible light spectrums. Herein, the proposal being that thermal energy now starts at the cut-off wavelength and extends into longer wavelengths, e.g., the far infrared, and perhaps even into the microwave.

Again, for condensed matter, thermal energy includes the energy spectrum associated with the vibrational energies inside that matter. It represents the wavelengths/frequencies of energy that are radiated and (most likely) absorbed by that matter.

Importantly, thermal energy is not limited to the discrete energies that are readily absorbed and radiated by electrons, i.e., the quantized energies often determined in infrared spectroscopy. When contemplating closed systems, thermal energy is the energy that is both radiated and absorbed by the walls, which often can be blackbody in nature.

Thermal energy is a broad continuous spectrum of energy. Is it plausible that such a broad spectrum is somehow absorbed by the atoms and/or molecules, as a whole? That would certainly help one to understand why thermal equations involve both the number of molecules and/or the number of atoms.

A possible implication being that this energy is absorbed by nuclei and/or their components. This plausibility has previously been briefly pointed out by this author [4], [12]. Whatever the exact mechanism for the absorption and emission of thermal energy, its result is the vibrational energy within

condensed matter. Importantly, since the heat capacities are based upon the number of atoms in molecules, there must be some sort of approximate universality. A universality not readily explained by either the configuration of its electrons, or the shapes of their electron clouds.

8. Gases

Can any of the above be applied to gases?

For monatomic gases the heat capacities have been deemed to be relatively constant. However, that is not the case for polyatomic gases over all temperature regimes.

Fig. 7 shows the isometric specific heat of air (99%: O_2 and N_2) over a broad temperature range: $0 < T < 2000$ K. Note that engineers prefer to use specific heat which is related to the gas's mass. Physicists and chemists prefer to use molar heat capacities, which are related to the number of moles of gas.

As shown in Fig. 7, for, $T < 200$ K, a polyatomic gas' isometric specific heat [heat capacity per unit mass (c_v)] has been deemed to be some rapidly increasing functions of decreasing temperature, e.g., as: $T \rightarrow 0\ K$.

Furthermore for, $200\ \text{K} < T < 375$ K, a polyatomic gas' isometric specific heat (c_v) has been considered to approximately be constant, as described by eq. 3.

Furthermore, for, $375\ \text{K} < T < 1750$ K, a polyatomic gas' isometric specific (c_v) has been considered as being a linear increasing function of temperature.

Note that Fig. 7 extends to 2000 K, while the analysis for solids stopped at 500 K. This was due to the previously stated weakness in this graphical analysis.

Interestingly, the fact that monatomic gases have a relatively constant heat capacity as defined by eq. 2, implies that not all gases behave the same. Seemingly, gases that have vibrational energy as part of their total thermal energy are the only gas's whose heat capacities have temperature dependence. That being the case, then the kinetic energy (translational plus rotational) [2]-[4] is not affected, at least in the same way that vibrational energy is.

Is there anything that confirms the above? An indirect proof resides with the density of gases being a function of temperature. Specifically, the mean

molecular volume of a gas should be related to its mean kinetic energy: $3kT/2$. Ditto, a gas' mean molar volume is related to its mean molar kinetic energy: $3RT/2$. In other words, as the gas' temperature increases its kinetic energy increases. Therefore, the gas' mean molecular volume should increase.

Conversely, as the gas' temperature decreases the number of moles of a gas per unit volume (m^3) should increase. As shown in Fig. 8, the number of moles of a gas per unit volume, increases linearly as the temperature decreases from 320 K to 160 K. As the temperature decreases below 160 K, i.e., $T \rightarrow 0\ K$, the number of moles per cubic meter increases rapidly.

The above is expected. That is if the gas' thermal energy density decreases rapidly as: $T \rightarrow 0\ K$. Perhaps, what was not expected is this. As shown in Fig. 8, this equally applies to both monatomic and diatomic gases, namely hydrogen (H_2), helium (He), nitrogen (N_2), argon (Ar) and oxygen (O_2). The implication being that both monatomic and diatomic gases witness the same degradation of kinetic energy, as: $T \rightarrow 0\ K$.

An explanation for the similar degradation of kinetic energy is as follows. This author's kinetic theory implies that the larger structured wall molecules impose their kinematics upon the smaller gas molecules [2]-[4]. This means that both the monatomic and diatomic gases will obtain the same mean kinetic energy from their collisions with the structured vibrating wall molecules, as is defined by: $3kT/2$.

The overall implication is that it is the changes to a polyatomic gas's absorption of vibrational energy that separates the energetics of polyatomic gases from monatomic gases, as: $T \rightarrow 0\ K$.

9. Thermal Energy Density of High T Gases

For a diatomic gas (e.g., 99% of air), eq. 3 can be used to approximate the isometric heat capacity: $C_{v-gas} \approx 5R/2$, which it clearly is for: $T = 250$ K (see, Fig. 7) and remains approximately so for: 250 K < T < 375 K. Unexpected is that its heat capacity then increases with temperature. It approaches the theoretical isobaric heat capacity for a diatomic gas, as defined by eq. 8. That being $C_{p-gas} \approx 7R/2$ at high temperatures (blast furnace temperatures, e.g.: 1,500 K)

How does one explain the seemingly heat capacity's increase for: 375 K < T < 1750 K, shown in Fig. 7? Consider the heat capacity to be constant,

then again, it is the required thermal energy in per degree temperature change that increases. In other words, $Q_{in\text{-}v}$ as defined in eq. 13 increases because there is an unexpected increase to the thermal energy density in relation to the gas's temperature increase. Obviously, the gas' thermal energy density increase is greater than eq. 13 implies, as illustrated in Fig. 7 for: $T > 375$ K.

An implication of Fig. 7 is that the thermal energy density of the surrounding thermal (or blackbody) radiation increases rather rapidly between: 450 K< T < 750 K. After which, the increase tapers off: 750 K < T < 1750 K. Seemingly approaching some linear increasing value as temperatures exceed 2000 K. It would be of interest to attain a superior analysis of the thermal energy density at higher temperatures than has been provided by the graphical analysis herein. Again, hopefully such an analysis may be improved, e.g., by using AI computing.

10. Thermal Energy Density of Low *T* Gases

The traditional explanation for the heat capacity of a gas increasing as temperatures approach absolute zero, (i.e. for: $T < 250$ K, as: $T \rightarrow 0$) was based upon the concept that states can be frozen-out. Specifically, the vibrational energy of gases (e.g., air), are increasingly frozen-out as the temperatures decrease. Perhaps, but air is 99% homonuclear O_2 and N_2, both of which traditionally speaking, are supposedly transparent to thermal radiation.

Imagine that O_2 and N_2 truly are transparent to thermal radiation/photons, as has been traditionally claimed. One, might then ask, what difference would being frozen-out make? One faces that enigma bestowed in 20th century thermodynamics. That being, energy does not simply exist, as is implied by equipartition and degrees of freedom, founded kinetic theory.

Energy associated with a gas molecule must have an origin. For the case of a diatomic gas molecule in a closed system, this author's kinetic theory's origins are [2]-[4]:

1) Kinetic energy (translational plus rotational) is primarily imposed onto the diatomic molecule through the gas molecule's collisions with structured vibrating wall molecules.
2) Vibrational energy is primary obtained from the absorption of thermal photons.

Additionally, if homonuclear diatomic gases (e.g., O_2 and N_2) actually

are transparent to all thermal radiation, then being frozen-out would have no consequences. In which case, the diatomic gas must obtain both its kinetic and vibrational energy from its collisions with walls. Based upon heat capacities, this seemingly is not the case [2]-[4].

Importantly, thermal energy consists of broad continuous spectrums of energy, e.g., blackbody spectrums. Again, this differentiates thermal energy from quantized energies associated with the discrete energy states that are associated with electrons. It raises the question, is there another plausible explanation?

The simplest explanation for what is witnessed for gases at low temperatures is that the thermal energy density rapidly approaches zero, as: $T \rightarrow 0\ K$. Thus, one has the illusion that the heat capacity has skyrocketed, when in fact it is thermal energy density that has crashed.

In terms of polyatomic gases (e.g., air: 99%: N_2 and O_2) any thermal energy absorption resulting in vibrational energy would rapidly approach zero as: $T \rightarrow 0\ K$. Hence, the vibrational energy of that gas would also rapidly approach zero.

One may prefer to think in terms of the gas' vibrational energy being frozen-out at low temperatures. In many ways both arguments have similar results. A point becomes that one is not restricted to quantum arguments in order to comprehend why air's heat capacity has the illusion of being some rapidly increasing function of temperature as: $T \rightarrow 0$.

Moreover, thermal energy concerns the motions and vibrations of atoms/molecules as wholes. The energy associated with such motions quickly becomes zero as: $T \rightarrow 0\ K$. This is not the same as the energy associated with electrons. It is one thing to say that molecular motions cease, however this does not imply that electrons necessarily stop moving.

11. O_2 and N_2 Are Not Completely Transparent

How can diatomic gases like O_2 and N_2 be transparent to thermal radiation, yet their heat capacities adhere to standardized equations 2, 3, 5 and/or 6?

Heat capacity experiments involve the measurements of thermal energy in (Q_{in}) versus the temperature change (dT). The required energy is based upon the gas's kinematics, i.e., the gas's kinetic plus vibrational energies. For all intents and purposes, thermal energy constitutes wavelengths that are greater than the cut-off wavelength. That being the previously described

theoretical division for thermal energy, i.e., the thermal part of the infrared spectrum.

The concept of certain gases being transparent is founded upon infrared spectroscopy, which often focuses upon shorter wavelengths photons (higher frequencies/energies). Those, being the photons that tend to interact (as waves) with various gases electron configurations, e.g., a gas' lopsided charge distribution. To what extent the absorption due to different electron configurations actually results in the heating of a gas, may become debatable on a case-by-case basis.

Many believe that the absorption of discrete wavelengths due to electron configurations is the primary mechanism by which gas molecules absorb thermal energy. In terms of this paper, so-called transparent gases likely absorb thermal photons. They do not absorb the higher energy (shorter wavelength) photons that tend to excite discrete energy states in gases like CO_2. Note that CO_2 also has a strong absorption peak near 15 μm.

It is of interest that in remote sensing, the wavelengths in the thermal part of the EM spectrum forms one of the windows for observing the Earth from satellites. Seemingly, the majority (up to 80%) of the photons in this window do readily pass through the atmosphere. An implication being that the absorption of thermal photons by gases is inconsequential.

Due to the speed of light, the absorption of thermal photons by gases can represent relevant quantities of thermal energy. Imagine a closed system where thermal photons are both radiated and absorbed by the walls. Certainly, the chances of a given photon scattering with and then being absorbed by a given gas molecule, remains low. However, the quantity of photons that can interact with that gas molecule over a given duration renders the absorption of thermal photons by gas molecules, real.

12. Infrared Spectroscopy

Would all of a gas' absorptions be witnessed in infrared spectroscopy? In dispersive infrared spectroscopy, the resulting sample's spectrum is obtained by subtracting a background (or zero) spectrum from one's measurements. The resultant spectrum then shows any uniqueness which often is based upon the sample gas's unique electron configuration, e.g., lopsided charge distributions. This uniqueness enables one to quickly identify the gas.

Consider that Fig. 9. Path 1 (reference cell path) will have the same interference (absorptions and radiances), as Path 2 (sample cell path). The

interference along Path 1 when measured gives the background spectrum. This interference comes from the air, contents of the reference cell, laboratory and/or apparatus etc. The subtraction of the background spectrum means that the recorded spectrum only shows uniqueness associated with the sample being tested. A uniqueness that is based upon discrete energy associated with specific wavelengths, which are amplified before the spectrum is recorded.

It should be emphasized that both the analyte cell (sample cell) and the reference cell are enclosures. The reference cell is either evacuated (vacuum) or is filled with a gas that is considered as being non-absorbing, e.g., air (99% homonuclear O_2 and N_2). As enclosures, both cells contain thermal (e.g., blackbody) radiation that is related to their temperature. Furthermore, the light source is a heated wire radiating a thermal (e.g., blackbody) spectrum that is associated with its higher temperature. Therefore, much of the subtracted background will constitute a broad continuous thermal (e.g., blackbody) spectrum, whose peak is in the vicinity of the previously described cut-off wavelengths, e.g., $\lambda_{cut} = 10\ \mu m$.

Few have asked, does the background subtraction have any consequences, other than enabling the identification of the gas? If the background spectrum includes some universal phenomenon, then the resulting spectrum becomes misleading from a thermal energy perspective. For example, if both the analyte and the reference gas absorbed (or emitted) the similar parts of the light source's spectrum. Then it becomes erroneous to assume that the parts of the subtracted background spectrum are in no way universal to all (or most all) gases. In which case, the background subtraction includes the subtraction of certain gas' thermal signature, or part thereof.

Similar argument holds for Fourier Transform Infrared Spectrometry (FTIR), where the background's subtraction occurs in its computer and programming. Note that in FTIR the background spectrum is often measured in the cell prior to testing the sample. Its data is stored in the computer, where the background spectrum is subtracted.

Interestingly, in inelastic collision studies, infrared spectroscopy is used. Furthermore, as previously stated most such studies are performed in ultracold experimental apparatus, hence certain aspects of the thermal spectrum would be eradicated.

The plausibility that some universal phenomena may not be witnessed in

the infrared spectroscopy, raises concerns that may help one's understanding.

13. Discussion

Nothing was proven here beyond all doubt. Ditto can be said for Einstein's photoelectron model which treats solids as a group of quantum oscillators. The same applies to Debye's T^3 law. Certainly, both Einstein's and Debye's models are based upon mathematical results. Results that can be tied to both statistical and quantum theory.

The issue with such results, is that one often places mathematics ahead of theoretical logic, i.e., one's pet theory is purely mathematical thus, leaving theoretical justification by the wayside. In this paper a theory was devised ahead of the math, a theory whose plausibility was verified using graphical analysis. A theory that fits with and clearly explains accepted thermodynamic relations.

It is interesting to note that both Stefan-Boltzmann's and Planck's energy density relations, are in many ways part of quantum theory's origins. Interestingly, this is the point that this theory separates from the traditional understandings. It raises questions, e.g., are such accepted relations founded upon mathematical tricks, or divine logic? Planck thought that the quantization of energy was a mathematical trick enabling one to advert the ultraviolet catastrophe [16]. Certainly, at that point Planck was thinking in terms of classical oscillators.

The issue is not with the quantization of a photon's energy, rather it is the notion that thermal energy is only adsorbed by electrons possessing discrete quantized energy states. The states that are found in infrared spectroscopy results, enabling one to identify specific gases. Energy states that when absorbed may result in thermal energy increases but equally may result in the emission of a photon of that discrete energy.

Thermal energy has a universality based upon the number of atoms in a molecule rather than some configuration of electrons. Again, this universality is witnessed in equations 1 through 6 and 11 through 15. Furthermore, thermal energy concerns broad continuous spectrums, spectrums whose total energy density can be best inferred by heat capacity experiments.

In terms of eq. 22, the energy density of a blackbody spectrum between λ and $d\lambda$ is the energy per mode, times the density of states per photon, times the probability that the mode is occupied. It remains valid as a

mathematical approximation. It is just that the "density of states" must rapidly decrease at the cut-off wavelength for shorter wavelengths (for higher energy photons/phonons), when contemplating thermal energy densities.

Again, the cut-off wavelength is likely not a sharp vertical divide as was graphically depicted herein. It must be acknowledged that the cut-off frequency may vary with states (solids, liquids and gases) as well as with the nature of the matter. Interestingly, some matter's absorption of thermal energy includes visible wavelengths, and the near infrared. These absorptions are primarily due to electrons absorbing energy (as waves), rather than the molecules/atoms themselves. Furthermore, for gases there should be a pressure dependence, which affects the mean free path of the thermal photons.

It is of further interest that one of our estimated cut-off wavelengths ($\lambda_{cut} = 10\ \mu m$) is at the end of what is referred to as the "fingerprint zone" ($2\ \mu m < \lambda < 10\ \mu m$). That being where there are many complex bands that form a molecule's fingerprint. The chosen cut-off also resides in what is often considered as being in the thermal infrared ($8\ \mu m < \lambda < 15\ \mu m$).

This author previously theorized that thermal radiation, e.g., blackbody radiation, may be due to inelastic collisions between atoms and/or molecules. Moreover, it was speculated that the emission of thermal photons was due to collision induced distortions of the electron clouds in both atoms and molecules [4], [12]. Thus, explaining the broad continuous nature of thermal spectrums, at least in the thermal infrared.

Logic implies that if matter radiates thermal photons then that matter should absorb thermal photons. Questions then arise concerning what is the mechanism of absorption? Is it by the electron clouds, or are thermal photons absorbed by another mechanism.

This author has previously discussed that absorption of thermal photons may involve photons behaving as particles thus passing their momentum onto the atoms/molecules [4], [12]. Thus, there may be more to the wave-particle duality of photons than has been accepted.

Whatever the mechanism, thermal equilibrium implies that matter absorbs as much thermal energy as it relinquishes (kinematic plus radiated thermal energy). This is certainly witnessed in enclosures where the walls must absorb as well as radiate thermal photons.

Accordingly, the mechanism of absorption and emission do not

necessarily have to be identical. The only criterion is that when in thermal equilibrium, the total thermal energy in equals the total thermal energy out. Although speculative, one could envision matter absorbing thermal photons as particles and emitting thermal photons due to inelastic collisions, e.g., collision induced distortions of electron clouds.

It should be stated that statistical thermodynamics describes all of a system's energy solely in terms of that system's kinematic energies. Such a description remains a valid approximation for closed systems where the system's total kinematic energy is significantly greater than its total radiative energy [4], [17]. And where the closed system's wall both radiate and absorb thermal photons, thus giving the illusion of elastic collisions [4], [12], [17]-[19].

14. **Conclusions**

We instinctively think in terms of temperature being a measure of warmth, realizing that as the temperature increases, then so too does the thermal energy. Our first experiences involve thermal energy being a linear function of temperature, as is measured in our daily lives using a thermometer. Therefore, when performing thermal energy experiments, one instinctively conforms to it being the matter's heat capacity that varies with temperature. As a powerful mathematical construct, statistical thermodynamics fortified our confidence in what may be erroneous logic.

Contemplating that it is the thermal energy density that varies with temperature, alters our thermodynamic perspective. A perspective that allows heat capacity to be considered as a constant over most temperature regimes. A new perspective that does explain our experimental findings in a simpler context.

Specifically, experiments based upon the thermal energy into (Q_{in}) a system may be better explained in terms of the system's relatively constant heat capacity multiplied by its temperature change (dT). However, the amount of thermal energy required to incrementally increase the temperature (dT) is a not always a linear function of temperature, over all temperature regimes.

There remains a relatively small temperature regime over which the thermal energy required to increase a system's temperature remains a linear function of temperature. That happens to be the temperature regime in which we tend to reside here on Earth's surface, i.e., 250 K < T < 400 K. Seemingly, this reality has skewed our perspective.

Graphs for Planck's blackbody energy density relation were obtained at 25 K intervals for: 50 K < T < 500 K. The total energy density based upon the plots were graphically calculated. Cut-off wavelengths of 8 μm, 10 μm, and 12 μm were then chosen based upon the accepted graph for the heat capacity of mercury, and the graph for the blackbody energy density at: T= 250 K.

All wavelengths longer than the chosen cut-off wavelength were considered to be part of the blackbody's thermal energy. The total blackbody thermal energy density was then graphically calculated, e.g. for a cut-off of: $\lambda_{cut} = 10\ \mu m$, the blackbody spectrum's total thermal energy density was considered to include: $10\mu m < \lambda < \infty$.

Plotting both the blackbody spectrum's total energy density at various temperatures, it became obvious that as expected, the blackbody's total energy density is a rapidly increasing function of temperature.

However, the blackbody spectrum's thermal energy density could be approximated as a linear function of temperature for: 250 K < T < 400 K for all three proposed cut-off wavelengths. Assuming that the blackbody spectrum's thermal energy density must be related to the thermal energy density in matter, gives clarity as to why most of our accepted thermal energy relations are linear increasing functions of temperature.

For temperatures below 250 K the thermal energy density decreases rapidly (e.g., T^4) as the temperature decreases, i.e., as: $T \rightarrow 0\ K$. At absolute zero the thermal energy density is considered to be zero, i.e., all molecular motions cease.

Conversely, for temperatures above 400 K the thermal energy increases more rapidly than a linear relation of temperature would indicate. Unfortunately, the graphical analysis became unsensible for: T > 500 K.

It must be emphasized that this is a preliminary paper, written to show that there is a simpler logic that explains what has been witnessed. The following all warrant more consideration:

- Cut-off wavelengths (e.g.,$\lambda_{cut} = 10\ \mu m$) for thermal energy.
- Nature of thermal energy density for: T > 500 K.
- Relationship between a blackbody spectrum's thermal energy density and thermal energy density in specific matter.

Ultimately, this preliminary analysis separates new thermodynamics from the traditionally accepted theories based strictly upon statistical

thermodynamics, and quantum physics.

Figures

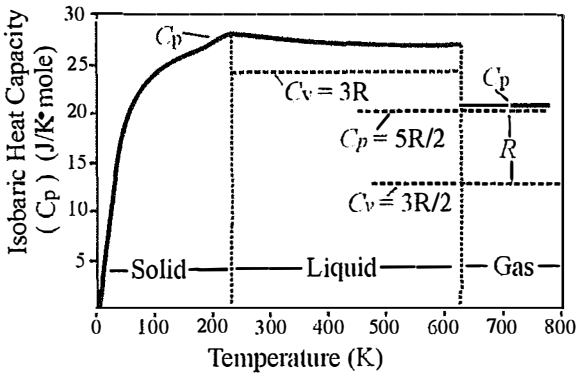

Fig. 1 is a sketch of the heat capacities versus temperature for mercury. Note that discontinuities exist where phase changes occur. Also note that mercury is unreactive, thus when in the gaseous state mercury tends to be a monatomic gas [1].

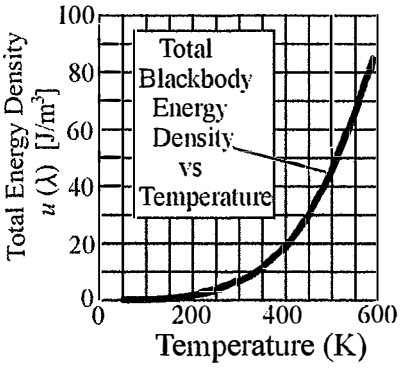

Fig. 2 is a sketch for the total energy density versus temperature, as described by eq. 22.

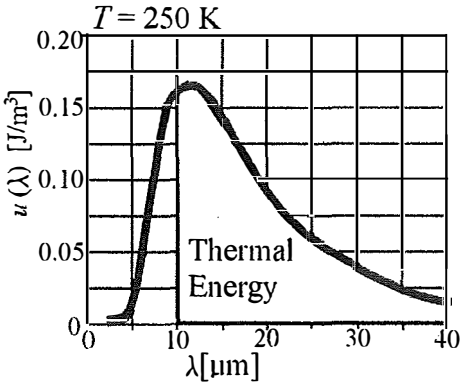

Fig. 3 is a sketch for the blackbody energy density versus wavelength at: $T = 250$ K

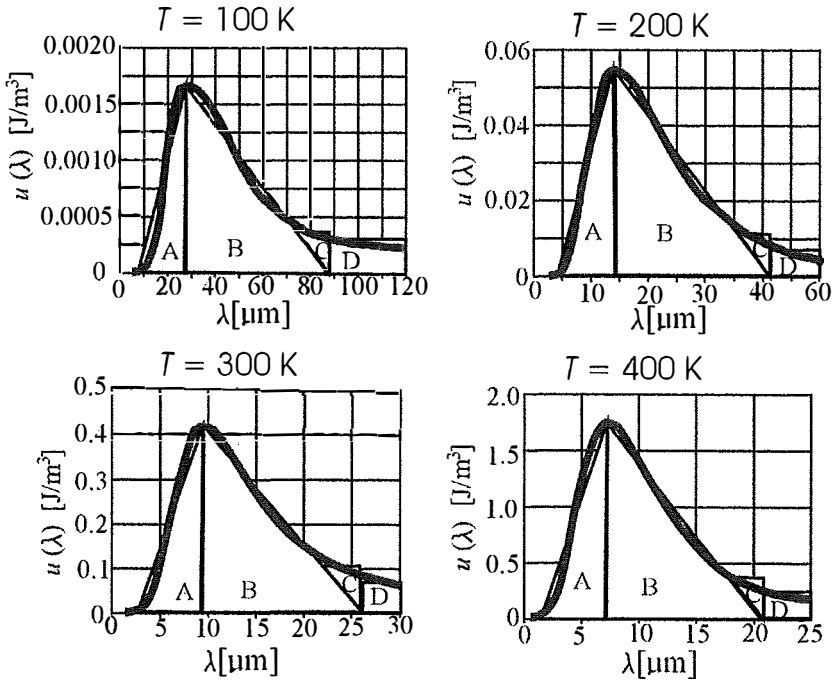

Fig. 4 shows the total energy density versus wavelengths for T=100, T=200, T=300 and T=400. The blackbody energy density is the summation of the areas in triangles A, B and C plus the rectangle D.

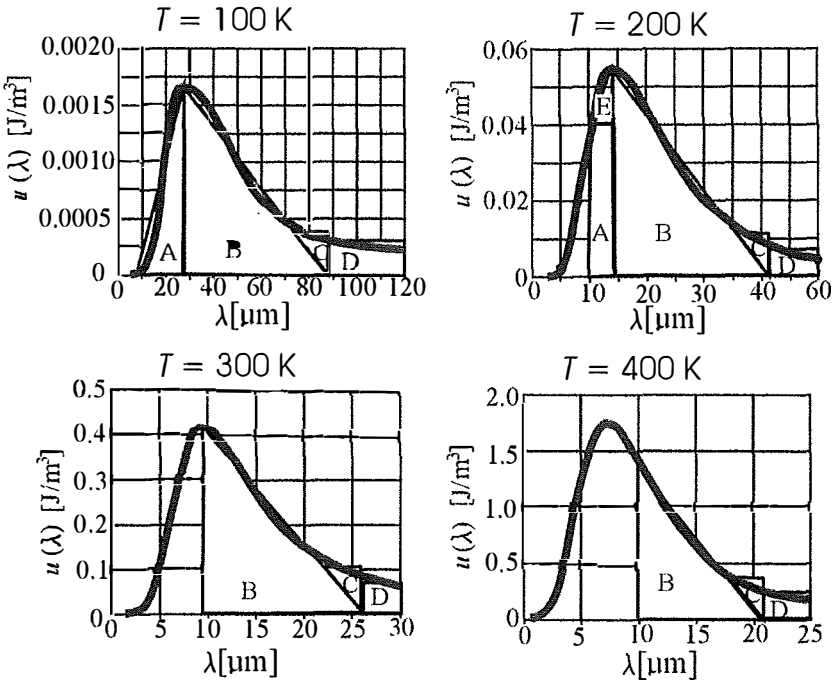

Fig. 5, shows the thermal energy density versus temperature for cut-off: $\lambda = 10\ \mu m$. For: $T = 100$ K it is the summation of: A, B, C& D. For: $T = 200$ K it is the summation of: A, B, C,D & E. For: $T = 300$ K and $T = 400$ K, it is the summation of B, C& D.

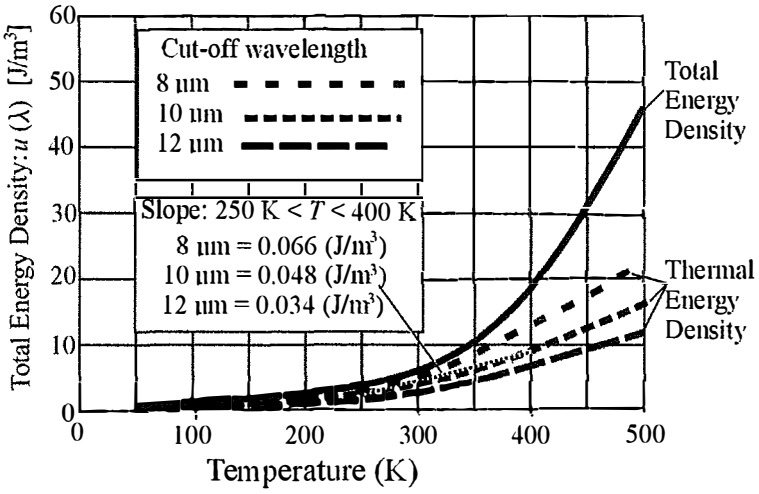

Fig. 6 shows both the total energy density and the thermal energy density versus temperature associated with blackbody radiation for the three chosen

cut-off wavelengths.

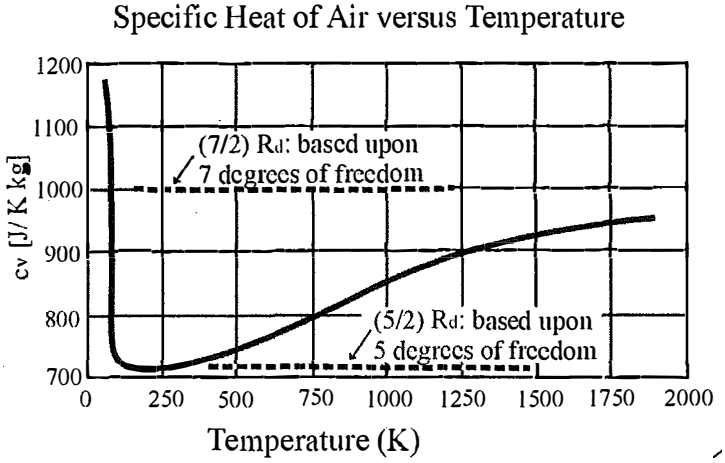

Fig. 7 is a sketch of the specific heat of air versus temperature. Note that: $R_d=RM_d$ that being the dry air constant where M_d is the dry air mass and R is the universal gas constant [14].

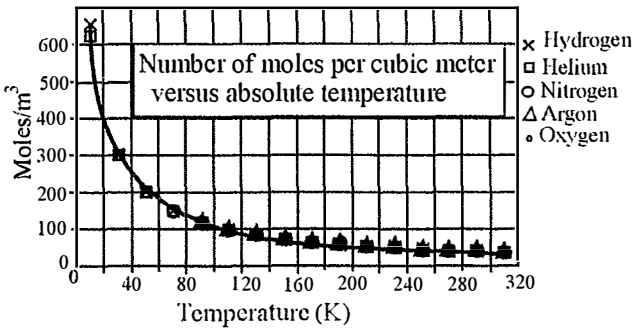

Fig. 8 shows the number of moles per cubic meter of various gases as a function of temperature. Data is in Table 2 at the end of this paper. It is based upon data from the "Handbook of Chemistry and Physics" [15]. Note that this also implies that Avogadro's hypothesis comes into question at low temperatures.

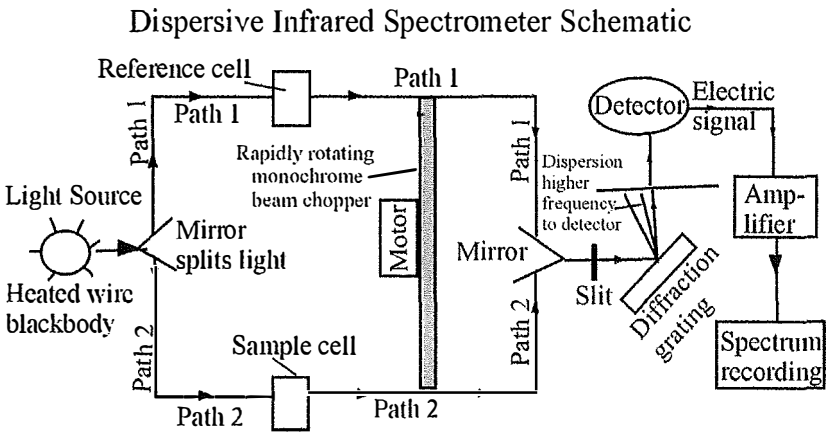

Fig. 9. Is a schematic for a dispersive infrared spectrometer.

Table 1: Gives Blackbody thermal energy at various temperatures

T (K)	Peak λ (um)	Peak $[u(v,T)]$ (J/m^3)	ρ_B Eq.20 (J/m^2)	Total Energy Density (J/m^3)	Thermal Energy Density At three chosen cut-offs (J/m^3)		
					$\lambda =$ 8 μm	$\lambda =$ 10 μm	λ =12 μm
50	60	0.000054	0.354	0.004	0.004	0.004	0.004
75	38.8	0.00041	1.79	0.0214	0.0214	0.0214	0.0214
100	27.5	0.0017	5.67	0.0655	0.065	0.065	0.0644
125	22.9	0.0053	13.8	0.166	0.167	0.166	0.164
150	19.1	0.0133	29	0.347	0.34	0.335	0.328
175	16.7	0.0285	53.2	0.664	0.662	0.643	0.613
200	14.1	0.055	90.7	1.11	1.031	0.971	0.881
225	13	0.1	145.3	1.78	1.74	1.586	1.41
250	11.4	0.167	221.5	2.76	2.59	2.27	1.95
275	10.6	0.27	324.3	3.99	3.58	3.06	2.54
300	9.2	0.42	459.3	5.63	4.72	3.9	3.08
325	8.3	0.625	632.6	7.78	6.1	4.87	3.67
350	8	0.91	850.9	10.53	7.89	6.19	4.69
375	7.5	1.33	1121	13.8	9.99	7.44	5.44
400	7.2	1.77	1452	18.62	12.58	9.45	6.99
425	6.8	2.4	1850	23.17	14.1	10.8	7.75
450	6.4	3.3	2325	30.09	17	12.35	8.85
475	6.1	4.11	2887	38.71	20.57	14.37	10.02
500	5.8	5.2	3544	46.4	23.68	16.48	11.48
525	5.6	6.8	4308	51.95	**	**	**
550	5.3	8.6	5189	68.52	**	**	**
575	5	11	6199	76.53	**	**	**
600	4.7	13.3	7349	84.14	**	**	**
** Non-sensible due to weakness in graphical analysis							

Table 2

	Density at 1 Bar pressure (kg/m^3)					Number of moles per m^3 at 1 Barr pressure				
T (K)	H_2	He	Ar	N_2	O_2	H_2 Atomic mass 2.016	He Atomic mass 4.002	Ar Atomic mass 39.95	N_2 Atomic mass 28.01	O_2 Atomic mass 32.00
0	1.32	2.50				656.25	624.19			
40	0.62	1.20				305.41	299.85			
60	0.41	0.80				201.09	200.05			
80	0.30	0.60		4.38		150.55	150.10		156.31	
100	0.24	0.48	4.92	3.44	3.94	120.78	120.11	123.03	122.69	123.16
120	0.20	0.40	4.06	2.84	3.25	100.20	100.12	101.58	101.38	101.63
140	0.17	0.34	3.46	2.42	2.77	85.86	85.83	86.64	86.53	86.69
160	0.15	0.30	3.02	2.12	2.42	75.10	75.11	75.60	75.53	75.63
180	0.13	0.27	2.68	1.88	2.15	66.77	66.77	67.09	67.04	67.09
200	0.12	0.24	2.41	1.69	1.93	60.07	60.09	60.30	60.26	60.31
220	0.11	0.22	2.19	1.52	1.75	54.61	54.65	54.80	54.40	54.78
240	0.10	0.20	2.01	1.41	1.61	50.10	50.10	50.19	50.15	50.19
260	0.09	0.19	1.85	1.30	1.48	46.58	46.25	46.31	46.30	46.31
280	0.09	0.17	1.72	1.20	1.38	42.93	42.93	42.98	42.98	43.00
300	0.08	0.16	1.60	1.12	1.28	40.06	40.08	40.13	40.09	40.13
320	0.08	0.15	1.50	1.05	1.20	37.56	37.58	37.60	37.59	37.59

Handbook of Chemistry and Physics: Editor: W.M. Haynes (CRC Press, New York, 2010) [14]

AW signifies Atomic Weight. Note: mols/m^3 calculated by: Density*1000/AW

References:

[1] https://chem.libretexts.org/Courses/Knox_College/Chem_321%3A_Physical_Chemistry_I/08%3A_The_Third_Law/8.01%3A_Heat_Capacity_as_A_Function_of_Temperature

[2] Mayhew, K.W., "A New Perspective for Kinetic Theory and Heat Capacity", Prog. in Phys., Vol. 13, 4 (2017) pg 166-173 https://www.researchgate.net/publication/332849728_A_New_Perspective_for_Kinetic_Theory_and_Heat_Capacity

[3] Mayhew, K.W., "Kinetic Theory: Flatlining of Polyatomic Gases", Prog. in Phys., Vol. 14, 2 (2018) pg 75-79. https://www.ptep-online.com/2018/PP-53-05.PDF

[4] Mayhew K,W., New Thermodynamics: Part A (2024). Self -published Amazon: https://www.amazon.com/dp/B0CWRLRBMR?ref_=pe_93986420_774957520&fbclid=IwAR3LQtjLw9Et5lhYCh3OczmQTCkK0IqSWmuU5HaDRkytfg_lZupUaPuXgk0

[5] Mayhew, K.W., Hernandez. H., " Entropy and Enthalpy: Reality or Grandiose Mistake? ForsChem Res. Rep. V0l 8, 2023-06. https://www.researchgate.net/publication/369487992_Entropy_and_Enthalpy_Reality_or_Grandiose_Mistake

[6] Mayhew, K.W. (2021). New Thermodynamics: Inelastic Collisions, Lost Work, and Gaseous Inefficiency. Hadronic Journal, 44 (1), 67-96. http://hadronicpress.com/docs/HJ-44-1E.pdf.

[7] Mayhew, K.W. (2020). New Thermodynamics: Reversibility and Free Energy. Hadronic Journal, 43 (1), 51-59. http://hadronicpress.com/docs/HJ-43-1B.pdf.

[8] Mayhew, K.W. (2020). New Thermodynamics: Inefficiency of a Piston-Cylinder. European Journal of Engineering Research and Science, 5 (2), 187-191. doi: 10.24018/ejeng.2020.5.2.1765.

[9] Mayhew, K.W. (2015). Second law and lost work. Physics Essays, 28 (1), 152-155. doi: 10.4006/0836-1398-28.1.152.

[10] Einstein, A.Podolsky, B., Rosen, N., "Can quantum-mechanical description if physical reality be considered complete?," Phys. Rev. 47, 777 (1935). http://www.eprdebates.org/docs/epr-argument.pdf

[11] Santilli, R. M. "Overview of the Einstein-Podolsky-Rosen Argument with Applications in Physics, Chemistry and Biology" APAV 2021. https://www.santilli-foundation.org/epr-overview-2021.pdf

[12] Mayhew, K.W.," New Thermodynamics: Wave-Particle duality in Radiative Heat Transfer" Hadronic Journal 44, 215-116 (2021)

[13] https://lampx.tugraz.at/~hadley/ss1/emfield/blackbody.php?T=5700, Jan. 2024

[14] https://en.wikipedia.org/wiki/Degrees_of_freedom_(physics_and_chemistry) Jan. 2024

[15] Handbook of Chemistry and Physics: Editor: W.M. Haynes (CRC Press, New York, 2010)

[16] https://en.wikipedia.org/wiki/Planck_postulate#:~:text=Planck%20was%20unable%20to%20justify,Planck%20then%20contemplated%20virtual%20oscillators. Jan. 2024

[17] Mayhew, K.W., "New Thermodynamics: Pictet, Epistemology and Philosophy", Sci. & Phil., Vol 11(1) 2023.
https://philpapers.org/rec/MAYNTP
[18] Mayhew, K.W., "New Thermodynamics: Inelastic Collisions, Blackbody Radiation, Entropy and Light", EJ-Physics, Vol 2, 6, pg -6 (2020).
https://www.researchgate.net/publication/345983105_New_Thermodynamics_Inelastic_Collisions_Blackbody_Radiation_Entropy_and_Light
[19] Mayhew, K.W., 2021. "New Thermodynamics: Inelastic Collisions, Lost Work, and Gaseous Inefficiency" Hadronic Journal, 44, pg 67-96.
https://hadronicpress.com/docs/HJ-44-1E.pdf